NASA CR-132549

DEVELOPMENT OF TECHNOLOGY FOR FLUID-STRUCTURE INTERACTION MODELING OF A 1/8-SCALE DYNAMIC MODEL OF THE SHUTTLE EXTERNAL TANK (ET)

Volume I: Technical Report

by

M. Bernstein, R. Coppolino, J. Zalesak, and P. W. Mason

August 1974

Final Report – Prepared Under Contract No. NAS 1-10635-13

by

Grumman Aerospace Corporation

Bethpage, New York 11714

Langley Research Center
Hampton, Virginia 23665

NATIONAL AERONAUTICS AND SPACE ADMINISTRATION

DEVELOPMENT OF TECHNOLOGY FOR FLUID-STRUCTURE INTERACTION MODELING OF A 1/8-SCALE DYNAMIC MODEL OF THE SHUTTLE EXTERNAL TANK (ET)

Volume I: Technical Report

Prepared under Contract NAS 1-10635-13

for the

Langley Research Center
National Aeronautics and Space Administration
Hampton, Virginia 23365

by

M. Bernstein, R. Coppolino, J. Zalesak, and P. W. Mason

Grumman Aerospace Corporation
Bethpage, New York 11714

August 1974

FOREWORD

The work described in this report was performed at the Grumman Aerospace Corporation, Bethpage, New York, and administered by the Vibration Section of the Structures and Dynamics Division, NASA Langley Research Center, Hampton, Virginia.

The work performed under NASA Contract NAS1-10635-13 included the construction and delivery of the 1/8-Scale Shuttle Model External Tank and the generation and delivery of a NASTRAN hydroelastic model of this tank. Prior to the manufacture of the model, the Space Division of Rockwell International funded a design effort to modify the forward attachments of the External Tank (ET) to the Solid Rocket Booster (SRB) so that they more closely represented the prototype attachments.

After it became apparent that modifications in NASTRAN hydroelastic formulation were advisable, additional funding was provided by the Space Division of Rockwell International to partially support the developments described in Section 4. Although not part of the task under NAS1-10635-13, Section 4 is included as information for potential NASTRAN users.

Many persons at Grumman and NASA Langley have contributed to the various phases of this program. The technical assistance and direction of Dr. L. P. Pinson and Mr. U. J. Blanchard of the NASA Langley Research Center is gratefully acknowledged. The following persons contributed significantly to this effort at Grumman:

- Master Agreement Program Management: E. F. Baird
- Task Order Management: M. Bernstein
- Design and Manufacturing Liason: A. P. La Valle
- Stress Analysis: W. P. Bierds
- Manufacture of Model: R. A. Wagensell
- Model Final Assembly: M. Gack, G. Stevens

- NASTRAN Dynamic Analysis: M. Bernstein, J. Zalesak, P. W. Mason, D. Gregory
- Modification of Hydroelastic Formulation: R. Coppolino
- NASTRAN Modification: R. Coppolino and A. Levy
- Shell Analysis: V. Svalbonas

This report consists of two volumes as follows:

- Volume I - Technical Report
- Volume II - Supporting Data

ABSTRACT

This report describes a NASTRAN analysis of the external tank (ET) substructure of the 1/8-scale space shuttle structural dynamics model.

The NASTRAN hydroelastic procedures were used to form a model of the liquid oxygen portion of the ET. Large computer storage requirements and running times were required unless these procedures were modified. Several possibilities were demonstrated including the substitution of the real for the complex eigenvalve routine and the use of the OMIT capability to reduce the number of fluid coordinates.

A NASTRAN model of the complete ET was then formed and reduced to 252 degrees of freedom using these procedures. A review of the eigenvector extracted, using the unsymmetrical inverse power method, indicated that the structural OMIT's resulted in unsatisfactory modal deflections. More basic modifications to the NASTRAN hydroelastic capability appeared necessary to generate a successful ET model.

An approach is described which, by assuming incompressibility, reduces the fluid representation to a symmetric mass matrix which can be added to the structural mass. The problem can then be solved using faster and more efficient eigenvalue routines. Using this approach the ET NASTRAN model was analyzed for three separate weight conditions. Computational efficiency was good, averaging less than 1 CPU minute for each mode.

NOTE

This report is one of a series describing analytical work at Grumman on the 1/8-Scale Structural Dynamics Model. The other reports are:

- Analytical and Experimental Investigation of a 1/8-Scale Dynamic Model of the Shuttle Orbiter:
  - Volume I, "Introduction" - NASA CR 132488 May 1974
  - Volume II, "Technical Report" - NASA CR 132489 July 1974
  - Volume IIIA, "Supporting Data" - NASA CR 132490 May 1974
  - Volume IIIB, "Supporting Data" - NASA CR 132491 May 1974
- Development of Technology For Modeling of a 1/8-Scale Dynamic Model of the Shuttle Solid Rocket Booster (SRB) - NASA CR 132492 July 1974

ABBREVIATIONS

ALARM FEER	computer programs to solve eigen-value problems of very large size
ALTER	modification of NASTRAN rigid formats
DOF	degrees of freedom
ET	External Tank
LH_2	liquid hydrogen
LO_2	liquid oxygen
MPC	multiple point constraint - NASTRAN
NASTRAN	NASA Structural Analysis System
SPC	single point constraint - NASTRAN
SRB	Solid Rocket Booster

VOLUME I TABLE OF CONTENTS

Section			Page
1	INTRODUCTION AND SUMMARY		1-1
2	DESCRIPTION OF THE 1/8-SCALE SHUTTLE EXTERNAL TANK MODEL		2-1
	2.1	Liquid Oxygen Tank	2-9
	2.2	Intertank Skirt	2-10
	2.3	Liquid Hydrogen Tank	2-13
	2.4	Aft Skirt	2-13
	2.5	Dimensions	2-13
3	NASTRAN MODEL AND RESULTS		3-1
	3.1	Investigations of Hydroelastic Analyses in NASTRAN Using a Small Hemispherical Tank Model	3-1
	3.2	Liquid Oxygen Tank Model	3-12
	3.3	Remainder of External Tank	3-34
	3.4	Complete Model of External Tank	3-40
4	NASTRAN MODIFICATIONS		4-1
	4.1	Development of the Modified NASTRAN Hydroelastic Analysis	4-1
	4.2	Analysis of the 1/8-Scale External Tank	4-2

VOLUME I LIST OF ILLUSTRATIONS

Figure		Page
2-1	Grumman Parallel - Burn Space Shuttle Design 619 Used as Reference Prototype for 1/8-Scale Model Design	2-3
2-2	Mockup of 1/8-Scale Shuttle Model Basic Configuration	2-4
2-3	Prototype External Tank	2-5
2-4	Elements of 1/8-Scale Shuttle Model External Tank	2-6
2-5	Partially Assembled External Tank	2-7
2-6	Liquid Oxygen Tank on Intertank Skirt	2-8
2-7	View of 1/8-Scale Shuttle Model Liquid Oxygen Tank	2-11
2-8	1/8-Scale Model Intertank Skirt - Developed View of One Side	2-12
2-9	View of 1/8-Scale Model Intertank Skirt	2-14
2-10	View of Partially Assembled Liquid Hydrogen Tank	2-15
2-11	View of Assembled 1/8-Scale Model Aft Skirt Attached to Liquid Hydrogen Tank	2-16
3-1	NASTRAN Model of Small Hemispherical Tank	3-3
3-2	First Mode of Small Hemispherical Tank	3-4
3-3	Second Mode of Small Hemispherical Tank	3-5
3-4	Third Mode of Small Hemispherical Tank	3-6
3-5	Fourth Mode of Small Hemispherical Tank	3-7
3-6	Fifth Mode of Small Hemispherical Tank	3-8
3-7	NASTRAN Model of Liquid Oxygen Tank for 1/8-Scale Shuttle Model	3-13
3-8	Original LO_2 Tank Dome Model	3-14
3-9	1/8-Scale Model LO_2 Tank Mode Shape at 22.9 Hz	3-18
3-10	1/8-Scale Model LO_2 Tank Mode Shape at 75.2 Hz	3-19
3-11	1/8-Scale Model LO_2 Tank Mode Shape at 91.5 Hz	3-20
3-12	1/8-Scale Model LO_2 Tank Mode Shape at 115.2 Hz	3-21
3-13	1/8-Scale Model LO_2 Tank Mode Shape at 129.3 Hz	3-22
3-14	1/8-Scale Model LO_2 Tank Mode Shape at 19.2 Hz	3-23
3-15	1/8-Scale Model LO_2 Tank Mode Shape at 60.5 Hz	3-24
3-16	1/8-Scale Model LO_2 Tank Mode Shape at 110.0 Hz	3-25
3-17	1/8-Scale Model LO_2 Tank Mode Shape at 134.3 Hz	3-26

VOLUME I LIST OF ILLUSTRATIONS (Cont)

Figure		Page
3-18	Original LO_2 Tank Model Under Static Pressure	3-27
3-19	Initially Revised LO_2 Tank Dome	3-28
3-20	Initially Revised LO_2 Tank Under Static Pressure	3-29
3-21	Refined 9 Row LO_2 Tank Dome Under Static Pressure	3-30
3-22	Tank with Revised 7 Row Dome Under Static Pressure	3-31
3-23	Revised 7 Row Tank Dome Under Static Pressure	3-32
3-24	1/8-Scale Model LO_2 Tank Mode Shape at 23.1 Hz (Dome Revised)	3-33
3-25	NASTRAN Model of External Tank Frames for 1/8-Scale Shuttle Model	3-36
3-26	NASTRAN Model of External Tank Shell Structure for 1/8-Scale Shuttle Model	3-37
3-27	1/8-Scale Model Liquid Hydrogen Tank, First Symmetric Mode - 139.25 Hz (Structure Only)	3-38
3-28	1/8-Scale Model Liquid Hydrogen Tank, Second Symmetric Mode - 155.58 Hz (Structure Only)	3-39
3-29	1/8-Scale Model External Tank NASTRAN Model	3-42
3-30	1/8-Scale Model External Tank - Comparison of Deflections of Light - LH_2 Tank Ring at Station X 188.75	3-45
3-31	Comparison of Deflections on LO_2 Tank	3-46
4-1	External Tank With Fluid, Liftoff Configuration	4-7
4-2	External Tank With Fluid, Liftoff Configuration	4-8
4-3	External Tank With Fluid, Liftoff Configuration	4-9
4-4	External Tank With Fluid, Liftoff Configuration	4-10
4-5	External Tank With Fluid, Liftoff Configuration	4-11
4-6	External Tank With Fluid, Liftoff Configuration	4-12
4-7	External Tank With Fluid, Liftoff Configuration	4-13
4-8	External Tank With Fluid, Liftoff Configuration	4-14
4-9	External Tank With Fluid, Liftoff Configuration	4-15
4-10	External Tank With Fluid, Liftoff Configuration	4-16
4-11	External Tank With Fluid, Liftoff Configuration	4-17
4-12	External Tank With Fluid, Liftoff Configuration	4-18
4-13	External Tank With Fluid, Liftoff Configuration	4-19

VOLUME I LIST OF ILLUSTRATIONS (Cont)

Figure		Page
4-14	External Tank With Fluid, Liftoff Configuration	4-20
4-15	External Tank With Fluid, Liftoff Configuration	4-21
4-16	External Tank With Fluid, Liftoff Configuration	4-22
4-17	External Tank With Fluid, Liftoff Configuration	4-23
4-18	External Tank With Fluid, Liftoff Configuration	4-24
4-19	External Tank With Fluid, Liftoff Configuration	4-25
4-20	External Tank With Fluid, Liftoff Configuration	4-26
4-21	External Tank With Fluid, Liftoff Configuration	4-27
4-22	External Tank With Fluid, Liftoff Configuration	4-28
4-23	External Tank With Fluid, Liftoff Configuration	4-29
4-24	External Tank With Fluid, Post Max Q Configuration	4-30
4-25	External Tank With Fluid, Post Max Q Configuration	4-31
4-26	External Tank With Fluid, Post Max Q Configuration	4-32
4-27	External Tank With Fluid, Post Max Q Configuration	4-33
4-28	External Tank With Fluid, Post Max Q Configuration	4-34
4-29	External Tank With Fluid, Post Max Q Configuration	4-35
4-30	External Tank With Fluid, Post Max Q Configuration	4-36
4-31	External Tank With Fluid, Post Max Q Configuration	4-37
4-32	External Tank With Fluid, Post Max Q Configuration	4-38
4-33	External Tank With Fluid, Post Max Q Configuration	4-39
4-34	External Tank With Fluid, Post Max Q Configuration	4-40
4-35	External Tank With Fluid, Post Max Q Configuration	4-41
4-36	External Tank With Fluid, Post Max Q Configuration	4-42
4-37	External Tank With Fluid, Post Max Q Configuration	4-43
4-38	External Tank With Fluid, Post Max Q Configuration	4-44
4-39	External Tank With Fluid, Post Max Q Configuration	4-45
4-40	External Tank With Fluid, Post Max Q Configuration	4-46
4-41	External Tank With Fluid, Post Max Q Configuration	4-47
4-42	External Tank With Fluid, Post Max Q Configuration	4-48
4-43	External Tank With Fluid, Post Max Q Configuration	4-49
4-44	External Tank With Fluid, Post Max Q Configuration	4-50

VOLUME I LIST OF ILLUSTRATIONS (Cont)

Figure		Page
4-45	External Tank With Fluid, Post Max Q Configuration	4-51
4-46	External Tank With Fluid, Post Max Q Configuration	4-52
4-47	External Tank With Fluid, Post Max Q Configuration	4-53
4-48	External Tank With Fluid, Post Max Q Configuration	4-54
4-49	External Tank With Fluid, Post Max Q Configuration	4-55
4-50	External Tank With Fluid, Post Max Q Configuration	4-56
4-51	External Tank Without Fluid	4-57
4-52	External Tank Without Fluid	4-58
4-53	External Tank Without Fluid	4-59
4-54	External Tank Without Fluid	4-60
4-55	External Tank Without Fluid	4-61
4-56	External Tank Without Fluid	4-62
4-57	External Tank Without Fluid	4-63
4-58	External Tank Without Fluid	4-64
4-59	External Tank Without Fluid	4-65
4-60	External Tank Without Fluid	4-66
4-61	External Tank Without Fluid	4-67
4-62	External Tank Without Fluid	4-68
4-63	External Tank Without Fluid	4-69
4-64	External Tank Without Fluid	4-70
4-65	External Tank Without Fluid	4-71
4-66	External Tank Without Fluid	4-72
4-67	External Tank Without Fluid	4-73
4-68	External Tank Without Fluid	4-74
4-69	External Tank Without Fluid	4-75
4-70	External Tank Without Fluid	4-76
4-71	External Tank Without Fluid	4-77
4-72	External Tank Without Fluid	4-78
4-73	Post Max Q External Tank 1st Bending Mode (Mode 6)	4-79
4-74	Post Max Q External Tank 1st Axial Mode (Mode 7)	4-80
4-75	NASTRAN Model of External Tank Structure	4-81
4-76	NASTRAN Model of External Tank Structure	4-82
4-77	NASTRAN Model of External Tank Structure	4-83

VOLUME I LIST OF TABLES

No.		Page
2-1	Pertinent Scaling Relationships for the 1/8-Scale Model.	2-9
2-2	Drawing Descriptions of 1/8-Scale Model	2-12
3-1	Comparison of Eigenvalues for Various Modifications	3-10
3-2	Comparison of Shapes of First Hydroelastic Mode for Various Model Modifications	3-11
3-3	Summary of Computer Runs in Rigid Format 7 to Calculate Liquid Oxygen Tank Hydroelastic Modes	3-17
3-4	Comparison of Computer Times for NASTRAN External Tank Hydroelastic Analysis	3-43
3-5	Comparison of Tank Model Pressures	3-47
4-1	1/8-Scale External Tank (ET) Hydroelastic Mode Summary (at Liftoff)	4-4
4-2	1/8-Scale External Tank (ET) Hydroelastic Mode Summary (Post Max Q)	4-5
4-3	Empty 1/8-Scale External Tank (ET) Mode Summary	4-6

VOLUME II TABLE OF CONTENTS

Appendix		Page
A	STARS-2 Vibration Analysis of 1/8-Scale Shuttle LH_2 Tank . . .	A-1
B1	Modification of the NASTRAN Hydroelastic Analysis	B1-1
B2	Hydroelastic Analysis - Progress Report	B2-1
B3	Elementary Verification Problems.	B3-1
B4	Modal Pressure Gain	B4-1
C	NASTRAN Input Data.	C-1

Section 1
INTRODUCTION AND SUMMARY

DEVELOPMENT OF TECHNOLOGY FOR FLUID-STRUCTURE INTERACTION MODELING OF A 1/8-SCALE DYNAMIC MODEL OF THE SHUTTLE EXTERNAL TANK (ET)

By M. Bernstein, R. Coppolino, J. Zalesak, and P.W. Mason

GRUMMAN AEROSPACE CORPORATION
Bethpage, New York 11714

1 - INTRODUCTION AND SUMMARY

This report discusses work performed by Grumman under Task Order 13 of Master Agreement Contract NAS1-10635 with the Structural Mechanics Branch, Structures and Dynamics Division, NASA/Langley Research Center, Hampton, Virginia.

The objectives of this task were:

- Formulation of an analytical NASTRAN representation of the significant dynamic characteristics of the 1/8-scale model of the shuttle external tank as specified by drawings and design details developed under NAS1-10636-11
- Construction of the external tank model
- Participation in a comparison of experimentally determined structural dynamic characteristics with results of the analysis, and proposing modifications in analysis technology as required.

The NASTRAN hydroelastic analysis capability was utilized to formulate a model of the liquid oxygen tank and a separate model of the remainder of the external tank. Early experience with this liquid oxygen tank model demonstrated the long computer running times and large core required for a moderately complete representation. Methods for reducing computation costs were evaluated in a small hemispherical tank model. It was determined that both the use of the OMIT capability to reduce the number of fluid coordinates, and modifications to avoid the use of the complex eigenvalue routine were helpful. The liquid oxygen tank lower dome representation was

improved by a series of modifications evaluated using static pressure loading in Rigid Format 1. The significant liquid oxygen tank modes for the zeroth and first harmonic were calculated for symmetric boundary conditions.

The intertank skirts and liquid hydrogen tank structure was modeled initially in Rigid Format 3. When weight representing the liquid hydrogen was added as non-structural mass, unusual shell deformations resulted and the model was not considered satisfactory. Therefore, a hydroelastic representation of the liquid hydrogen was added and the problem formulated in Rigid Format 7. Difficulties with the NASTRAN System are described on page 183 of Reference 5-1.

The complete model consisting of the two tanks and the intermediate structure was submitted for modal analysis in Rigid Format 7 at Langley. However, the problem was too large to run successfully. Simultaneously, a reduced version of the model obtained by using the OMIT feature of NASTRAN to decrease the number of structural coordinates and to omit all the interior fluid coordinates was submitted for computation at Grumman. Only the zeroth fluid harmonic was permitted. One mode at 46.5 Hz was obtained, characterized primarily by longitudinal motion. A review of the modal deformation pattern indicated anomalous behavior associated with the use of OMIT's of fluid loaded structure.

Development work on the external tank model was suspended at this point to devote all available effort toward reconciling the discrepancy between measured and calculated orbiter modes (Task 12 of NAS1-10635). It was apparent that additional modifications in NASTRAN were required to alleviate the large computation time requirements for the external tank.

Although not funded under this task, an approach to modifying the NASTRAN hydroelastic analysis was developed by R. Coppolino and is noted herein. On the basis of assumed fluid incompressibility, the fluid representation can be reduced to a symmetric mass matrix which is added directly to the structural mass matrix. The assembled hydroelastic problem can then be solved in Rigid Format 3 using the faster eigenvalue routines. In addition, a harmonic reduction scheme which expresses finite element structural deformation in terms of circumferential harmonics has been introduced for tanks of revolution. This technique has been demonstrated to be more accurate and efficient than conventional Guyan reduction for structures of revolution.

Harmonic reduction is ideal for the NASTRAN hydroelastic analysis. Circumferential displacement harmonics automatically enforces strict compatability with the fluid which is developed in terms of the pressure harmonics. These developments, described in Appendix B, are expected to materially enhance the use of the NASTRAN hydroelastic analysis for large problems.

Section 2
DESCRIPTION OF THE 1/8-SCALE SHUTTLE EXTERNAL TANK MODEL

2 - DESCRIPTION OF THE 1/8-SCALE SHUTTLE MODEL EXTERNAL TANK

The 1/8-scale shuttle dynamic model is based on Grumman's parallel-burn Space Shuttle Design 619 shown schematically in Fig. 2-1. A mockup of the 1/8-scale Shuttle model basic configuration is shown in Fig. 2-2. Fig. 2-3 shows a detailed structural arrangement of the prototype External Tank (ET). In simplifying the design, a major objective was to keep the model fabrication cost within target while retaining as many of the significant structural dynamic characteristics as possible. For the allotted funds it was impossible and also technically unnecessary to consider an exact or "replica" model at the small scale necessary for testing in the existing NASA/Langley facilities. Therefore, only the general characteristics of the major external tank elements were simulated without attempting to model local details.

The external tank consists of four elements which can be physically separated as schematically shown in Fig. 2-4. The 1/8-scale external tank is partially assembled in Fig. 2-5 between supporting SRB components. The forward element of the external tank is the liquid oxygen tank which is assembled into the intertank skirt in Fig. 2-6. The intertank skirt provides the two support points for the model suspension system, and the forward ET/SRB interstage connections. A short aft skirt furnishing the aft supports for attaching the solid rocket boosters forms the last element. The structure is described in NASA CR 112205 (Ref. 5-2), and previously in Ref. 5-1. However, a relatively complete description is included within for ready reference.

The scaling relationships that must exist between the model and the prototype are indicated in Table 2-1. These follow directly from a dimensional analysis of the various parameters that influence the dynamic behavior of the structure, and from the choice of the model material. Extrapolating prototype behavior from model test data is accomplished by using these scaling relationships directly. It should be noted that because of design expediency, some of the scaling rules have been compromised. For example, the local skin stiffness on the model is less than the required scaled value of the prototype for preventing buckling. Some liberty was also taken in modeling the stiffness characteristics since some lumping was necessary

in order to avoid the large expense of exact scaling of very small dimensions. Thus, stiffeners have been lumped to some extent but not eliminated completely. If they were completely eliminated, since the local stiffness of the skins was not duplicated, premature buckling would occur.

While accurate modeling of the prototype was desirable for extrapolating basic Shuttle dynamic characteristics, another prime object of the study was the NASTRAN dynamic analysis and its correlation with model test data. A complete static and dynamic analysis was made using NASTRAN with the structure modeled to a degree of refinement considered sufficient for preliminary design purposes. Thus the need for direct scaling of the prototype design to obtain an exact model in every detail was not considered crucial. It should also be pointed out that the Shuttle design was still in a state of flux at the beginning of this study, hence any attempt to model the then current vehicle exactly would not be overly beneficial to the Shuttle Project.

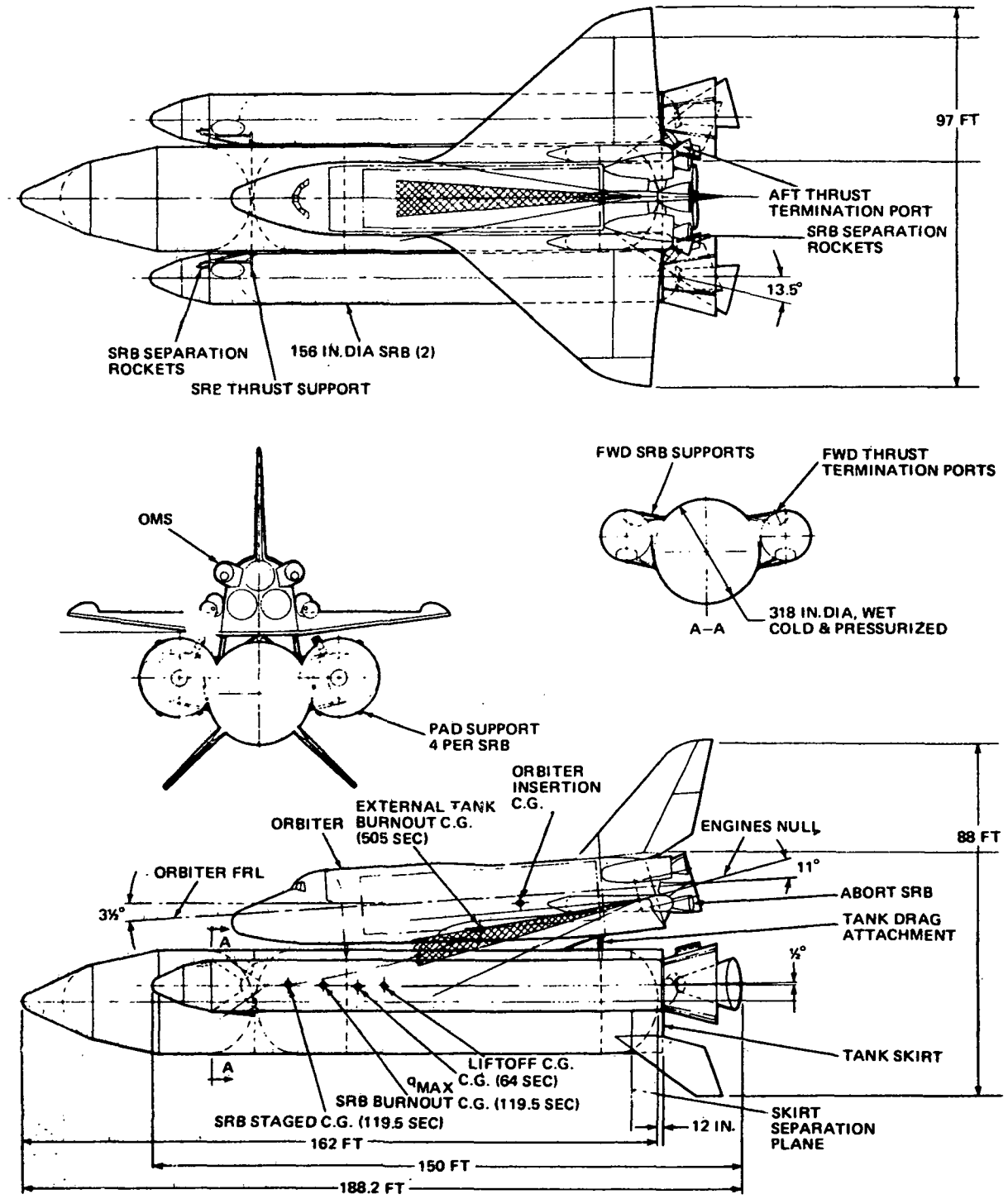

T14-1
T13-1

Fig. 2-1. Grumman Parallel Burn Space Shuttle Design 619 Used as Reference Prototype for 1/8-Scale Model Design

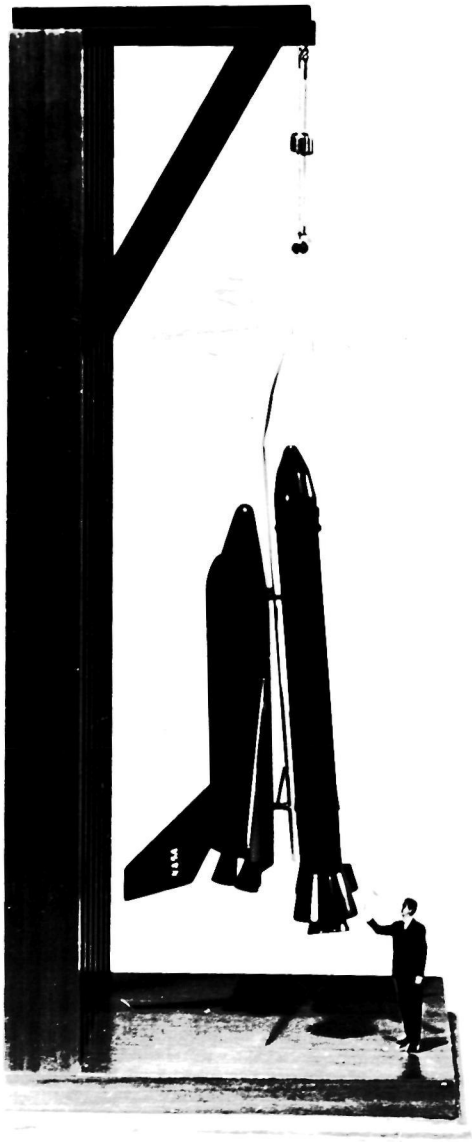

S-3
T13-2

Fig. 2-2 Mockup of 1/8-Scale Shuttle Model Basic Configuration

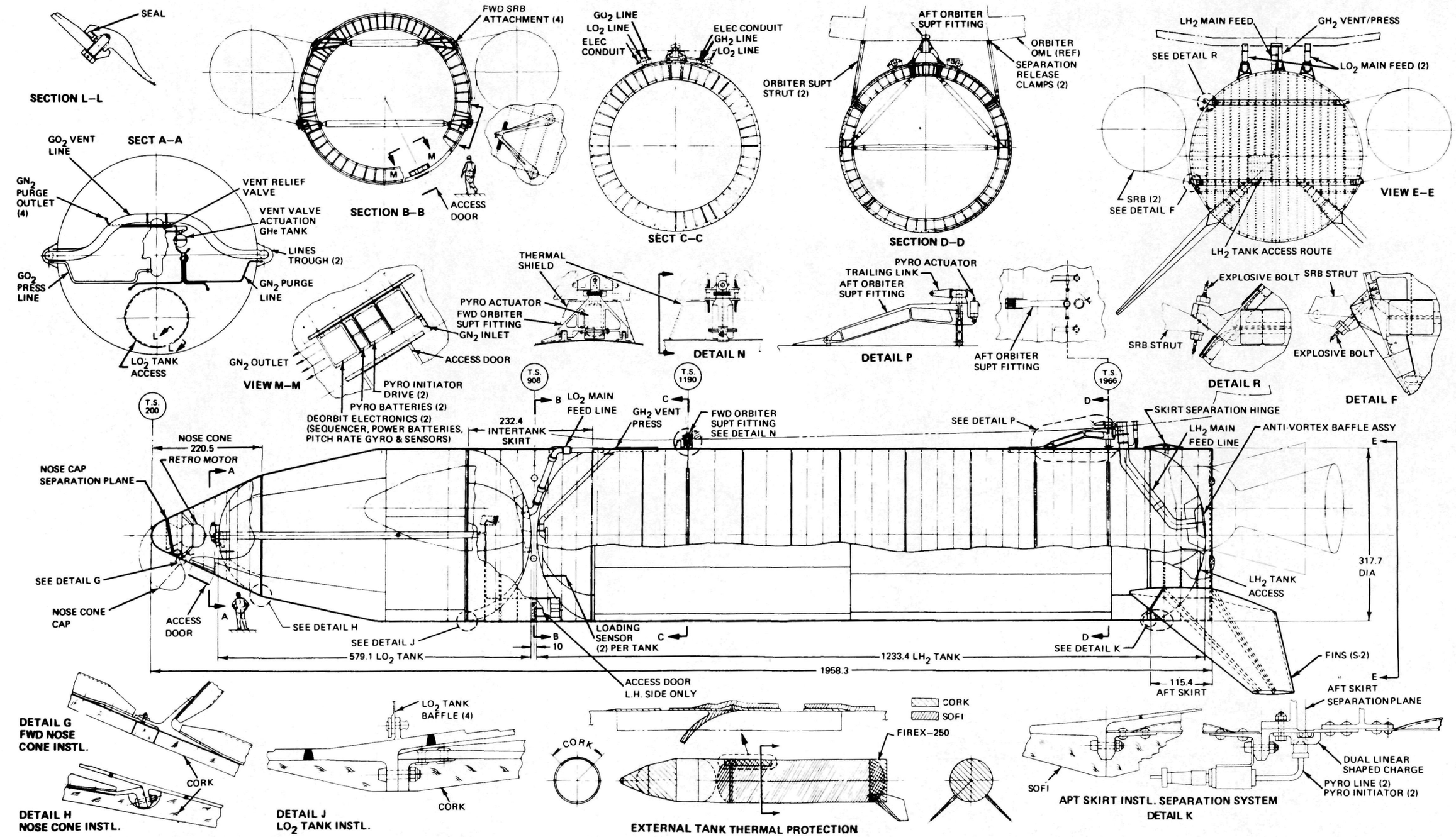

3-608
T13-3

Fig. 2-3 Prototype External Tank

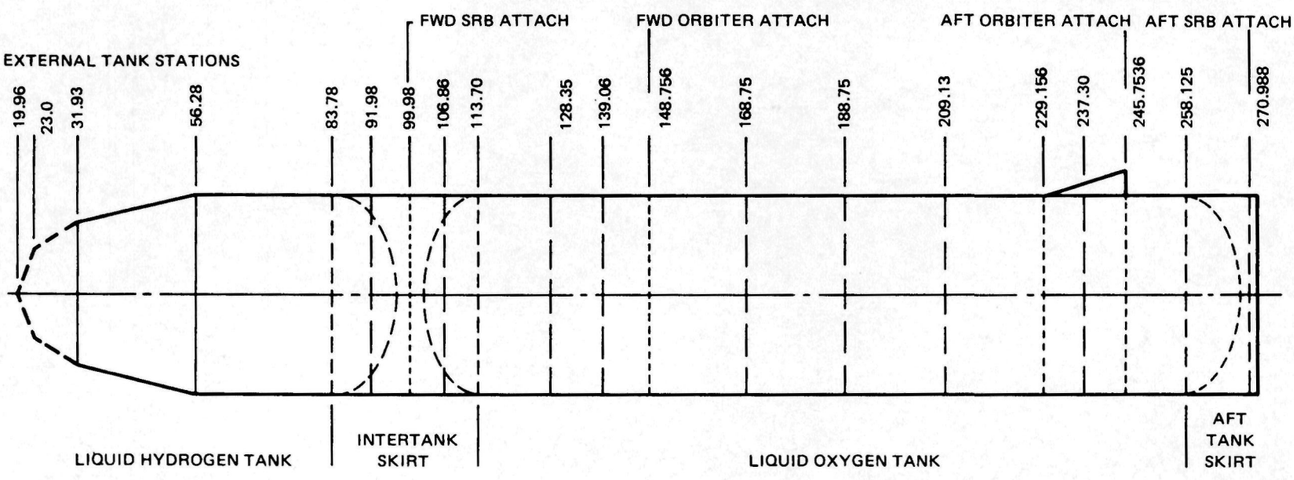

NOTE: DASHED VERTICAL LINES INDICATE FRAME LOCATIONS

T13-4

Fig. 2-4 Elements of 1/8-Scale Shuttle Model External Tank

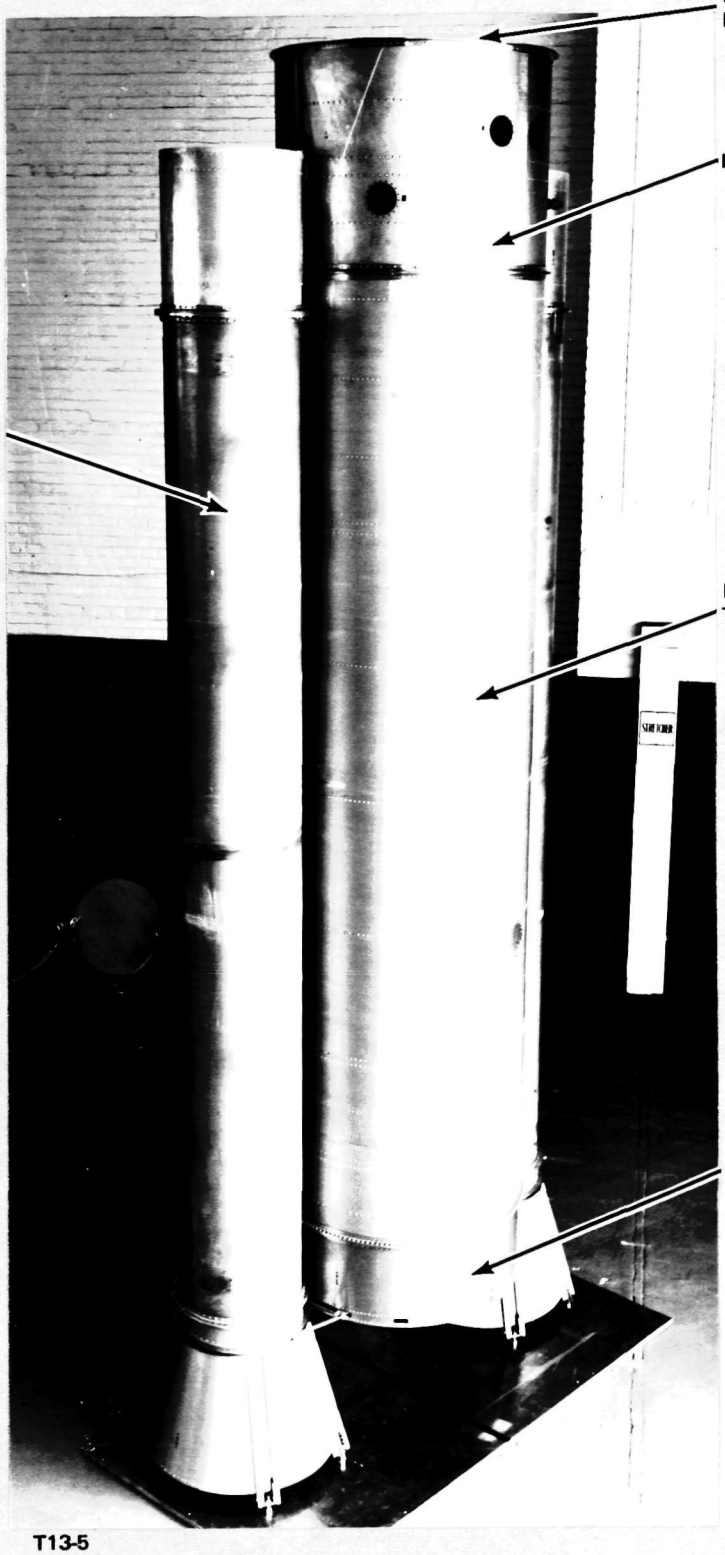

T13-5

Fig. 2-5 Partially Assembled External Tank

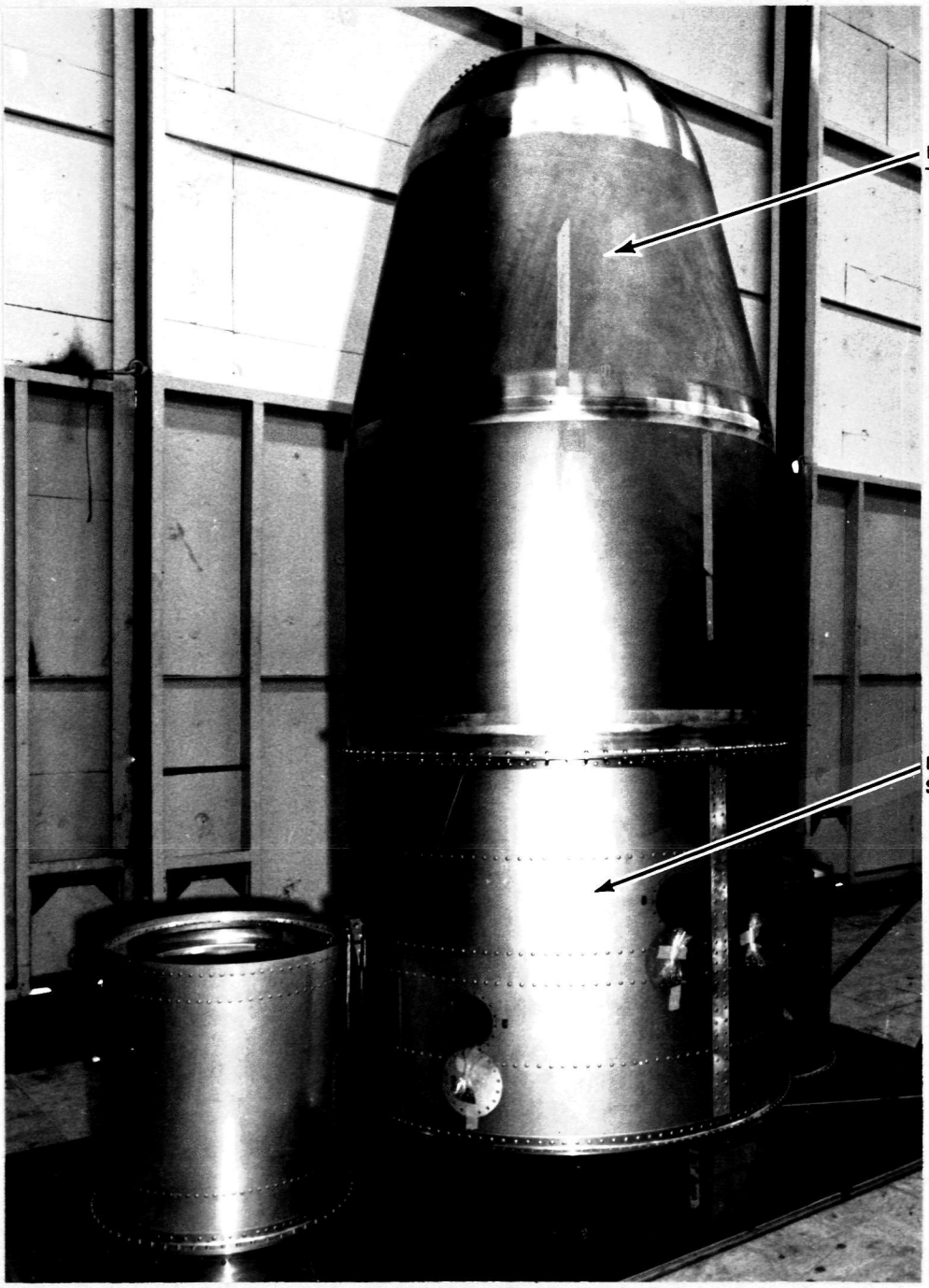

T13-6

Fig. 2-6 Liquid Oxygen Tank on Intertank Skirt

Table 2-1 Pertinent Scaling Relationships for the 1/8-Scale Model

Physical Quantity	Magnitude[a]	Physical Quantity	Magnitude[a]
Length and displacements	$\frac{L_m}{L_p} = \frac{1}{8}$	Stress ($\sigma = E\epsilon$)	$\sigma_m = \sigma_p$
Poisson's ratio, ν	$\nu_m = \nu_p$	Force ($F = \sigma A$)	$\frac{F_m}{F_p} = \left(\frac{1}{8}\right)^2 = \frac{1}{64}$
Mass density	$\frac{\rho_m}{\rho_p} = 1$	Longitudinal stiffness, EA	$\frac{(EA)_m}{(EA)_p} = \left(\frac{1}{8}\right)^2 = 1/64$
Modulus of elasticity, E	$\frac{E_m}{E_p} = 1$	Bending stiffness, E1	$\frac{(EI)_m}{(EI)_p} = \left(\frac{1}{8}\right)^4 = 1/4096$
	$\epsilon_m = \epsilon_p$	Torsional stiffness, GJ	$\frac{(GJ)_m}{(GJ)_p} = \left(\frac{1}{8}\right)^4 = 1/4096$
Area	$\frac{A_m}{A_p} = \left(\frac{1}{8}\right)^2 = \frac{1}{64}$	Weight ($W = \rho V$)	$\frac{W_m}{W_p} = \left(\frac{1}{8}\right)^3 = \frac{1}{512}$
Area moment of inertia, I	$\frac{I_m}{I_p} = \left(\frac{1}{8}\right)^4 = \frac{1}{4096}$	Acceleration ($F = ma$)	$\frac{a_m}{a_p} = \frac{8}{1}$
Mass moment of inertia, I'	$\frac{I'_m}{I'_p} = \left(\frac{1}{8}\right)^5 = \frac{1}{32,768}$	Natural Frequency, ω	$\frac{\omega_m}{\omega_p} = \frac{8}{1}$

TT-1

T13-1(T)

[a]Subscript "m" refers to the model; subscript "p" refers to prototype.

2.1 LIQUID OXYGEN TANK

The 1/8-scale model llquid oxygen tank (Fig. 2-7 and Drawing AD 383-505 listed in Table 2-2) is a monocoque welded structure (2219 aluminum) consisting of:

- A quasi-elliptical aft dome
- A cylindrical portion
- A conical portion
- A removable spherical cap.

The dome which extends from X Station 83.78 is formed from two tangential spherical segments in order to approximate an ellipse. The central 77° is formed to a 23.6 in. radius. The outer portion, to the full tank diameter of 39.75 in. is formed from a 18.35 in. radius centered 2.2 in. away from the tank axis. The central 12° of the dome is 0.040 in. thick to allow for installation of a pressure transducer and for a drain/fill fitting. The remainder of the dome is 0.016 in. thick. The dome is welded to the lower side of a machined ring and the cylindrical portion of the tank is welded to the upper side. The central portion of the ring is a flange drilled to accept the bolts which fasten to the intertank skirt. Above the ring the tank is cylindrical to X Station 56.28 and then is conical to X Station 31.93 where the radius has been reduced from 19.5 in. to 14 in. A sharper conical taper to X Station 23 reduces this to an open top of 9 in. radius. The sidewalls of the tank are of constant thickness, 0.020 in. A spherical segment .025 in. thick covers the top of the tank. The cover segment has a cutout, and a removable cap for access to the interior of the tank.

2.2 INTERTANK SKIRT

The intertank skirt (2024 Aluminum) extends from X Station 83.78 to 113.70. The intertank skirt is designed with two SRB/ET interstage connections that are representative of the proposed Rockwell International Shuttle configuration of November 6, 1972. This was a modification to the original Grumman design for the 1/8-scale shuttle model. The intertank structure is designed to provide attachment points for the model suspension system used during simulated free-body testing. The shell is milled to three thickness (t) as illustrated in Figure 2-8 (also refer to Fig. 2-6). The heaviest regions are close to the solid rocket booster interstage attachments and the model suspension lugs where the thickness is 0.1 in. A partial longeron which transmits load from the skin to the model suspension lug and interstage connection pin reenforces this region. The shell thickness reduces to 0.055 in. and then to 0.025 in. away from this region as indicated on the figure. Three ring frames are riveted to the shell. The heaviest frame consisting of back-to-back channels is located at the SRB/ET interstage (X Station 99.98). This ring frame also has a lateral strut extending between the interstage points to distribute the forward SRB loads. The other two are single rings and are located at approximately the quarter points along the length. These were added to minimize buckling. Riveted construction is used throughout. The intertank skirt is shown attached to the liquid hydrogen tank in Fig. 2-9.

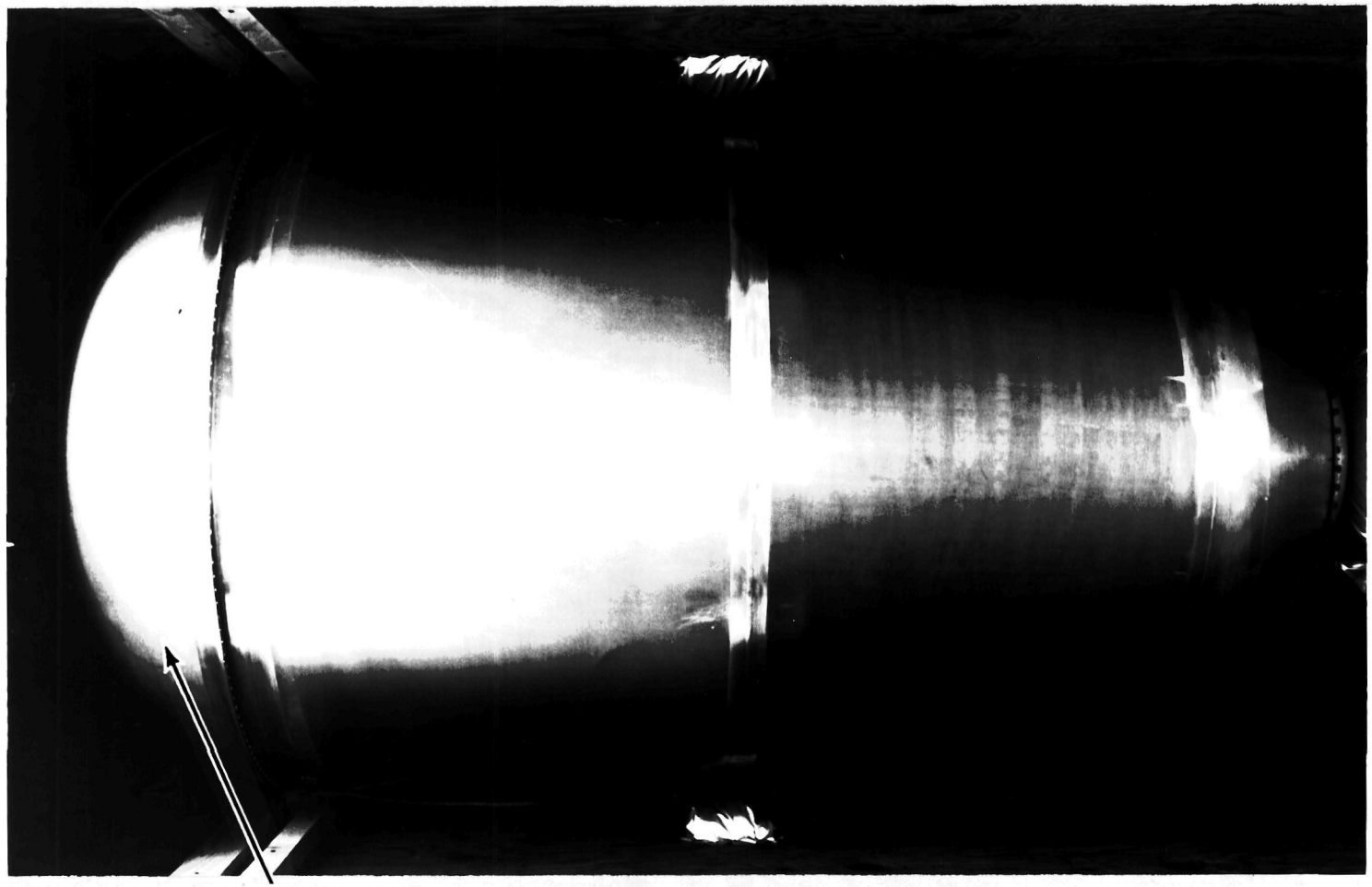

T13-7

Fig. 2-7 View of 1/8-Scale Shuttle Model Liquid Oxygen Tank

Table 2-2 Drawing Descriptions of 1/8-Scale Model

Drawing Number	Description
AD383-502 A	External Tank Assembly
-505 N/C	LO_2 Tank Assembly (2 sheets)
-506 N/C	Intertank Skirt Assembly
-507 A	LH_2 Tank Assembly (2 sheets)
-508 N/C	Aft Skirt Assembly
-514 N/C	LH_2 Tank Fitting Installation
-515 A	Rings for External Tank
-516 A	Intertank Skirt Frame Assembly
-517 N/C	LH_2 Tank Frame Assembly
-518 N/C	External Tank Aft Skirt Frame Assembly
-541 N/C	Intertank Skirt Assembly (NAR Configuration)
-542 N/C	Frame Installation Intertank Skirt (NAR Configuration)
-543 N/C	SRM Forward Skirt Assembly (NAR Configuration)
-544 N/C	Thrust Fitting-Intertank Skirt (NAR Configuration)
-545 N/C	Thrust Pin (NAR Configuration)
-546	Comparison NAR Shuttle Configuration and 1/8-Scale Dynamic Model
-568	ET and SRB Measurements

NOTE:
1. Copies of each of the above drawings have been submitted separately to NASA/Langley and to Rockwell International.
2. These drawings are available from the Vibration Section, Structures and Dynamics Division, NASA/Langley Research Center, Hampton, Virginia 23365.

T14-1(T)
T13-2(T)

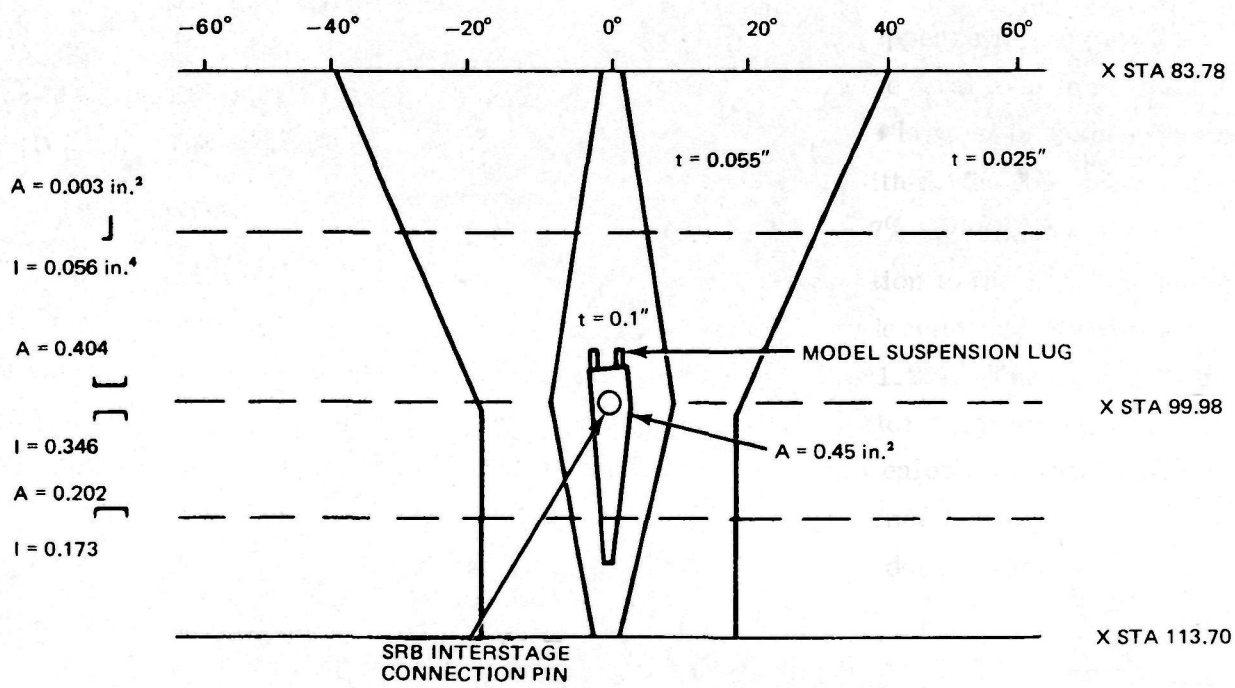

T13-8

Fig. 2-8 1/8-Scale Model Intertank Skirt - Developed View of One Side

2.3 LIQUID HYDROGEN TANK

The liquid hydrogen tank is a ring frame stiffened cylinder (2024 Aluminum) of riveted construction extending from X Station 113.7 to X Station 258.125, shown schematically in Fig. 2-4. Figure 2-9 is a photograph of the partially fabricated tank showing the internal members. Three major ring frames provide support for the orbiter attachment while six others are inserted to minimize buckling. The cylindrical portion of the skin is milled to be 0.025 in. on the side adjacent to the orbiter and 0.016 in. at other locations. The front and back domes are 0.020 in. and are the same dimensions as that on the liquid oxygen tank. The lower dome is attached with removable fasteners for access to the interior. There are three major ring frames formed from back-to-back channels while the others are single angles. The aft major frames of X Station 229.156 and 245.536 are reenforced by internal struts in a triangular pattern to distribute the orbiter load. These struts are also formed from channel sections fastened together. Fittings for attaching to the orbiter including a drag support and two struts in the Z direction are included as part of the tank (Fig. 2-10).

2.4 AFT EXTERNAL TANK SKIRT

The aft skirt is a simple riveted cylindrical extension (2024 Aluminum) of the liquid hydrogen tank. There is an interior stiffener frame (single angle) and an aft frame (back-to-back channels) which contains two lateral struts for distributing the aft SRB loads. The aft skirt attached to the liquid hydrogen tank is shown in Fig. 2-11.

2.5 DIMENSIONS

Numerical dimensions of all parts of the external tank may be determined from the drawings listed in Table 2-2. During the manufacture of the model, dimensions of various parts were measured. These are listed on a three sheet drawing, "ET and SRM Measurements". All drawings have been submitted to the NASA Langley Research Center along with the NASTRAN model.

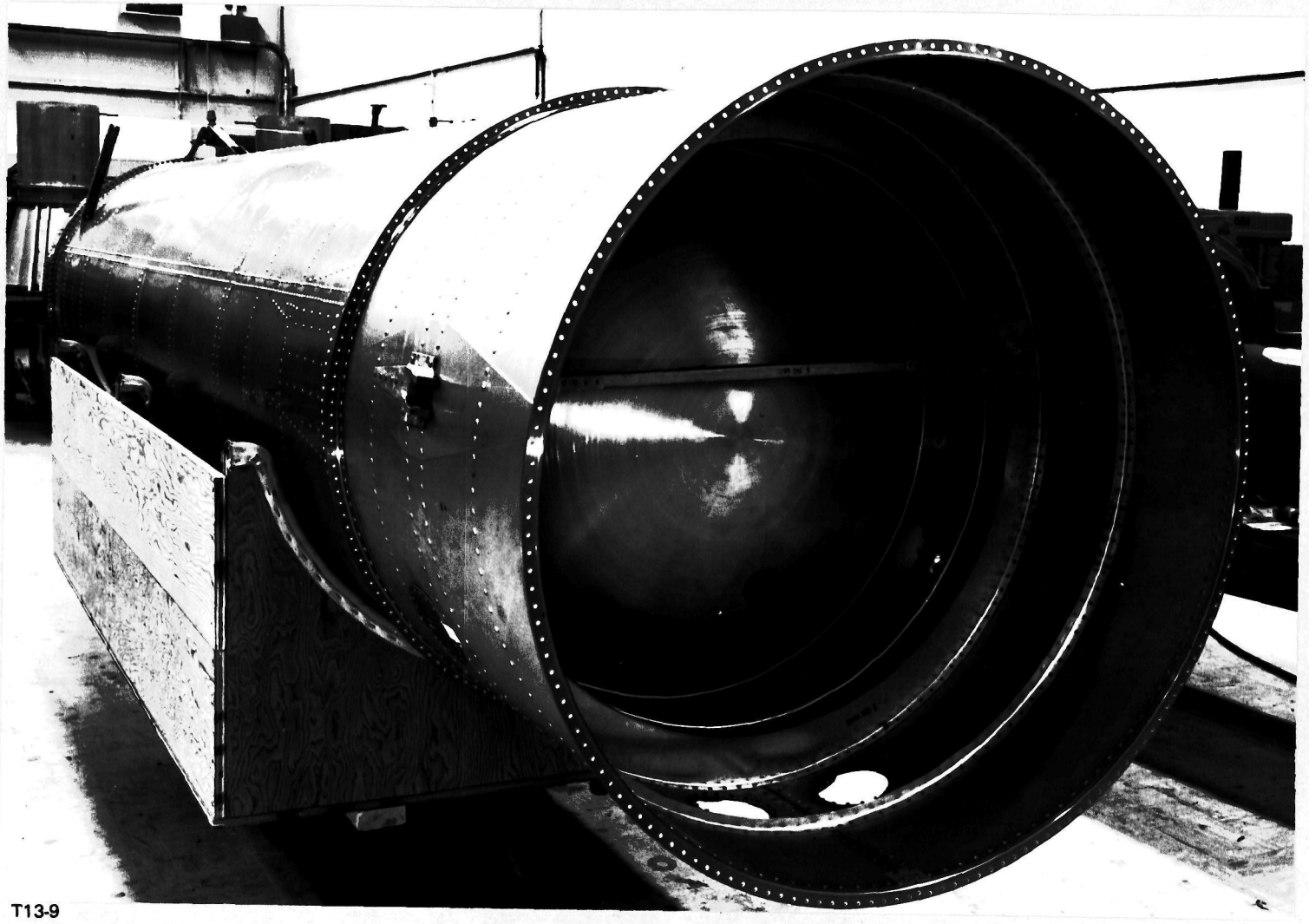

Fig. 2-9 View of 1/8-Scale Model Intertank Skirt

T13-10

Fig. 2-10 View of Partially Assembled Liquid Hydrogen Tank

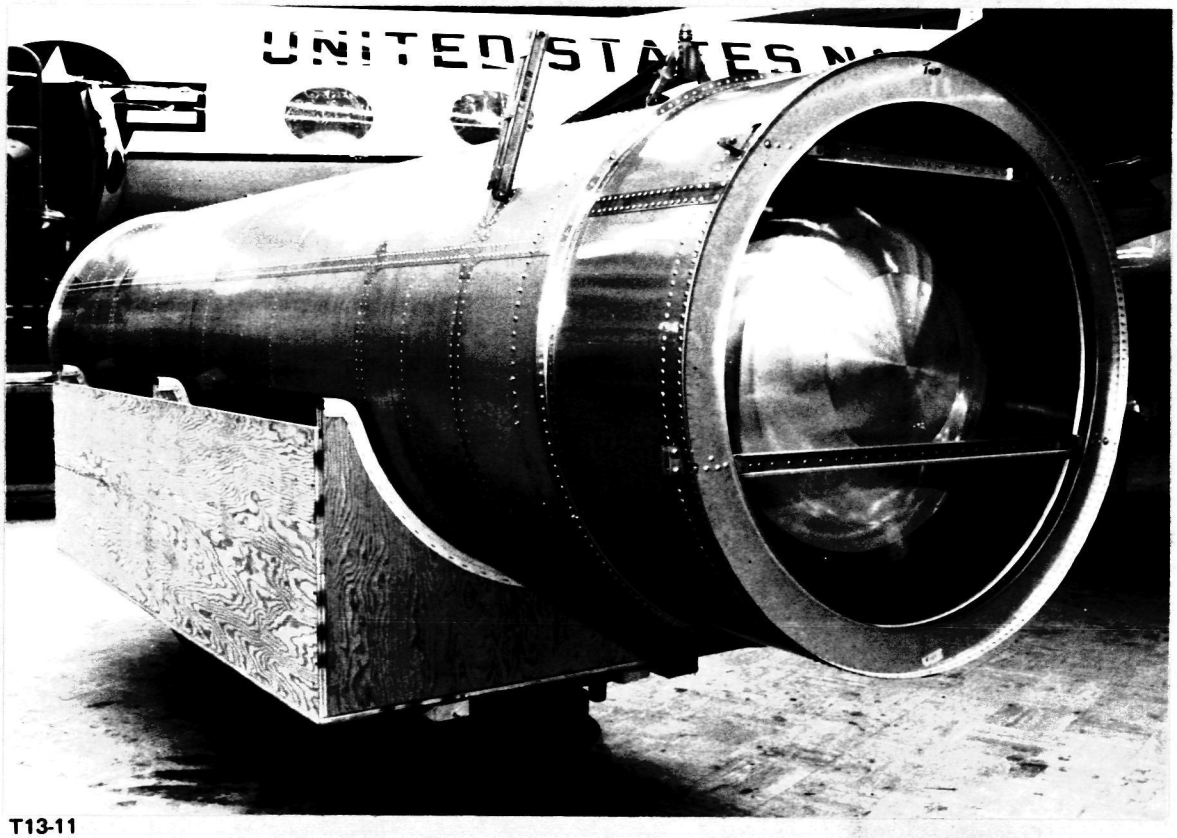

T13-11

Fig. 2-11 View of Assembled 1/8-Scale Model Aft Skirt Attached to Liquid Hydrogen Tank

Section 3
NASTRAN MODEL AND RESULTS

3 - NASTRAN MODEL AND RESULTS

3.1 INVESTIGATIONS OF HYDROELASTIC ANALYSIS IN NASTRAN USING A SMALL HEMISPHERICAL TANK MODEL

In developing and conducting the hydroelastic analyses of the 1/8-scale model tanks, a series of exploratory calculations were made using NASTRAN models of small hemispherical tanks. One of those analyzed had a 10 in. radius and walls of 0.022 in. aluminum for the upper 45 degrees, and 0.028 in. aluminum for the lower 90 degree segment including the apex. Boundary conditions in the analysis consisted of fixing five of the coordinates at the equator and permitting the shell to rotate about the tangential direction. These tank dimensions were selected to approximate one of a series tested at SWRI and reported by D. D. Kana and A. Nagey in May 1971 under contract NAS8-30167. The NASTRAN model (Fig. 3-1), consisted of 19 fluid rings and 22 grid points to represent a 45 DOF segment of the tank. QUAD2 bending and membrane quadrilateral elements were used for the shell and TRIA2 bending and membrane triangular elements for the apex. The Analyses Displacement Set consisted of 114 DOF including 38 for the fluid (half for the 0th and half for the 4th cosine harmonic). The 0th harmonic was selected to agree with the test data and technique. Testing was limited to vibration of the entire tank parallel to the axis through the apex of the hemisphere. The fourth harmonic was added because it was the next highest compatible with the symmetric boundary conditions, and it was advisable to include at least two harmonics in this check problem. Only symmetric boundary conditions were run. Some of the calculated mode shapes for this model are shown in Fig. 3-2 through 3-6. The deflected shapes for the 0th harmonic show reasonable agreement with reported experimental data but the frequencies are 10 to 25% higher as shown in the table on the following page.

Comparison of Nastran Model and Experiment

No. of Nodal Circles	SWRI Measured Frequency Hz	NASTRAN Calculated Frequency Hz	Increase
2 (Near Boundary)	750	940	1.25
2	1310	1335	1.10
3	1510	1714	1.13
4	1760	2074	1.18

T13-1(T)

The disagreement could be due to the assumptions concerning the thickness of the tank or the boundary conditions at the support. The major purpose of this small model was to investigate the readiness of NASTRAN hydroelastic analyses as required to support the 1/8-scale model. The small size and low computation costs were a decided advantage. The agreement between calculated and measured mode shapes and the approximate agreement in frequencies was sufficient to proceed in evaluating various computational possibilities as discussed in the following paragraphs.

The basic difficulty in assembling a suitable model was the high core and long computation time required in the direct application of the NASTRAN hydroelastic analyses to the 1/8-scale liquid oxygen tank. It was also obvious that the combined liquid oxygen and hydrogen tanks model would be too large, therefore, reductions in both the computer core requirements and running time were mandatory. Mr. R. E. Gillian of NSMO at NASA Langley suggested reducing the required core size by setting up the eigenvalue problem as an unsymmetric real matrix using the READ module from Rigid Format 3 in place of the CEAD module required in Rigid Format 7. This step could halve the core requirement for the eigenvalue portion of the analysis. Dr. R. Coppolino of Grumman suggested considering the fluid incompressible (Appendix B) and employment of structural harmonics as well as fluid harmonics.

NOTE: (1) 45° SEGMENT USED (SEE SKETCH ON TABLE 3-2).
(2) UNDERLINED NUMBERS ARE FLUID RINGS, REMAINDER ARE STRUCTURAL GRID POINTS.

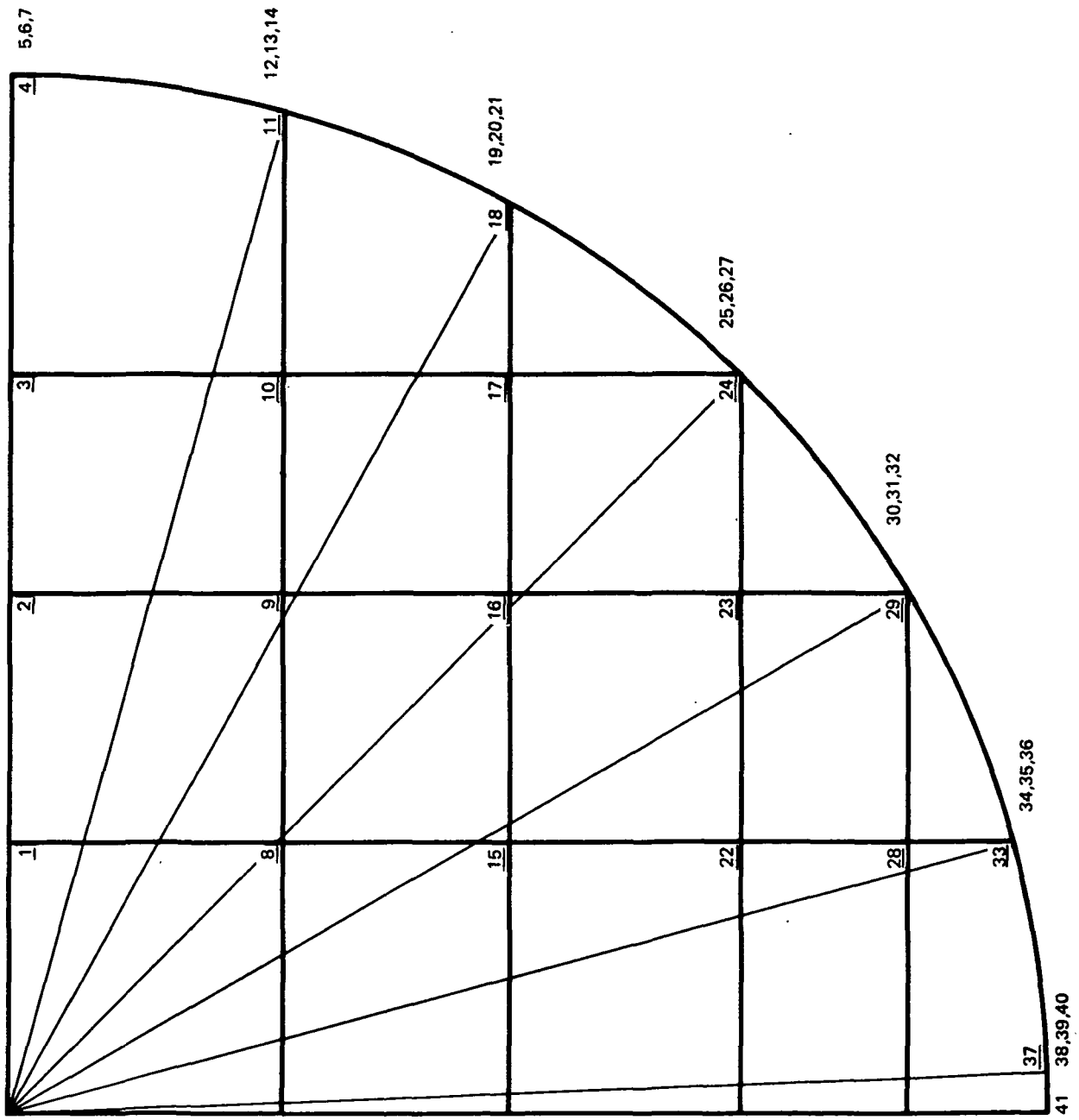

T13-12

Fig. 3-1 NASTRAN Model of Small Hemispherical Tank

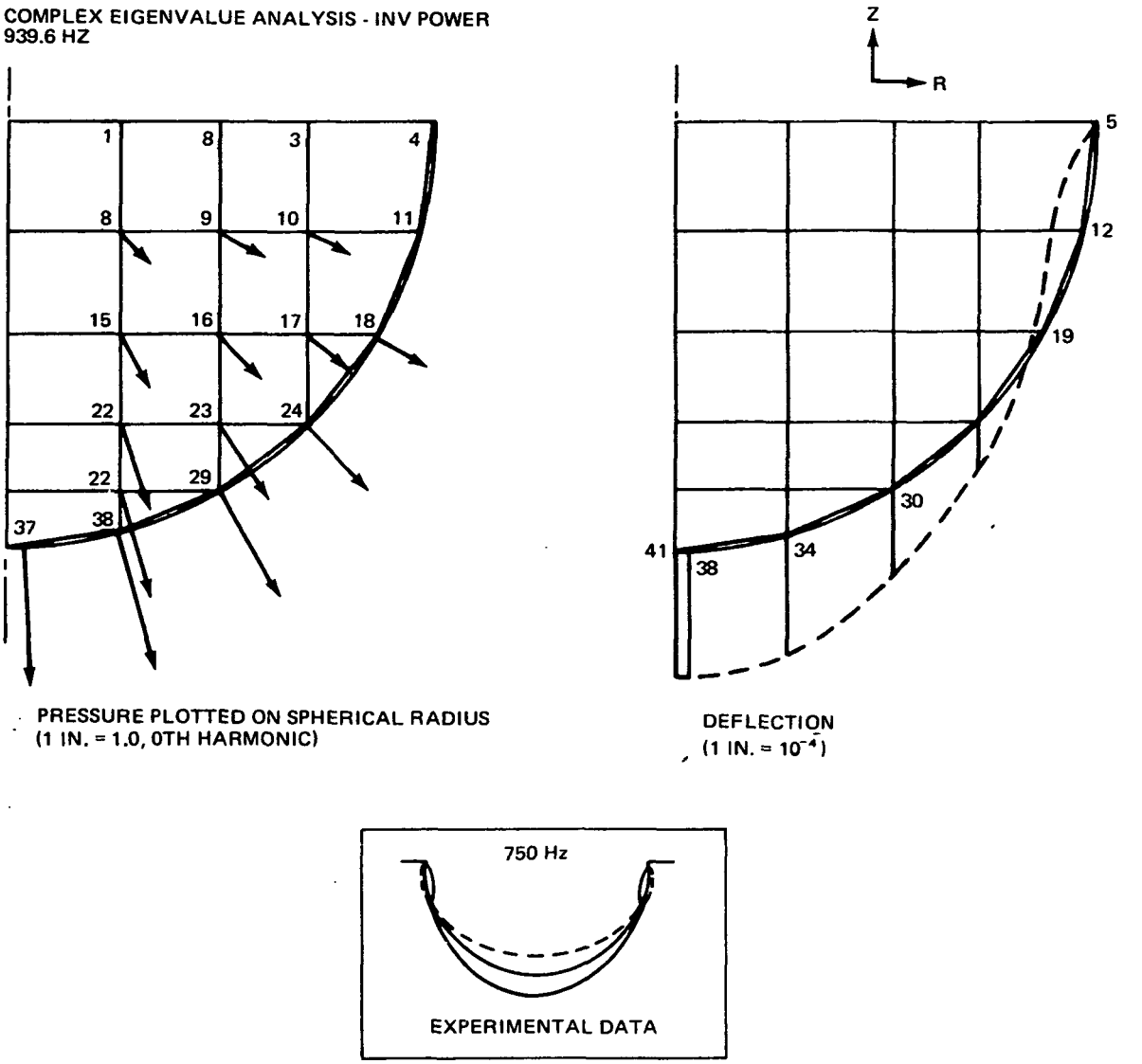

T13-13 **Fig. 3-2 First Mode of Small Hemispherical Tank**

COMPLEX EIGENVALUE ANALYSIS – INV POWER
1335.4 HZ

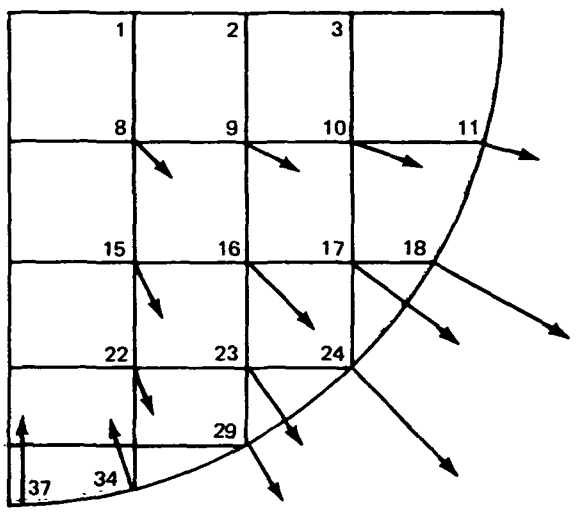

PRESSURE PLOTTED ON SPHERICAL RADIUS
(1 IN. = 1.0, 0TH HARMONIC)

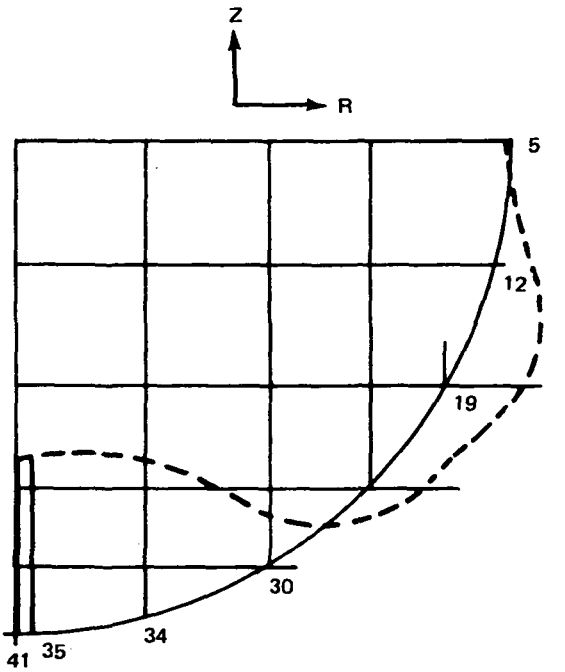

DEFLECTION
(1 IN. = 10^{-4})

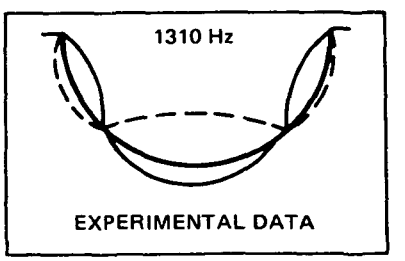

Fig. 3-3 Second Mode of Small Hemispherical Tank

T13-14

COMPLEX EIGENVALUE ANALYSIS – INV POWER
1713.7 HZ

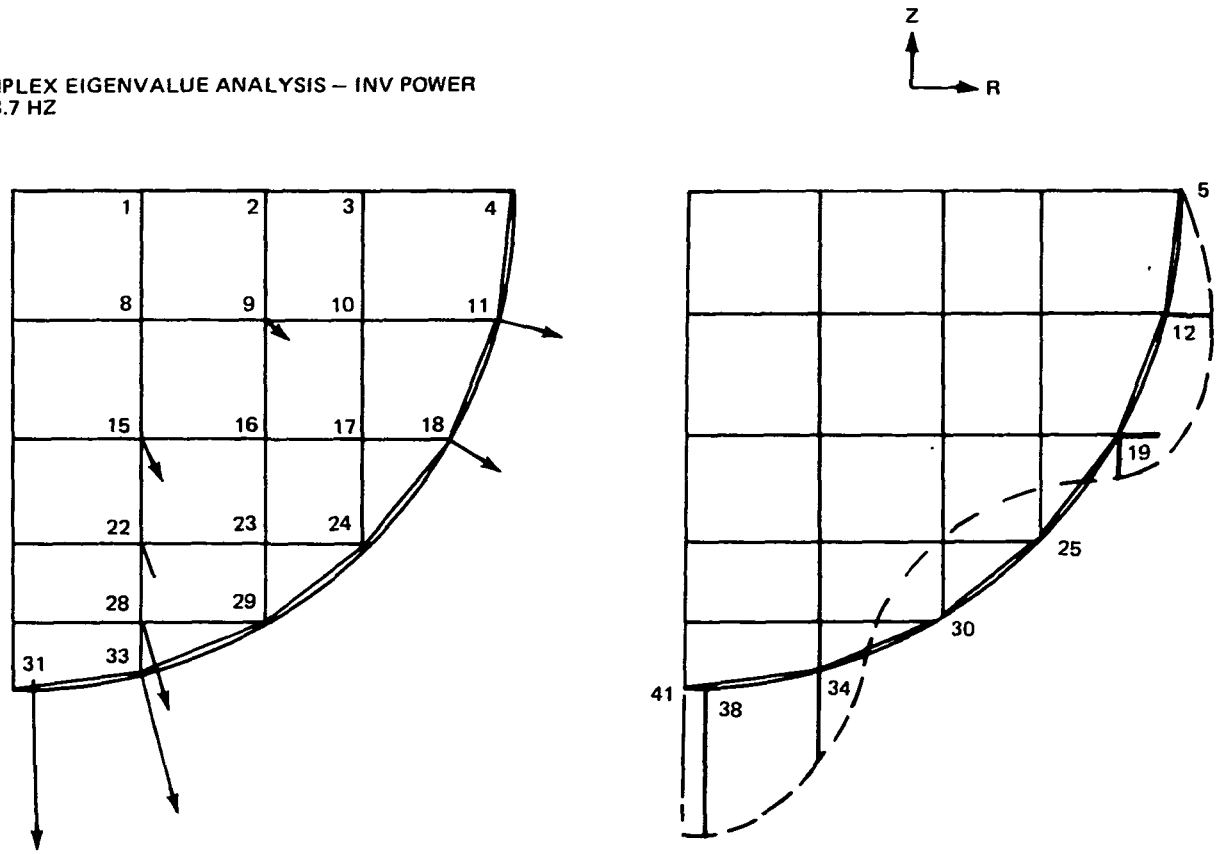

PRESSURE PLOTTED ON SPHERICAL RADIUS
(1 IN. = 1.0, 0TH HARMONIC)

DEFLECTION
(1 IN. = 10^{-4})

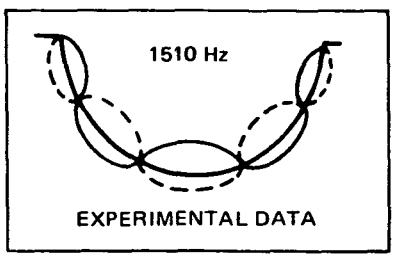

T13-15

Fig. 3-4 Third Mode of Small Hemispherical Tank

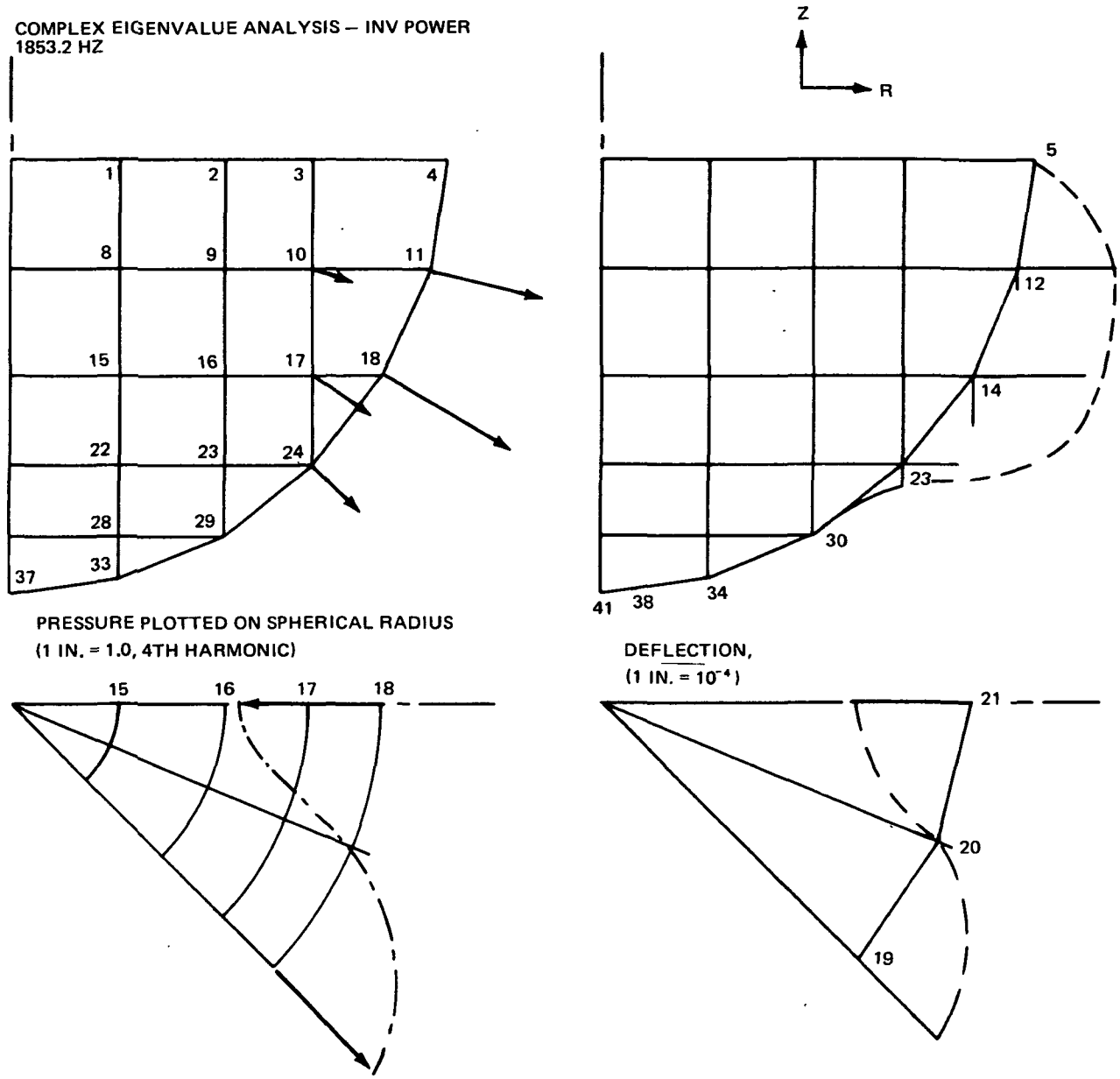

Fig. 3-5 Fourth Mode of Small Hemispherical Tank

T13-16

COMPLEX EIGENVALUE ANALYSIS – INV POWER
2074.1 HZ

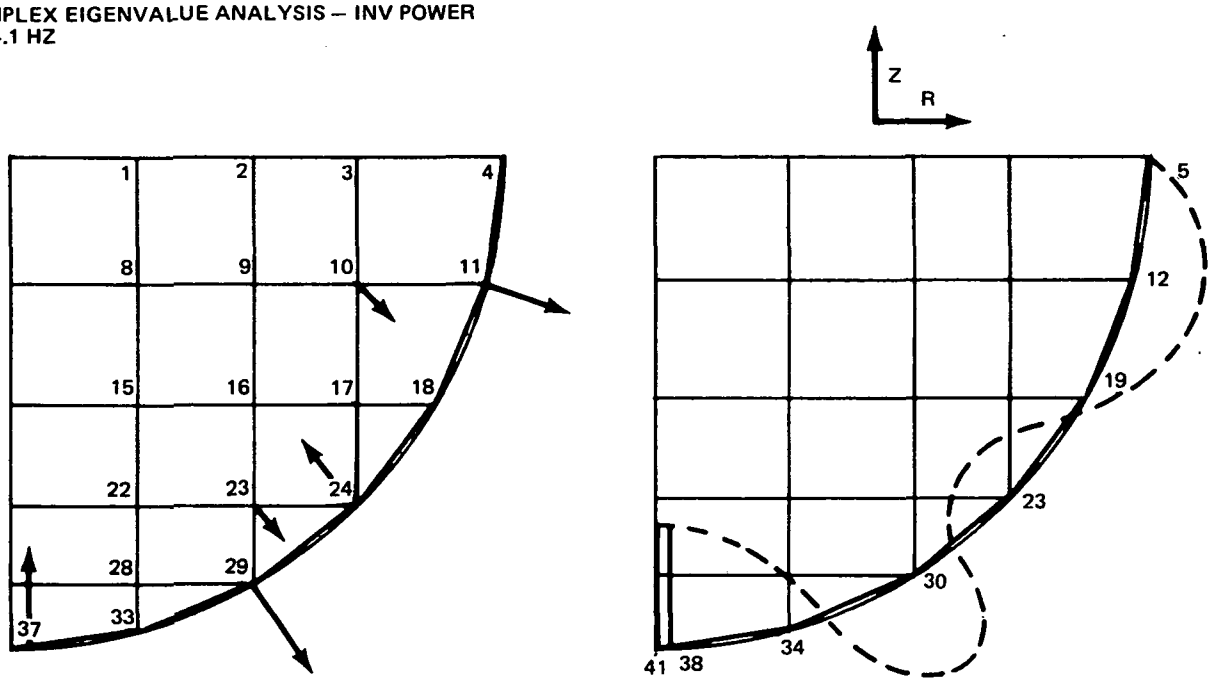

PRESSURE PLOTTED ON SPHERICAL RADIUS
(1 IN. = 1.0, 0TH HARMONIC)

DEFLECTION
(1 IN. = 10^{-4})

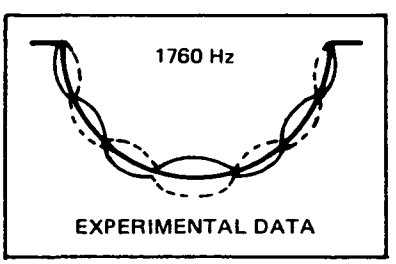

T13-17

Fig. 3-6 Fifth Mode of Small Hemispherical Tank

An immediate method for implementing the latter suggestion is to OMIT all interior fluid coordinates. This is equivalent to assuming an incompressible fluid as may be noted from Equations 4 and 5 of Appendix B1. A more conventional method for reducing the problem size is to OMIT structural coordinates, although this is a questionable procedure for a uniformly loaded shell. All three procedures were evaluated in the hemispherical tank model by modifying it into various sets as follows: (refer to Fig. 3-1).

- Set 1 - The READ (real eigenvalue) module was substituted for the CEAD (complex) module in Rigid Format 7
- Set 2 - The interior fluid elements (RINGFL 8, 9, 15, 16, 22) were set up for Guyan reduction using OMIT 1 cards
- Set 3 - A moderate number of structural coordinates (13, 26, 35) along the tank shell between boundaries were set up for Guyan reduction
- Set 4 - A larger number of structural coordinates including all those along the tank shell between boundaries (13, 20, 26, 31, 35, 39) were set up for Guyan reduction
- Set 5 - Finally, portions of Steps 2 and 4 were combined to reduce the size of the model.

A comparison of the eigenvalues obtained for these various models is listed in Table 3-1. There is agreement among all models for those modes which involve motion in the 4th fluid pressure harmonic because this induces a pressure node along the meridian line where the structural points are omitted. This occurs in the 4th, 6th, 8th and 9th eigenvalues. Review of the mode shapes indicates a node line through the location of the omitted structural coordinates. These modes therefore, do not evaluate the effect of omitting coordinates. Comparison of the other modes indicates that omitting interior fluid coordinates (at grid points 8, 9, 15, 16, 22) did not change the eigenvalues as may be seen by comparing Sets 1 and 2 and Sets 4 and 5. In other work, when omitting both interior and boundary fluid coordinates it was found that the eigenvalues changed by small amounts in the lowest modes and significant amounts at higher frequencies.

Table 3-1 Comparison of Eigenvalues for Various Modifications

Base		Set 1	Set 2	Set 3	Set 4	Set 5
	CEAD	No Omits	5 Fluid Omits	3 Struct. Omits	6 Struct. Omits	6 Struct. + 5 Fluid Omits
1	939.6	939.7	939.7	997.9	1059.5	1058.9
2	1335.4	1335.5	1335.5	1486.0	1756.7	1753.4
3	1713.7	1713.9	1713.9	1848.1	–	–
4	1853.2	1853.2	1853.2	1853.2	1853.2	1853.2
5	2074.1	2074.2	2074.2	2348.9	–	–
6	2229.8	2229.8	2229.8	2229.8	2229.8	2229.8
7	2356.7	2356.3	2356.3	–	–	–
8	–	2571.2	2571.2	2571.2	2571.2	2571.2
9	–	2873.4	2873.4	2873.5	2873.5	2873.5
10	–	–	–	3058.6	3203.8	3199.7
11	–	3695.0	3659.0	3754.5	3768.4	3764.9
A set-114		93	83	78	63	74
Time (minutes)						
Sys	26.2	12.4	11.0	12.3	7.4	14.9
Cpu	5.3	2.6	2.3	2.6	1.7	2.7

Note: The Inverse Power Method in Release 15.5 was Used for All Calculations.

T13-3(T)

Table 3-1 also permits comparison of eigenvalues obtained by omitting only structural coordinates. Set 1 differs from the Base set by having all rotations about coordinate 5 (tangential motion) omitted. This produced no calculable change in eigenvalues or vectors as was anticipated. In Set 3, three grid points located as sketched in Table 3-2 (13, 26, 35) had the remaining 5 coordinates omitted so that they were unconstrained by any applied forces. Set 4 was run with all structural points on the same meridian omitted (13, 20, 26, 35, 39). This magnitude of reduction would be necessary to reduce the current external tank model to about 200 DOF. There is a noticeable shift in the lower frequency eigenvalues and a change in the eigenvectors. Table 3-2 also compares the relative responses in the first mode. The radial and axial deflections change at locations where the coordinates are omitted. Tank fluid pressures at the boundary do not change much at the higher modal pressure locations.

Calculations indicate the READ module could be substituted for CEAD at a considerable savings of computer time nor did omitting all interior fluid coordinates change the computed eigenvalues or eigenvectors. The inaccuracies inherent in omitting tank coordinates with significant fluid loading is also apparent.

Table 3-2 Comparison of Shapes of First Hydroelastic Mode for Various Model Modifications

	Axial Deflection				Radial Deflection			
Coord	Set 1	Set 3	Set 4	Set 2	Set 1	Set 3	Set 4	Set 2
12	0.36	0.30	0.26	0.36	2.31	2.35	2.28	2.31
13	0.36	0.32	0.26	0.36	2.31	2.26	1.83	2.31
14	0.36	0.30	0.26	0.36	2.31	2.35	2.28	2.31
19	1.51	1.33	1.19	1.51	1.96	2.19	2.31	1.96
20	1.51	1.33	0.85	1.51	1.96	2.19	2.22	1.96
21	1.51	1.33	1.19	1.51	1.96	2.19	2.31	1.96
25	4.04	3.73	3.49	4.04	2.12	0.59	0.66	2.12
26	4.04	2.32	2.02	4.04	2.12	2.00	0.18	2.12
27	4.04	3.73	3.49	4.04	2.12	0.59	0.66	2.12
30	6.50	6.60	6.11	6.50	−.70	−.63	−.40	−.70
31	6.50	6.60	3.72	6.50	−.70	−.63	1.02	−.70
32	6.50	6.60	6.11	6.50	−.70	−.63	−.40	−.70
34	8.56	8.80	8.89	8.86	−.70	−.66	−.66	−.70
35	8.56	6.59	6.88	8.56	−.70	−.66	0.02	−.70
36	8.56	8.80	8.89	8.56	−.70	−.66	−.66	−7.0
38	9.19	9.58	9.83	9.19	−.10	−.10	−.10	−.10
39	9.19	9.58	9.81	9.19	−.10	−.10	−.01	−.10
40	9.19	9.58	9.83	9.19	−.10	−.10	−.10	−.10
41	9.14	9.53	9.78	9.14	–	–	–	–
	Tank Wall Fluid Pressure							
11	16	8	22	16				
18	182	127	92	182				
24	471	387	346	471				
29	761	741	656	761				
33	959	950	944	959				
37	1000	1000	1000	1000				

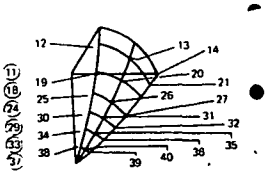

Schematic Location of Grid Points

● Fluid Points are circled.

T13-4(T)

3.2 LIQUID OXYGEN TANK MODEL

The liquid oxygen tank shell structure is represented by QUAD2 and TRIA2 bending and membrane quadilateral and triangular elements. The size of the elements used was a compromise between a reasonable representation of the simpler shell modes and the necessity to reduce the number of DOF's for the model. Therefore, a 22-1/2 degree arc length was selected for the span of each shell element giving 8 grid points about a semi-circle. Figure 3-7 represents the current model. The number of diametrical circles necessarily corresponds to the number of exterior fluid rings used. Two were selected for the cylindrical portion to maintain panel aspect ratios close to one for most locations. The dome representation was considered most important and 6 fluid rings were used in the original model, therefore 6 diametrical circles were used and the apex point was connected by MPC's. This original dome representation is depicted in Fig. 3-8. Previous work on a small hemispherical dome with uniformly spaced fluid rings resulted in an irregular deformation pattern close to the apex point, therefore, the lowest fluid rings were placed as shown. The dome representation was later modified as discussed below. Four fluid rings were used for the top conical section of the tank which was considered less significant than the dome; three interior fluid rings were used throughout most of the tank. Close to the bottom of the dome, where the pressures were most important, the fluid elements were made smaller (Fig. 3-7).

This model, which consisted of about 740 DOF's in the analysis set (50 fluid elements and 136 structural elements), was assembled into a NASTRAN model and submitted for computer analysis after a small hemispherical tank problem similar to that described in Subsection 3.1 had been successfully run. Difficulties encountered with this large problem were:

1. Hydroelastic problems would not run in Level 15.5. A system ØC-1 error occurred while executing module GKAD. This error was listed as SPR 1020. In order to avoid this problem, Level 15.1 was used for most analyses. The error was later fixed in Level 15.6.5 and should be correctable according to the NASTRAN System Monitoring Office.

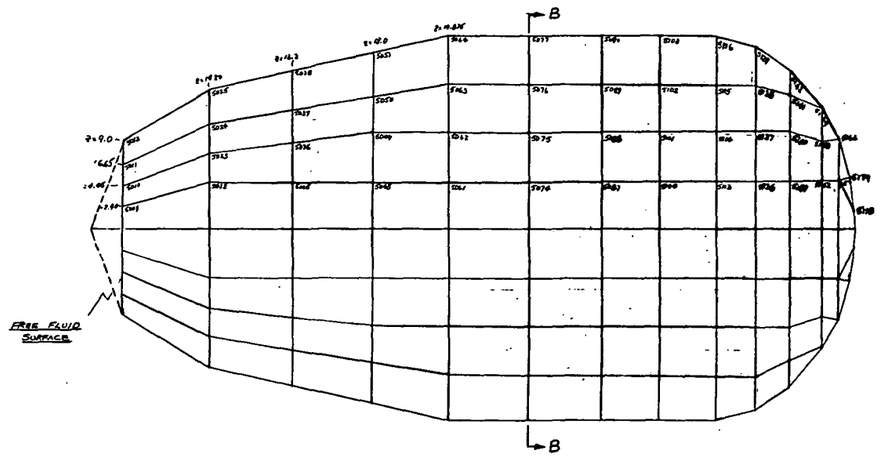

FLUID IDEALIZATION (RINGS)

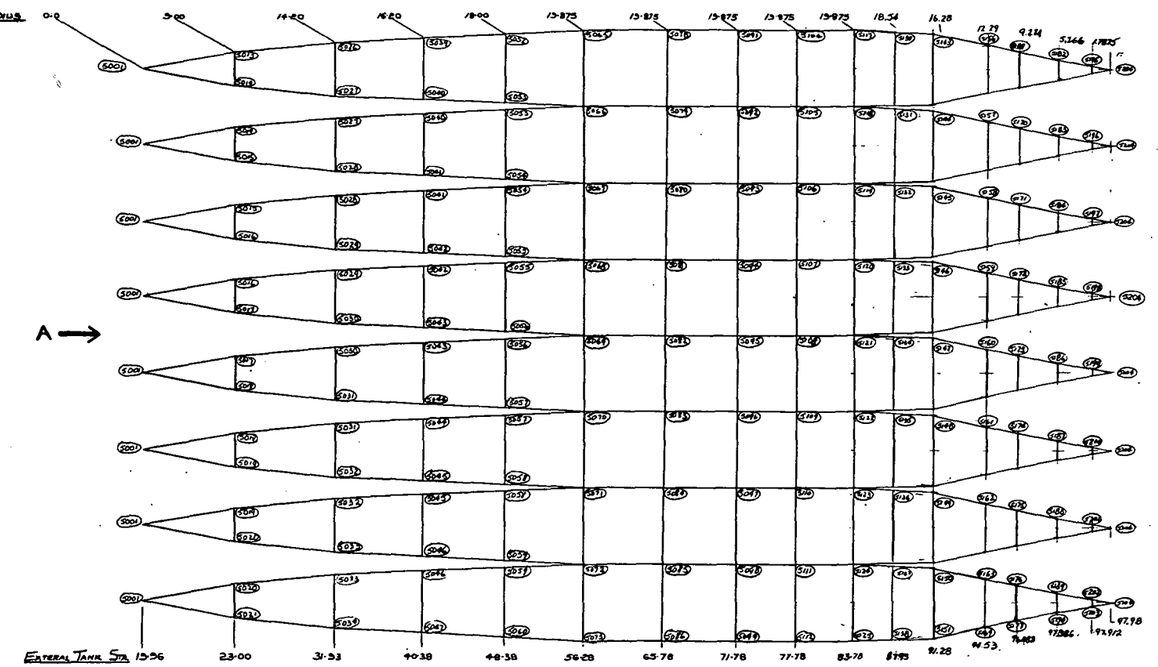

DEVELOPED TANK IDEALIZATION

REVISED 8/24/73 TO SHOW ADDITIONAL ELEMENTS AND REVISED GEOMETRY ON DOME DEVELOPED BY STATIC ANALYSIS

REVISED 2/26/73 TO SHOW FINER GRID ON LOWER DOME, AND MORE FLUID RINGS, AS SUGGESTED AT LANGLEY MEETING ON 2/22/73

ORIGINAL 2/20/73

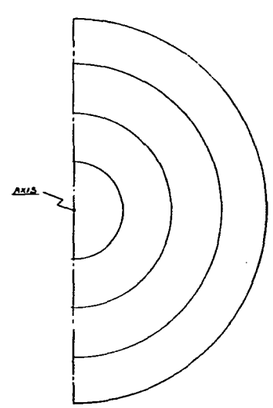

SECTION BB THROUGH FLUID RINGS

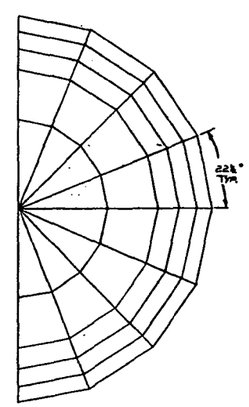

VIEW A OF UNDEVELOPED TANK

T13-18

Fig. 3-7 NASTRAN Model of Liquid Oxygen Tank for 1/8-Scale Shuttle Model

6/23/73

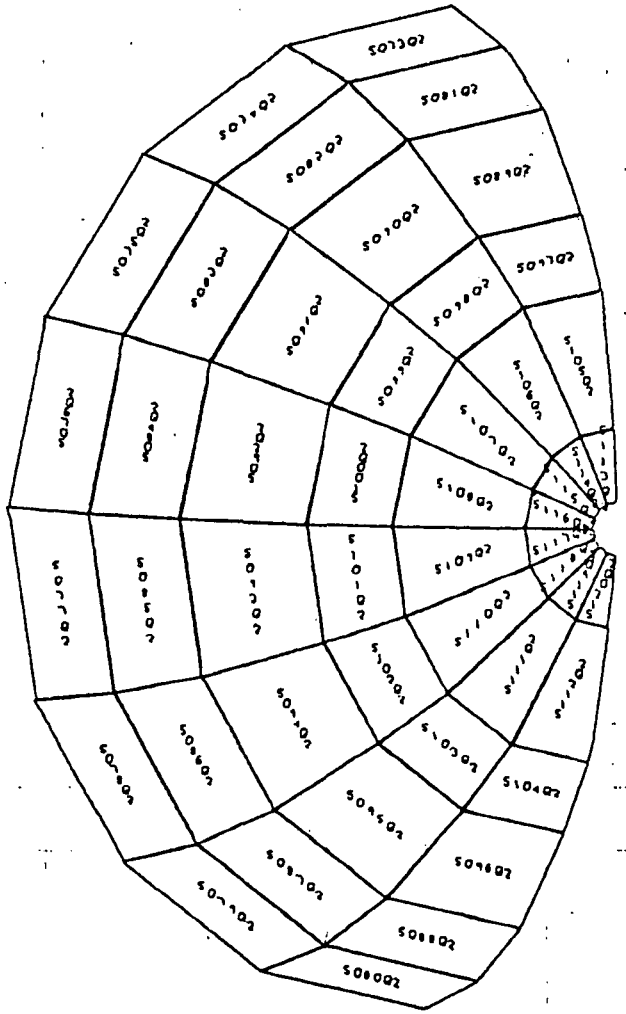

Undeformed Shape

T13-19

Fig. 3-8 Original LO_2 Tank Dome Model

2. Often, only a single eigenvalue was extracted using the Inverse Power Method although more were present. This error was listed as SPR 998.

   It is probably a function of the completion codes. It occurred for both Level 15.1 and 15.5. In order to avoid this problem the Determinent Method was used, which is somewhat slower.

3. Fluid ring element numbers must be entered in ascending order and they cannot be numbered higher than 33000. Violating the first rule results in a fatal message that the SEQGP card references an undefined grid point. Violating the second rule causes an ØC-5 system error in Module TA1. These errors were listed as SPR 1017 and 1016. They were identified after several exploratory computer runs and avoided by renumbering the fluid elements.

Several other errors were encountered and overcome by modifying the data or the analysis options. The problem was submitted for analysis with only one pressure harmonic (the zeroth) and a limited frequency sweep range requested, to reduce the computer running time. Computer submittals for the model after it had been developed are summarized in Table 3-3. There was no reduction in coordinates attempted in these runs. The only coordinates initially included in the OMIT set were those required to avoid singularities. Boundary conditions for this analysis consisted of restraints against motion in the X direction (parallel to the tank axis) at all coordinates at X Station 83.78. A total of five elastic modes was obtained for the zeroth harmonic and four for the first harmonic as indicated in Table 3-3.

The mode shapes obtained are shown plotted in Fig. 3-9 through 3-17. The predominant characteristic is the number of nodal pressure surfaces through the fluid, which varies from none for the lowest frequency to three for the highest. Structural deflections are also shown. They generally tend to follow the pressure variations. The pressures and deflections are only shown along one meridional line since they are essentially axisymmetric for the zeroth harmonic and antisymmetric for the first harmonic. The deflections differ from the pressure patterns at the higher frequencies at 110 and 134 Hz for the first harmonic. At these modal patterns, the grid point spacing is too coarse to be adequate.

An anomalous behavior notable in the deflections is the small magnitude on the dome at the third set of grid points from the apex. This "kink" in the deflections along the diametrical ring through the center of the dome is obvious in the lower zeroth harmonic modes. The pressure pattern in the first mode is quite regular and the dome thickness is a uniform 0.016 in. through the adjacent grid points. A change to 0.040 in. does occur closer to the dome center but this does not explain the deformation pattern.

The near uniform pressure on the tank dome in the first mode facilitated an analytical determination of the dome deformation under uniform pressure at reduced computation cost. The deformation pattern obtained for the original 6 rows of elements is shown in Fig. 3-18 and the dome deformation similar to that in Fig. 3-9. Replacing the central elements and multipoint constraints (MPC) at the apex with triangular elements as shown in Fig. 3-19 and using CQDMEM2 quadulateral membrane elements in place of QUAD2 plates, still resulted in an unsatisfactory deformation pattern illustrated in Fig. 3-20. Adding additional rows of elements for a total of 9 and modifying the geometry resulted in an improved deformation pattern (Fig. 3-21). However, in veiw of the necessity to keep down the number of DOF's, a compromise configuration of 7 rows of elements was attempted. The results are seen in Fig. 3-22 and 3-23. The apex deformation appear irregular and more flexible than the adjacent dome regions, however, the remainder of the dome appears satisfactory. This apex anomaly is not considered significant since it is expected to have little effect on the local pressures.

The revised apex was then incorporated into the liquid oxygen tank model and the first mode recalculated. The frequency shifted slightly from 22.9 Hz to to 23.1 Hz. The mode shape in Fig. 3-24 is an improvement over the original in the dome region.

Table 3-3 Summary of Computer Runs in Rigid Format 7 To Calculate Liquid Oxygen Tank Hydroelastic Modes

Fluid Harmonic Specified	Frequency Range Scanned (Hz)	Frequencies (Hz)	Reason for Termination	Computer (1) System Minutes Required
0	8 to 24	5.2 (Slosh)	Out of Time	92 (Inverse Power)
0	8 to 24	11.1 (Slosh)	Out of Time	63 (Determinant)
0	16 to 40	22.9	Out of Time	65
0	40 to 53	None	None in Range	41
0	40 to 72	None	Out of Time	100
0	72 to 95	75.2, 91.5	No More In Range	85
0	95 to 135	115.2, 124.3	"	88
1	95 to 135	100, 134.3	"	123.5
1	72 to 95	None	"	48
1	40 to 72	60.5	"	65
1	72 to 13	19.2, 27.3 (Slosh)	"	118

(1) Nominal Budgetary Value is $7 per System Minute (on the IBM 370/165).

T13-5(T)

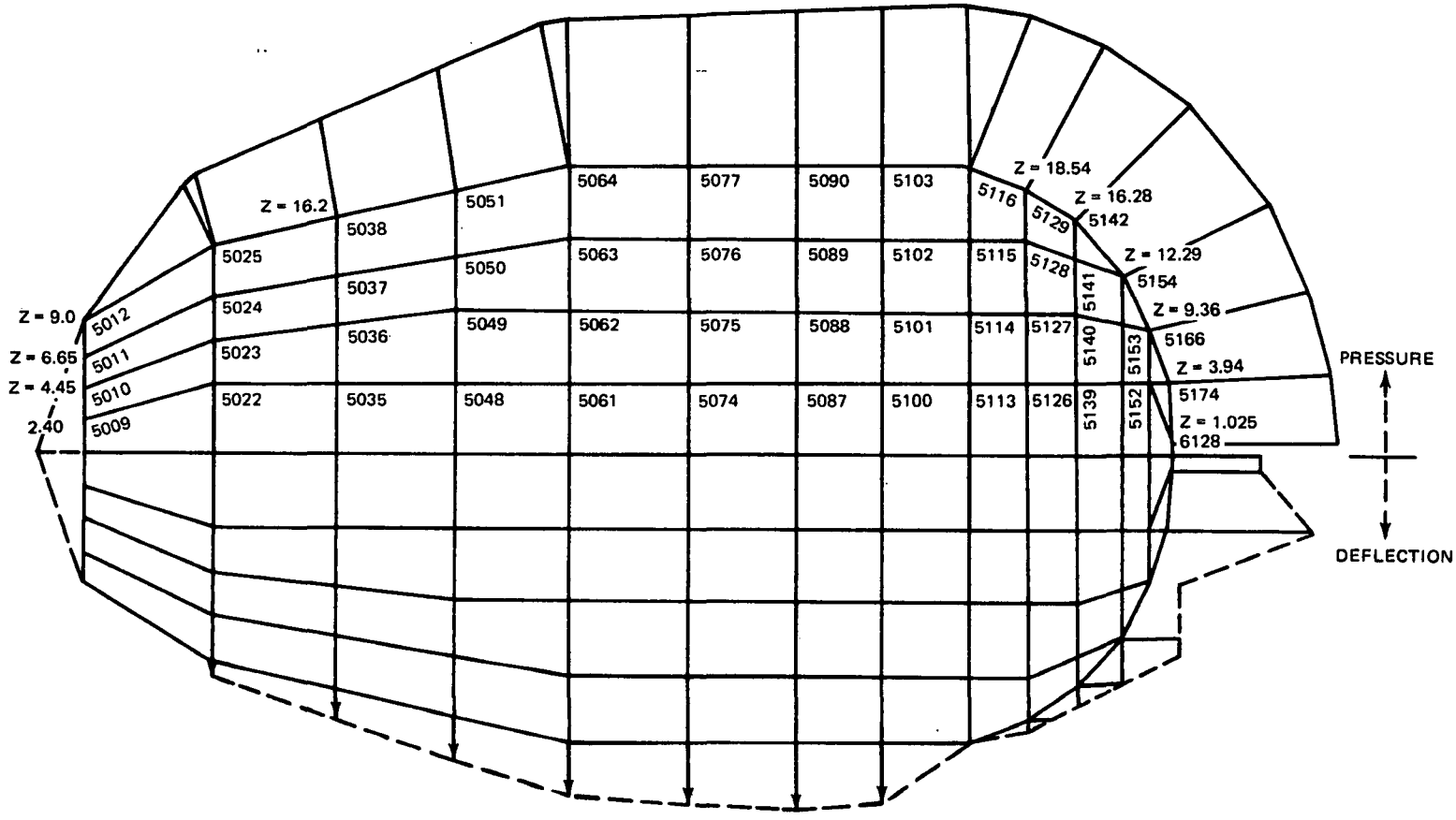

Top pattern represents pressure distribution; Bottom pattern represents shell deformation: n = 0 (Zeroth circumferential harmonic)

T13-20

Fig. 3-9 1/8-Scale Model LO_2 Tank Mode Shape at 22.9 Hz

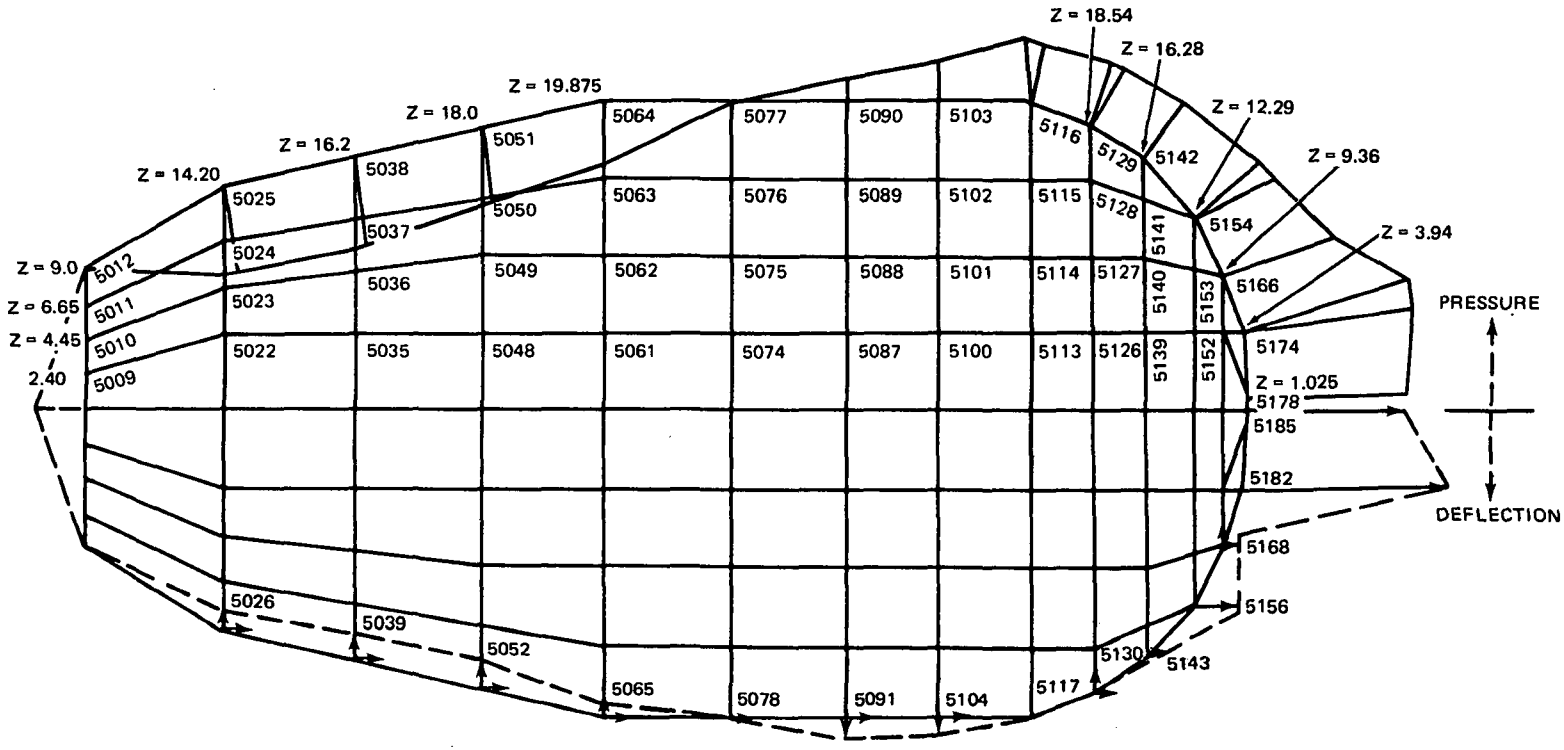

Top pattern represents pressure distribution; Bottom pattern represents shell deformation: n = 0 (Zeroth circumferential harmonic)

T13-21

Fig. 3-10 1/8-Scale Model LO_2 Tank Mode Shape at 75.2 Hz

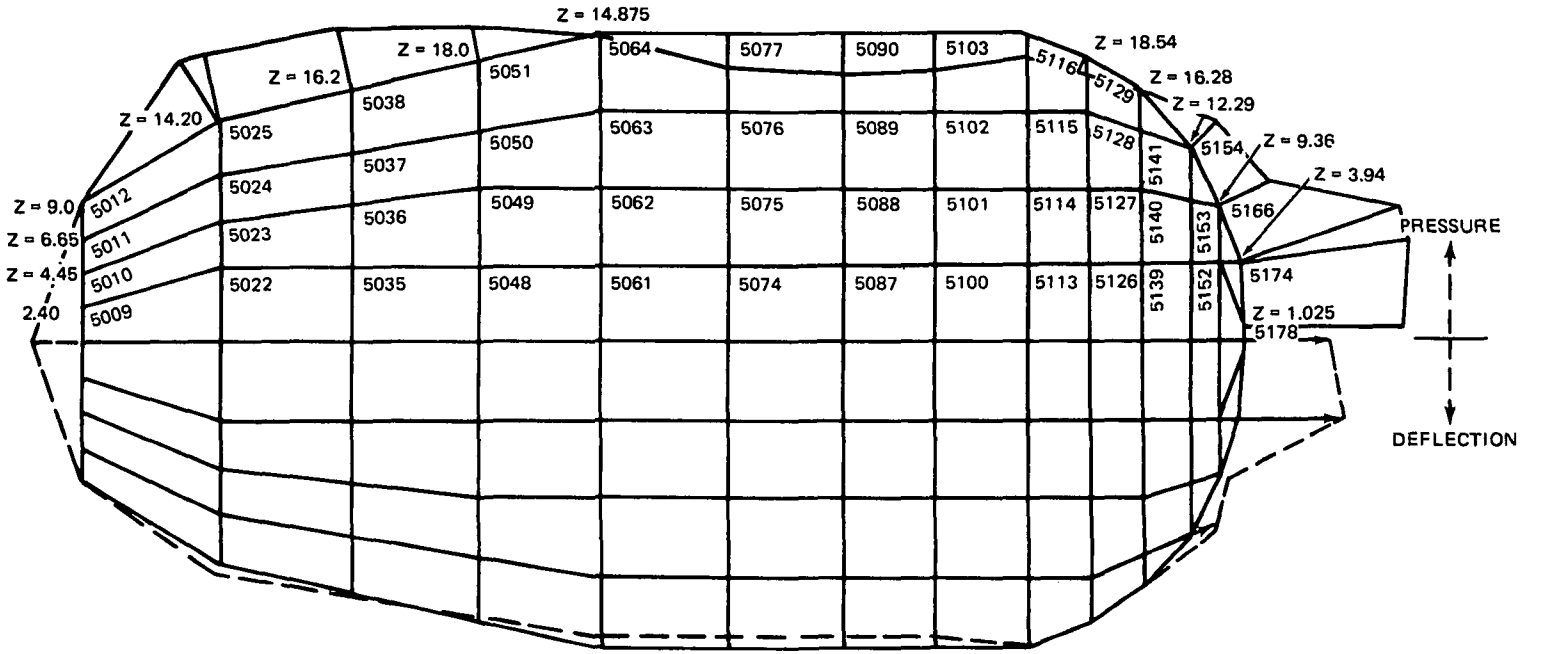

Top pattern represents pressure distribution; Bottom pattern represents shell deformation: n = 0 (Zeroth circumferential harmonic)

T13-22

Fig. 3-11 1/8-Scale Model LO_2 Tank Mode Shape at 91.5 Hz

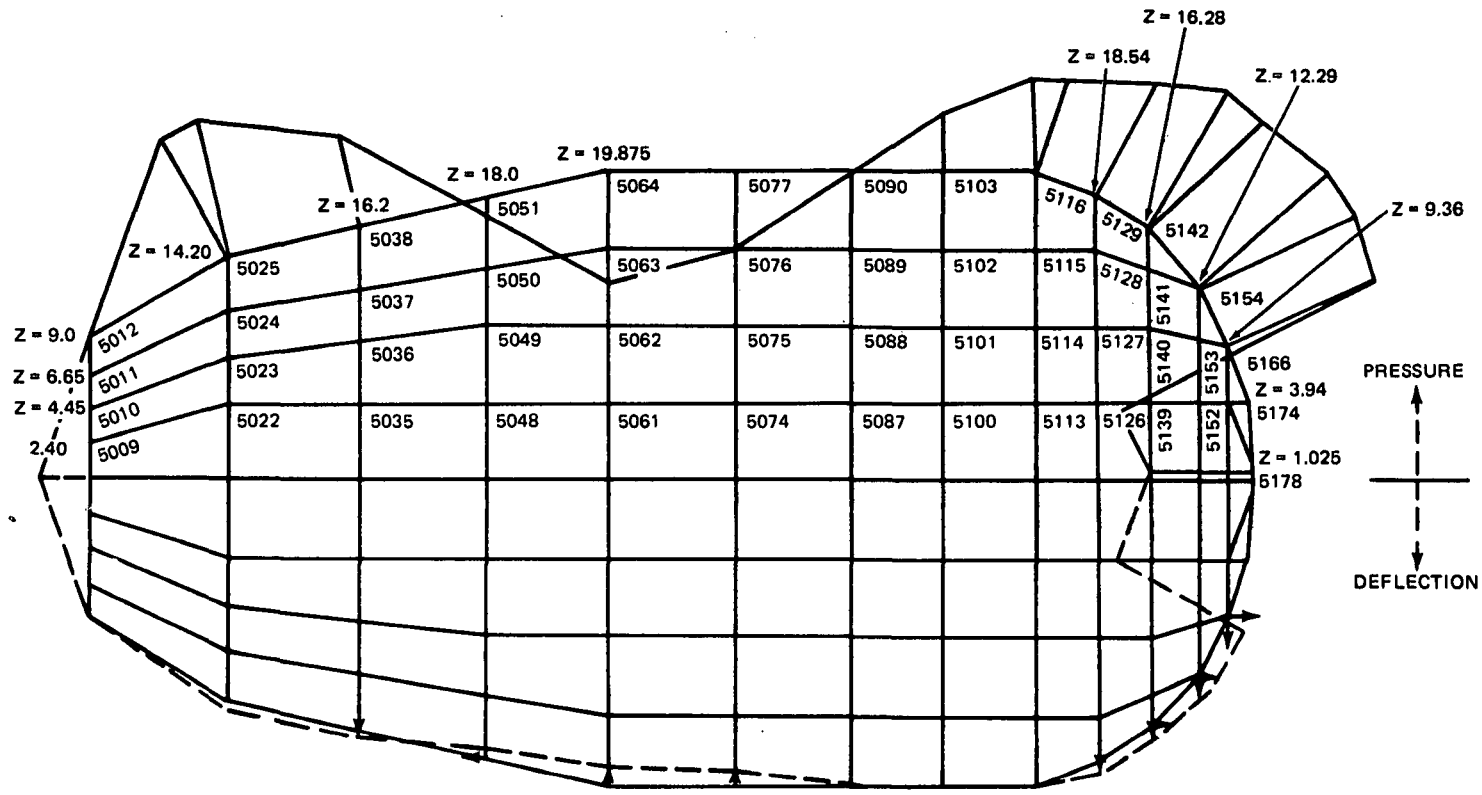

Top pattern represents pressure distribution; Bottom pattern represents shell deformation: n = 1 (First circumferential harmonic)

T13-23

Fig. 3-12 1/8-Scale Model LO_2 Tank Mode Shape at 115.2 Hz

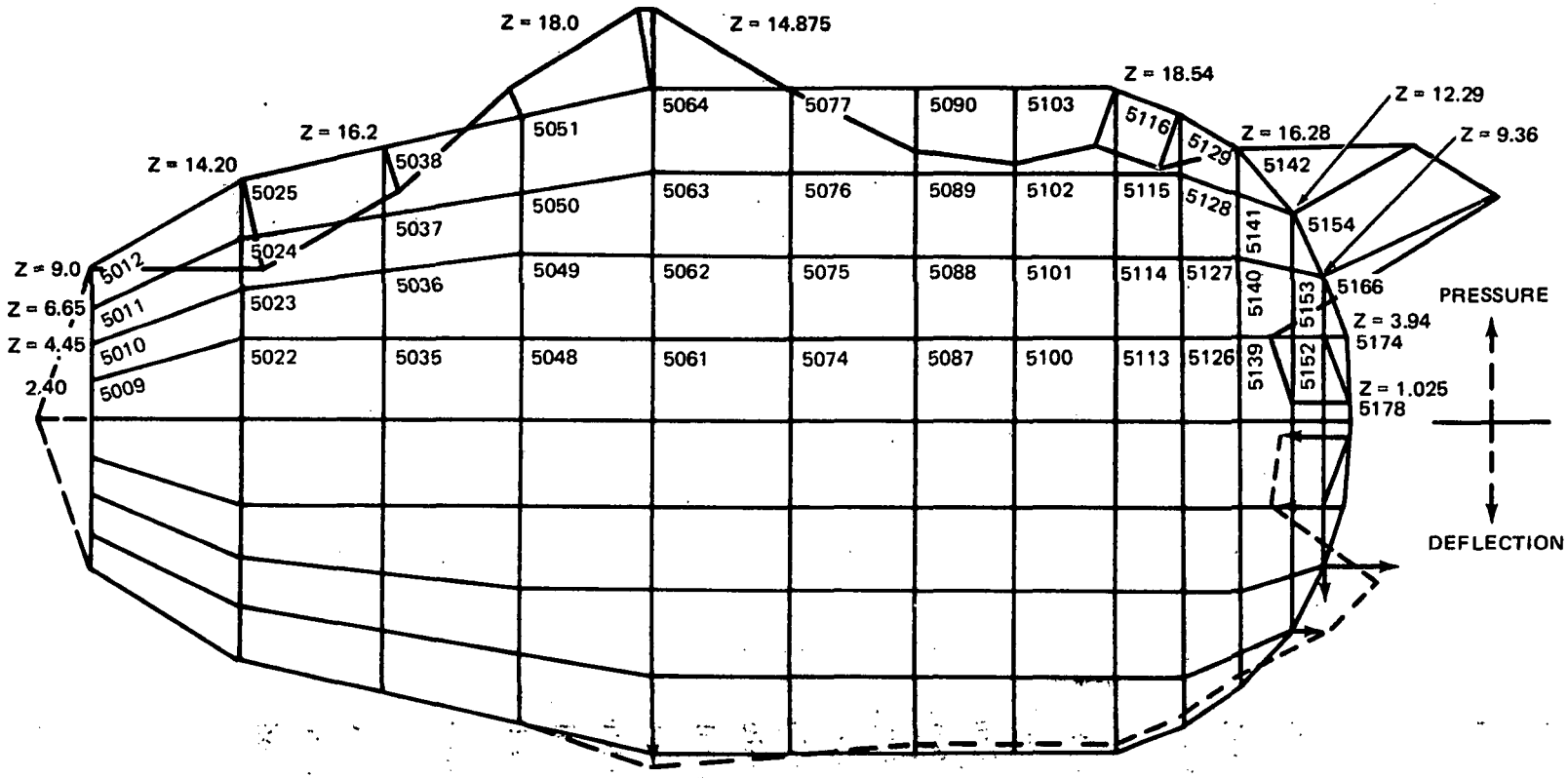

Top pattern represents pressure distribution. Bottom pattern represents shell deformation: n = 0 (Zeroth circumferential harmonic)

T13-24

Fig. 3-13 1/8-Scale Model LO_2 Tank Mode Shape at 129.3 Hz

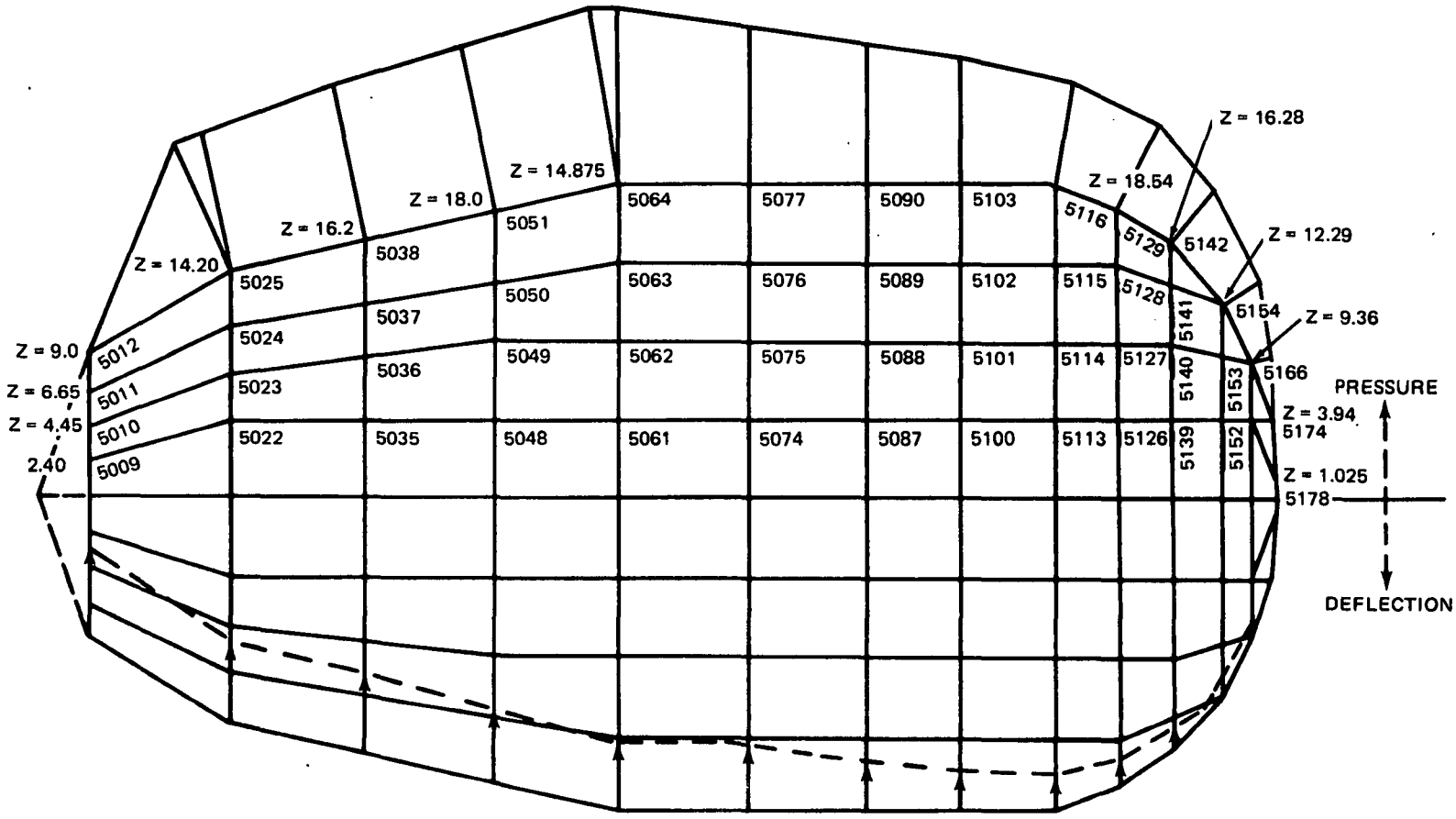

Top pattern represents pressure distribution. Bottom pattern represents shell deformation: n = 1 (First circumferential harmonic)

T13-25

Fig. 3-14 1/8-Scale Model LO_2 Tank Mode Shape at 19.2 Hz

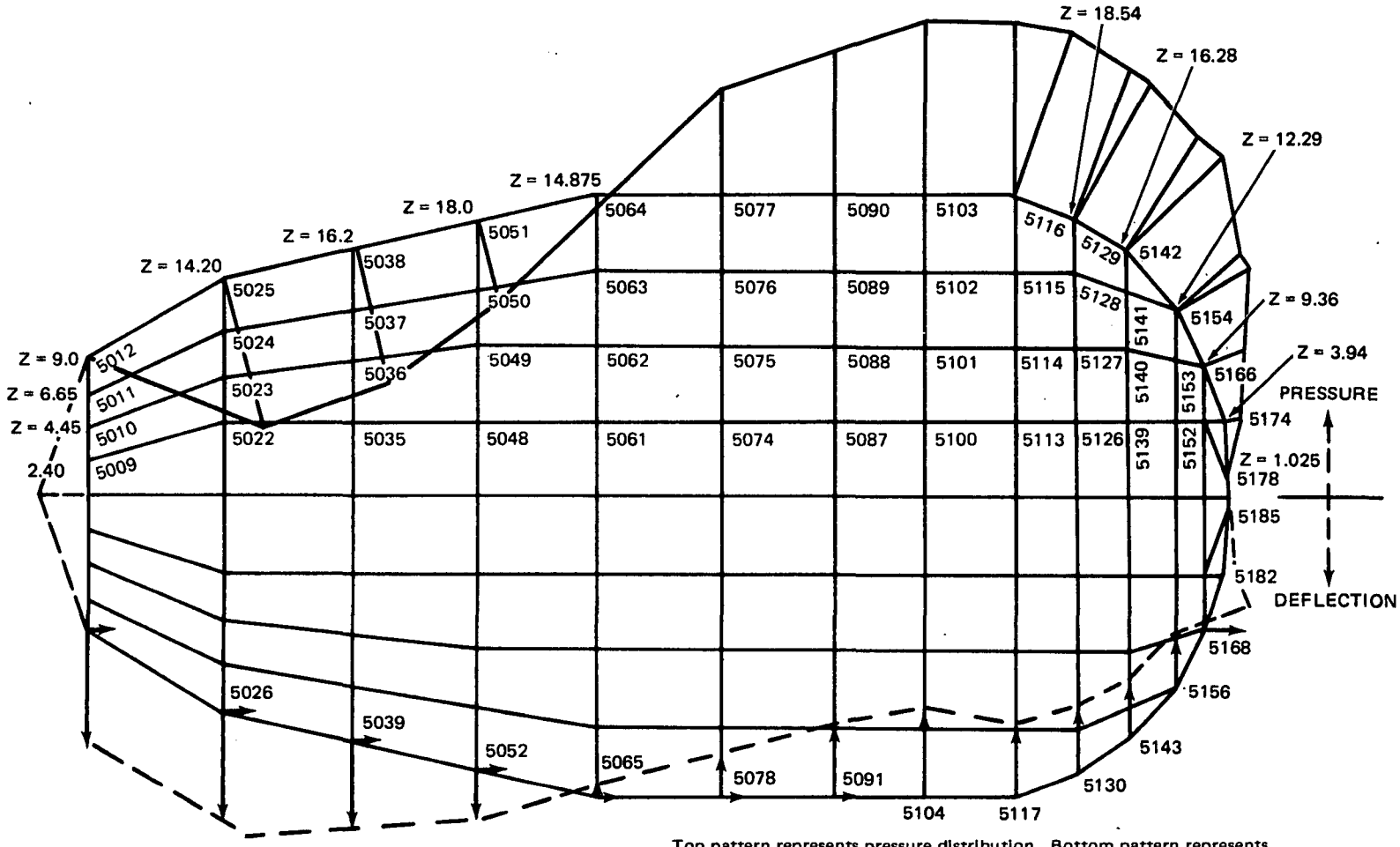

Top pattern represents pressure distribution. Bottom pattern represents shell deformation: n = 1 (First circumferential harmonic)

Fig. 3-15 1/8-Scale Model LO_2 Tank Mode Shape at 60.5 Hz

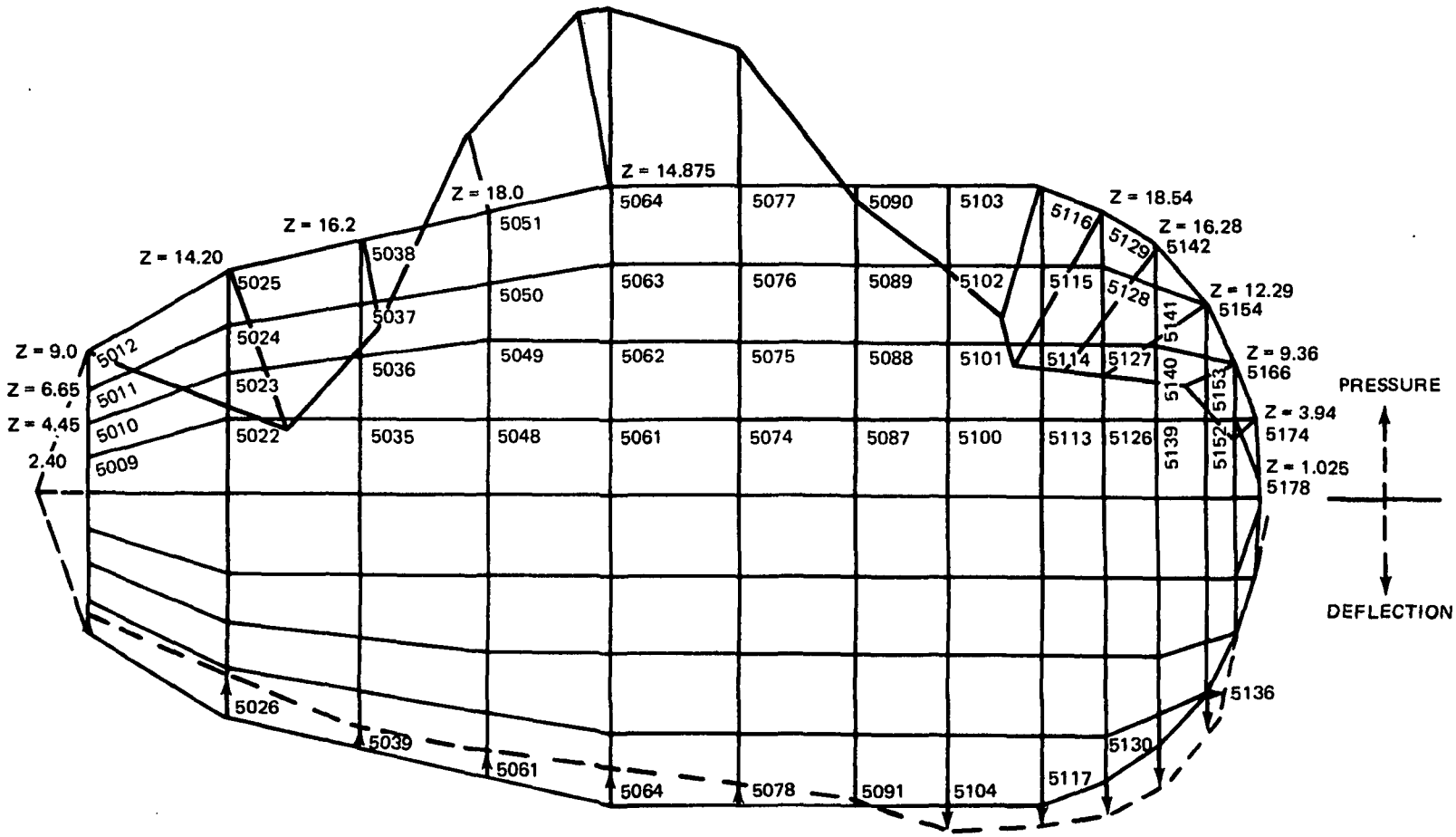

Top pattern represents pressure distribution. Bottom pattern represents shell deformation: n = 1 (First circumferential harmonic)

T13-27

Fig. 3-16 1/8-Scale Model LO_2 Tank Mode Shape at 110.0 Hz

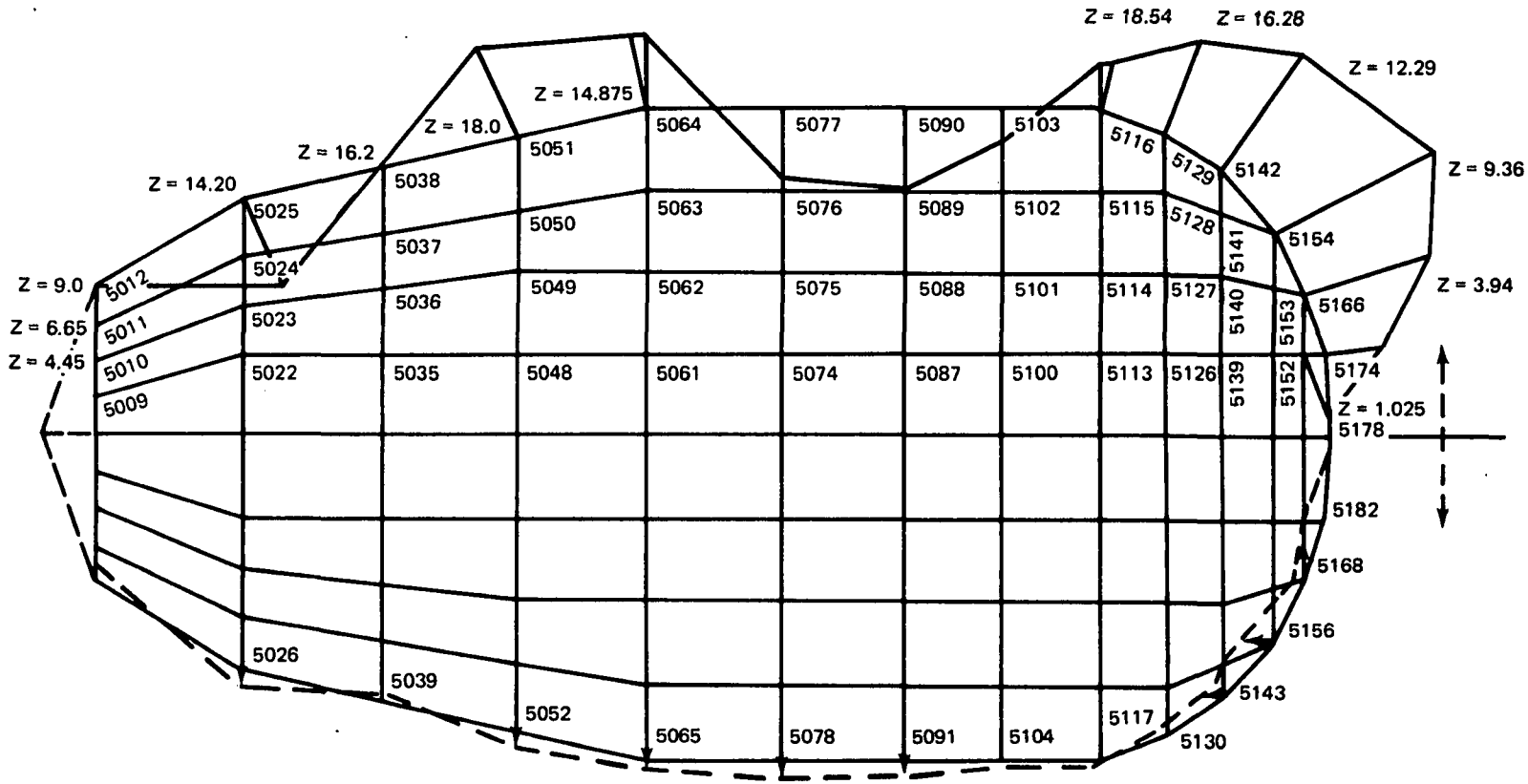

Top pattern represents pressure distribution. Bottom pattern represents shell deformation: n = 1 (First circumferental harmonic)

T13-28

Fig. 3-17 1/8-Scale Model LO_2 Tank Mode Shape at 134.3 Hz

6/23/73 MAX-DEF.=0.00397498

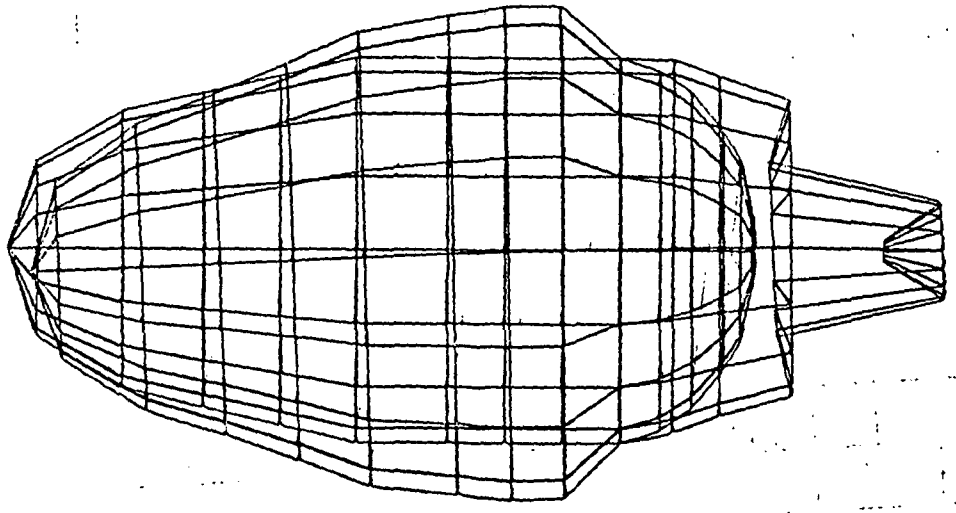

DEFORMATION OF TANK UNDER STATIC LOAD = FLUID HEAD
PRESSURE SCALED TO MAX. OF 1.0 psi
STATIC DEFOR. SUBCASE 1 LOAD 1

T13-29

Fig. 3-18 Original LO_2 Tank Model Under Static Pressure

6/30/73 MAX-DEF. = 0.00412321

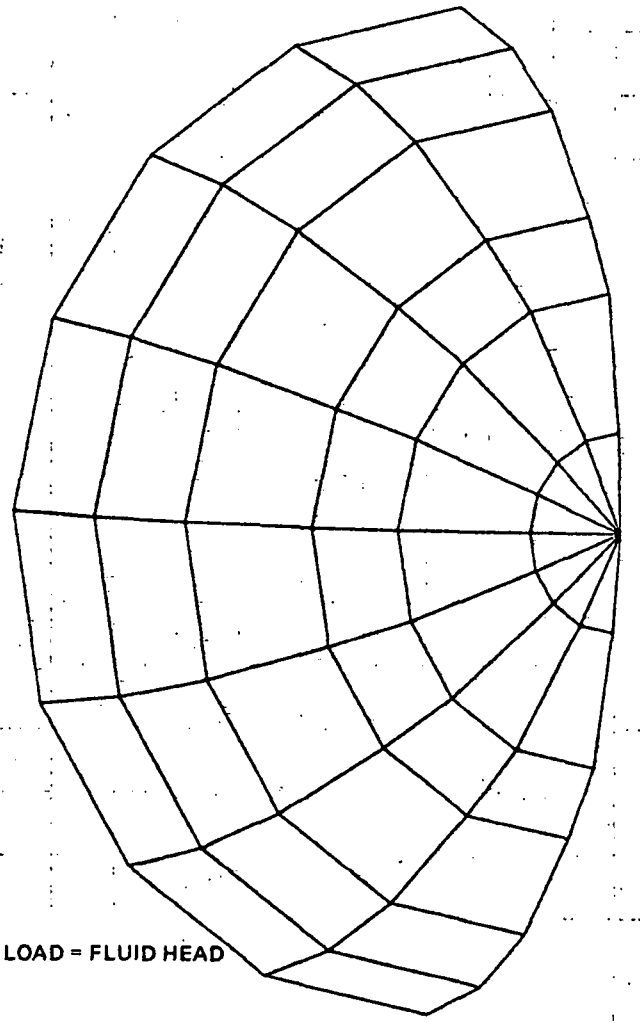

DEFORMATION OF TANK UNDER STATIC LOAD = FLUID HEAD
PRESSURE SCALED TO MAX OF 1.0 psi
STATIC DEFOR. SUBCASE 1 LOAD 1

T13-30

Fig. 3-19 Initially Revised LO_2 Tank Dome

6/30/73 Max-Def. = 0.00412321

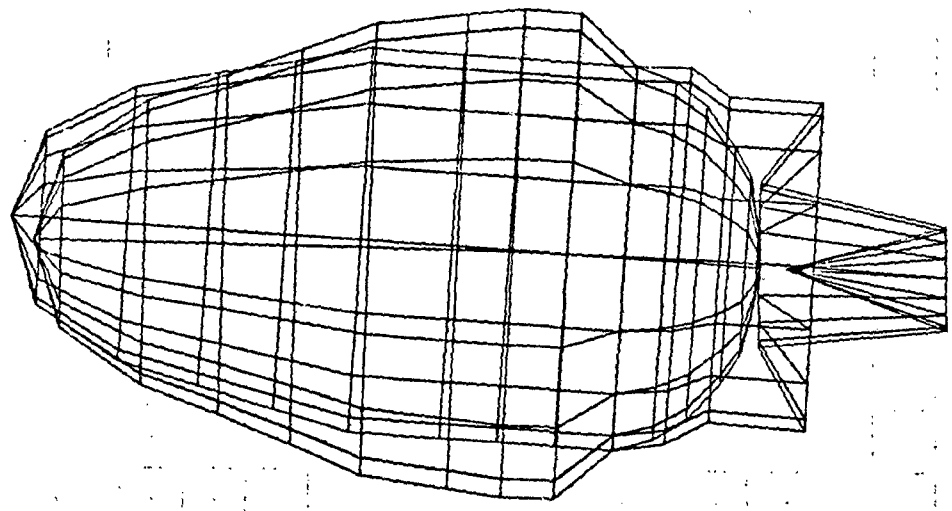

(CQDMEM2 USED IN PLACE OF CQUAD 2 (5073 TO 5112))
CTRIA 2 USED IN PLACE OF MPCS
DEFORMATION OF TANK UNDER STATIC LOAD = FLUID HEAD
PRESSURE SCALED TO MAX OF 1.0 PSI
STATIC DEFOR, SUBCASE 1 LOAD 1

T13-31

Fig. 3-20 Initially Revised LO_2 Tank Under Static Pressure

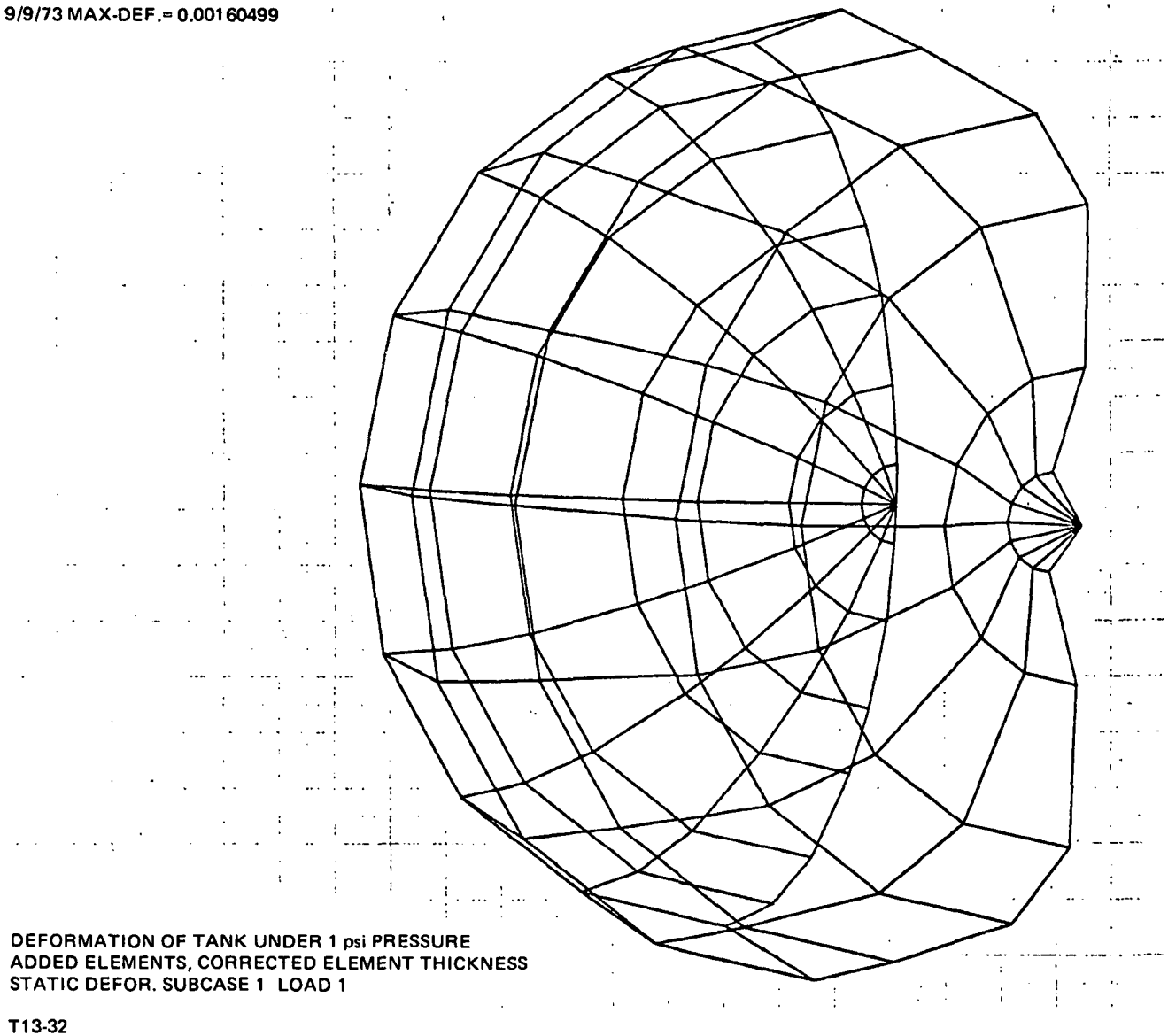

Fig. 3-21 Refined 9 Row LO_2 Tank Dome Under Static Pressure

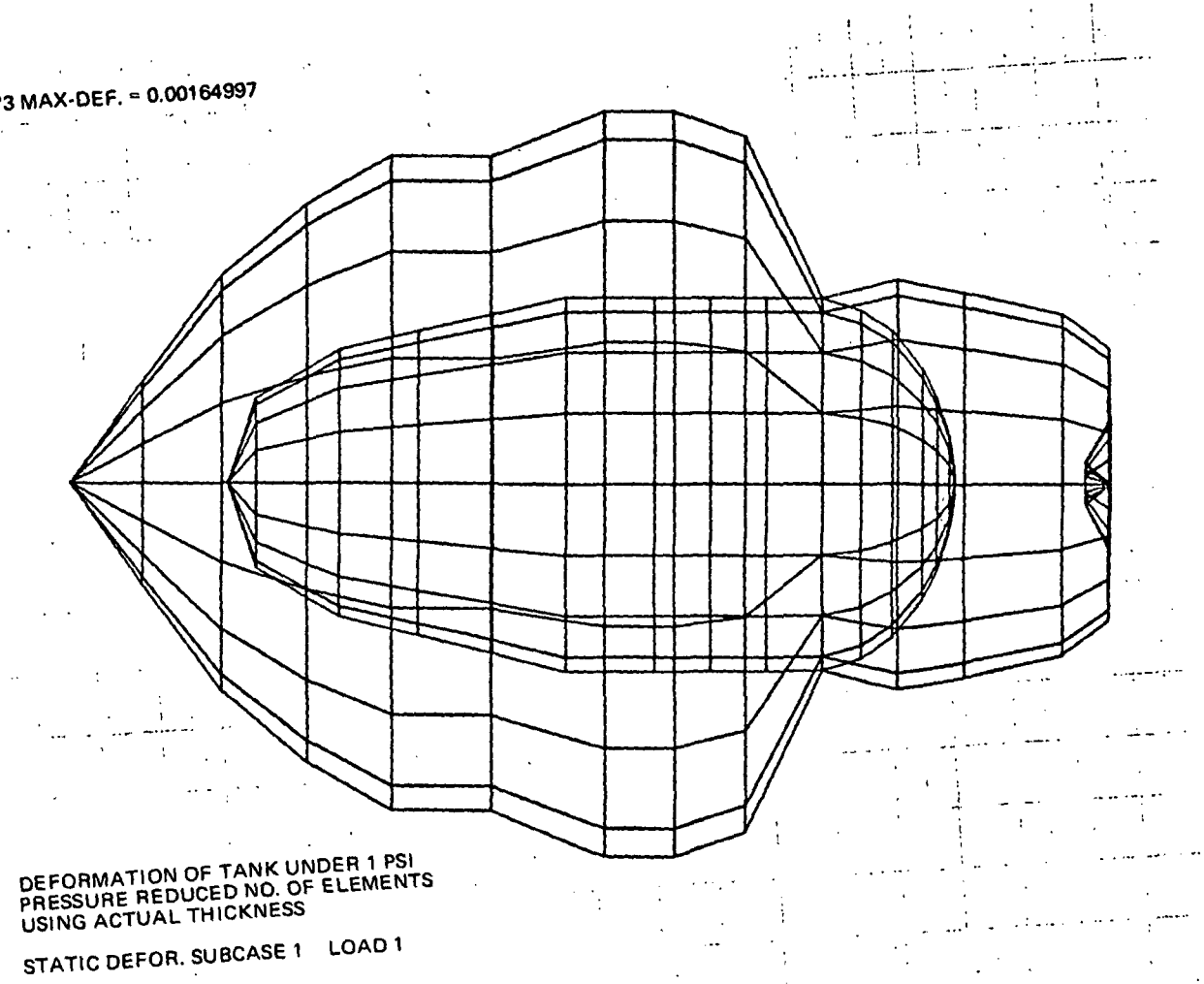

T13-33

Fig . 3-22 Tank with Revised 7 Row Dome Under Static Pressure

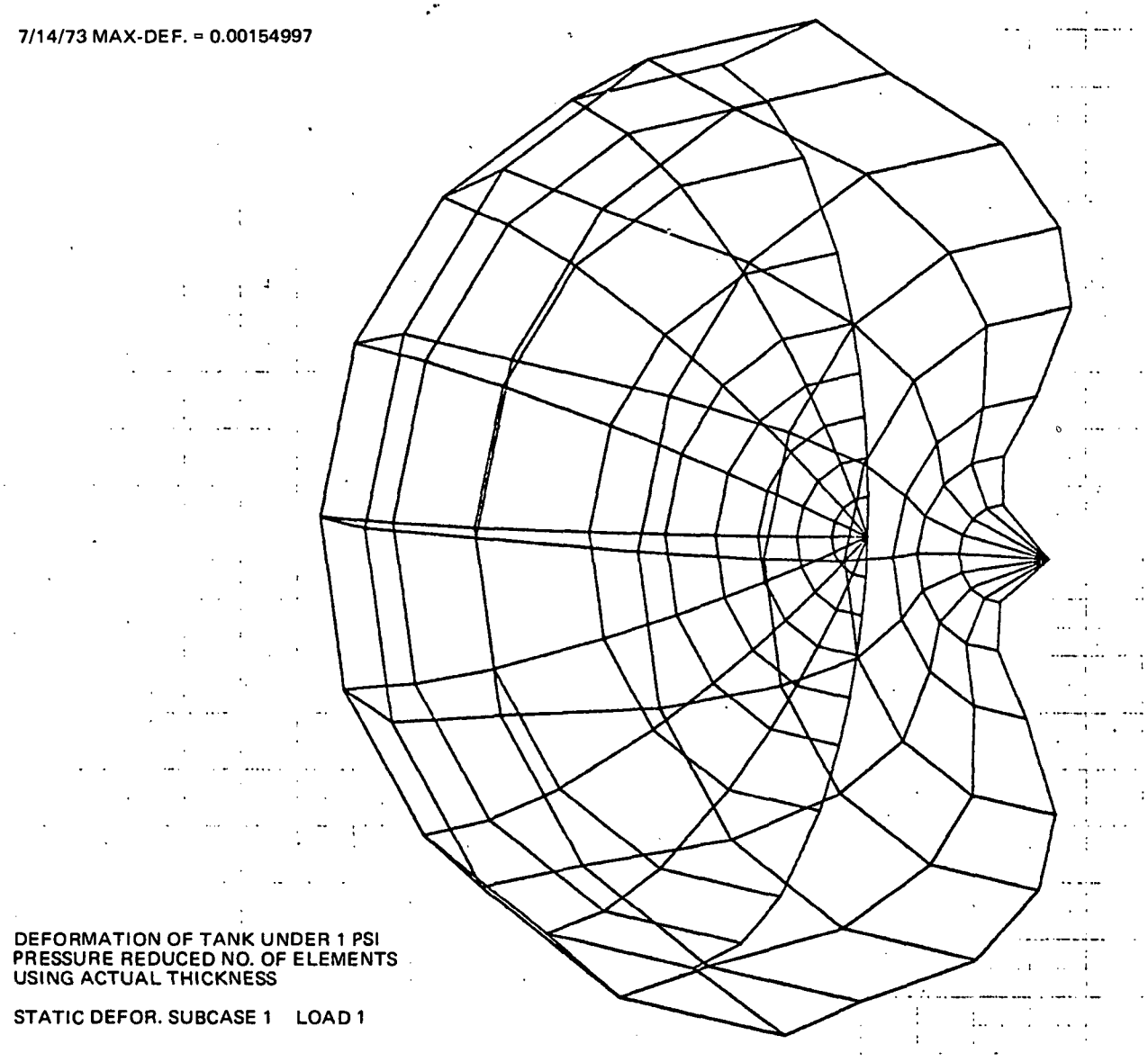

T13-34

Fig. 3-23 Revised 7 Row Tank Dome Under Static Pressure

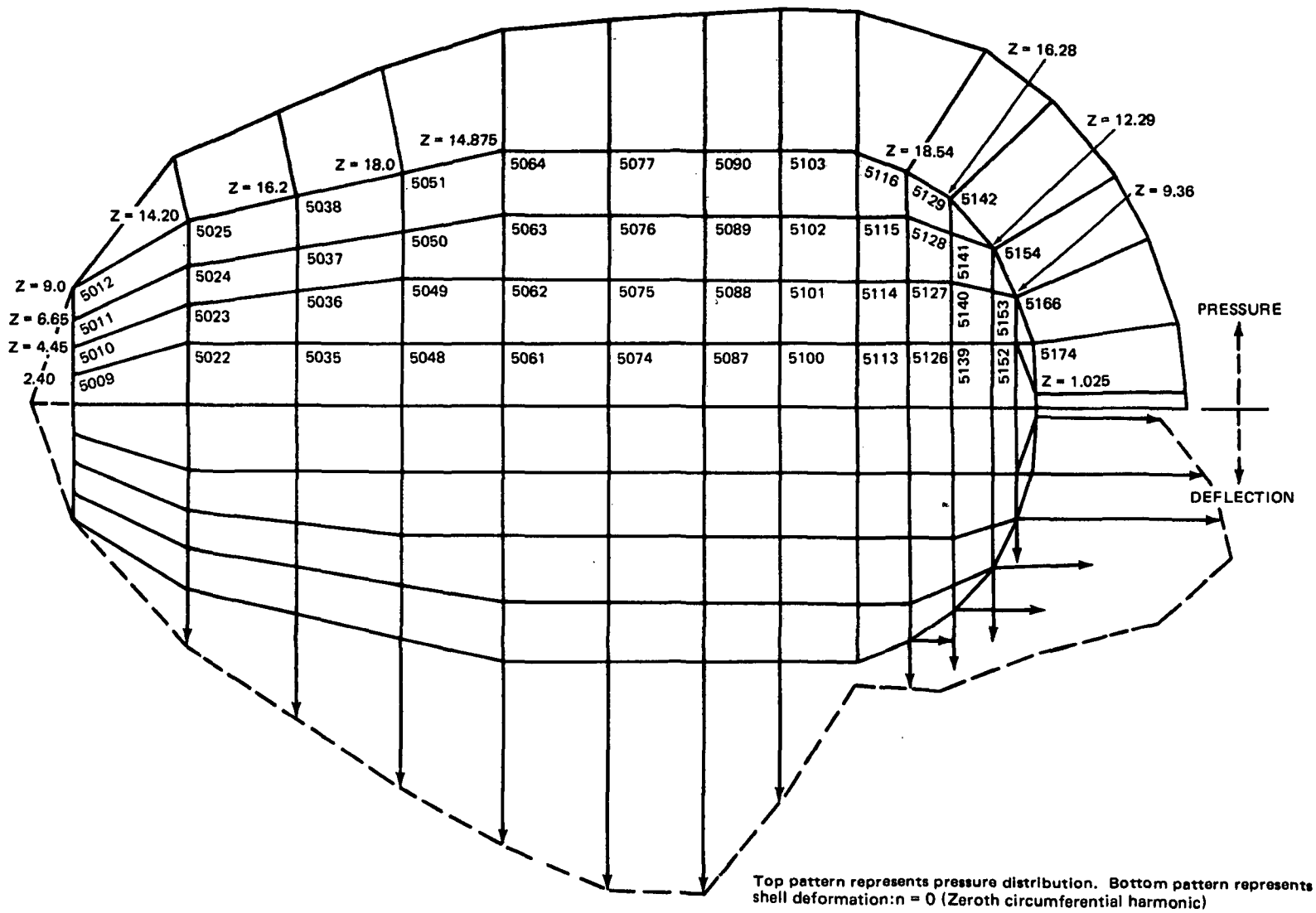

Top pattern represents pressure distribution. Bottom pattern represents shell deformation: n = 0 (Zeroth circumferential harmonic)

T13-35

Fig. 3-24 1/8-Scale Model LO_2 Tank Mode Shape at 23.1 Hz (Dome Revised)

3.3 REMAINDER OF EXTERNAL TANK

The intertank skirt, liquid hydrogen tank, and aft skirt were modeled using:

- CQUAD2 bending and membrane elements for the shell
- CBAR beam elements with offsets for the frames
- CONROD rod elements for the internal struts
- CONM concentrated masses to simulate fittings and non-structural weights.

MPC was used to restrain attachment locations intended for later use when coupling with the other parts of the NASTRAN model. Figures 3-25 and 3-26 show the model frames and shell.

The weight of this portion of the structure was calculated independently for comparison with the NASTRAN model. The weight calculated for half the structure was 67.8 lb compared to 66.2 lb for the NASTRAN model. The location of the center-of-gravity was calculated as 75.14 in. aft of the forward dome compared to 75.3 in. from the NASTRAN model. Free modes for the symmetric case were calculated for the structure without fluid loading. The first mode (Fig. 3-27) was predominantly bending while the second (Fig. 3-28) was a breathing mode with the central thinner portion of the liquid hydrogen tank deforming the most. The higher modes consisted primarily of local shell deformations of the central region. After the modes for the empty shell had been calculated, the weight of the hydrogen was distributed as non-structural mass. The resulting modes contained considerable panel motion and this procedure did not yield a satisfactory model. Therefore, it was decided to incorporate the hydrogen as a fluid using the hydroelastic capability.

Another separate study of the central portion of the liquid hydrogen tank was conducted using the STARS-2 shell vibration program. It was necessary to assume that the skin was of uniform 0.016 in. thickness in the region to use this program. Several analyses were made to determine whether local vibratory motion could be anticipated, and to estimate the effects of fluid pressure upon the shell frequencies.

These calculations, which are briefly summarized in Appendix A, consisted of determining modes and frequencies for:

- Effects of Pressure on Frequencies
  - Zero pressure
  - Fluid pressure
  - Ten times fluid pressure
- Effects of Edge Restraints
  - Fixed ends
  - Pinned ends
  - Free axially, pinned laterally

Results of the pressure variation are listed in Table A-1 of Appendix A. The effect of fluid pressure is less than 2%. Even an increase to ten times this pressure only raised the frequencies for the lowest mode ($n = 2$) by about 3% and the $n = 5$ mode by about 18%.

Results of the effects of edge restraints were interesting in that the mode shape for the pinned end conditions were characterized by deflections adjacent to the boundaries. These calculations summarized in Appendix A also demonstrated the susceptibility of this region of the tank to local vibration modes. The NASTRAN model of this region is probably too coarse for an adequate representation. This effect however is not considered significant in the overall modes of the combined shuttle and therefore could be neglected initially, particularly since the number of elements in the model were already too high.

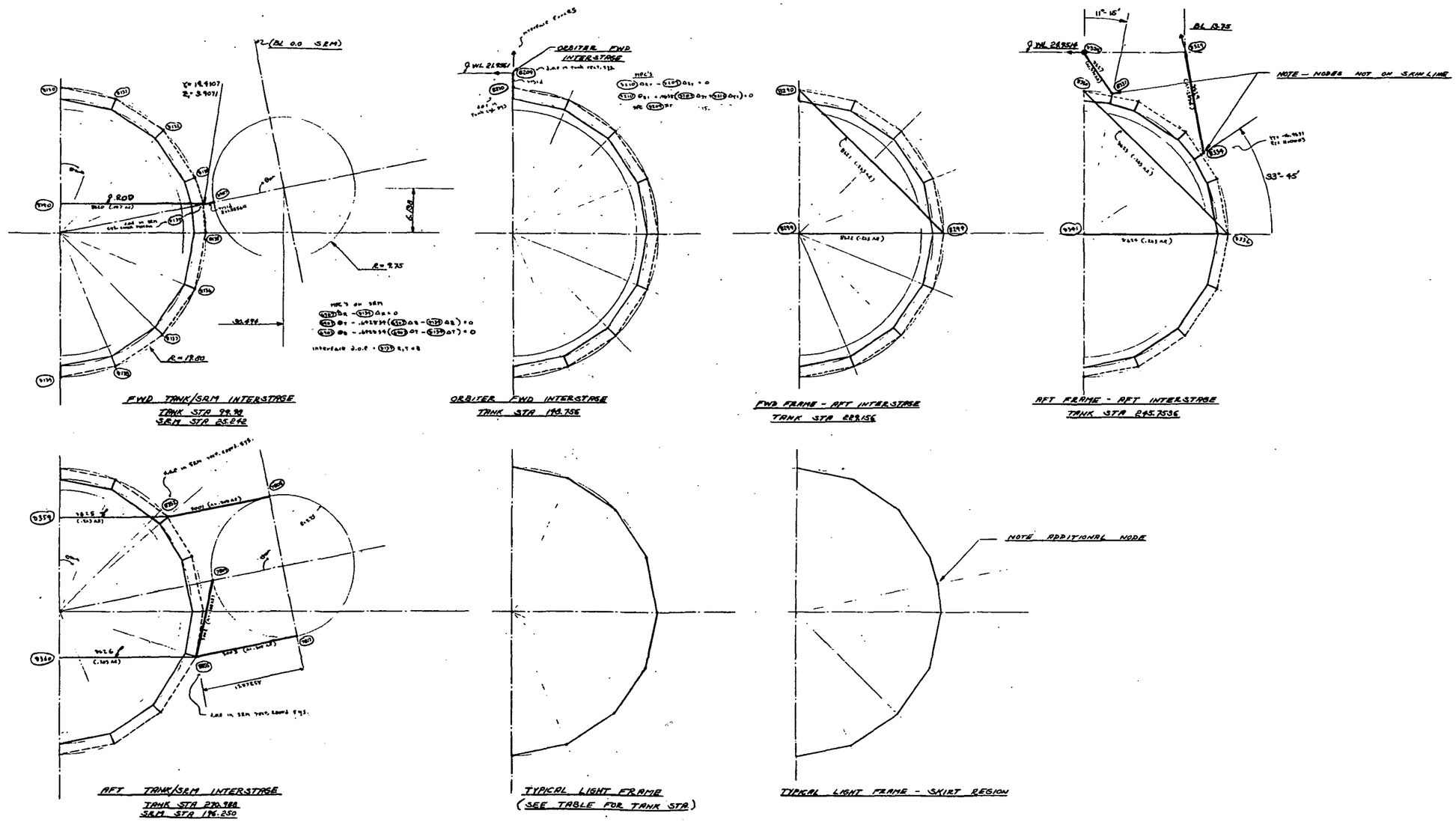

Fig. 3-25 NASTRAN Model of External Tank Frames for 1/8-Scale Shuttle Model

T13-37

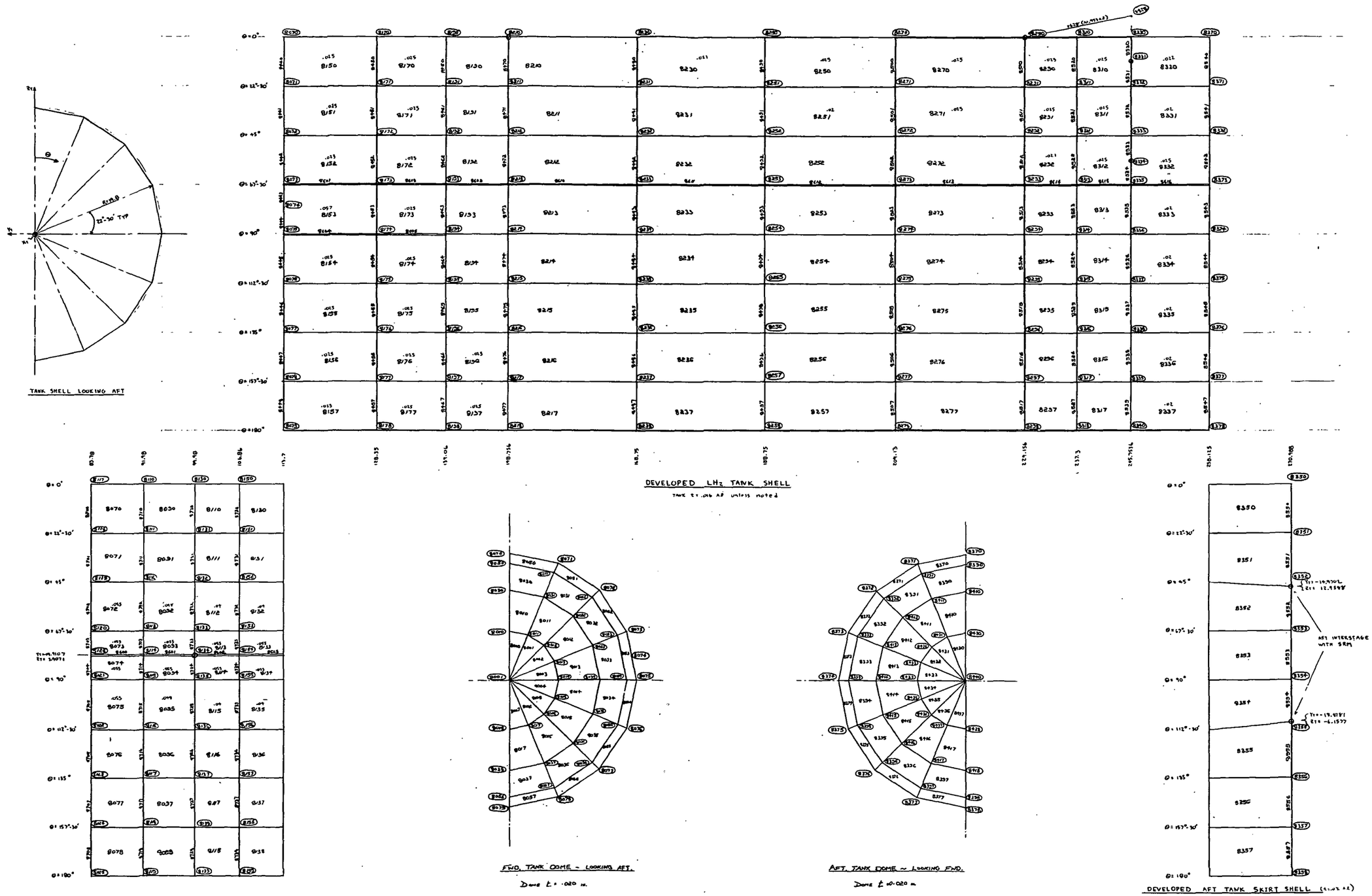

T13-37

Fig. 3-26 NASTRAN Model of External Tank Shell Structure for 1/8-Scale Shuttle Model

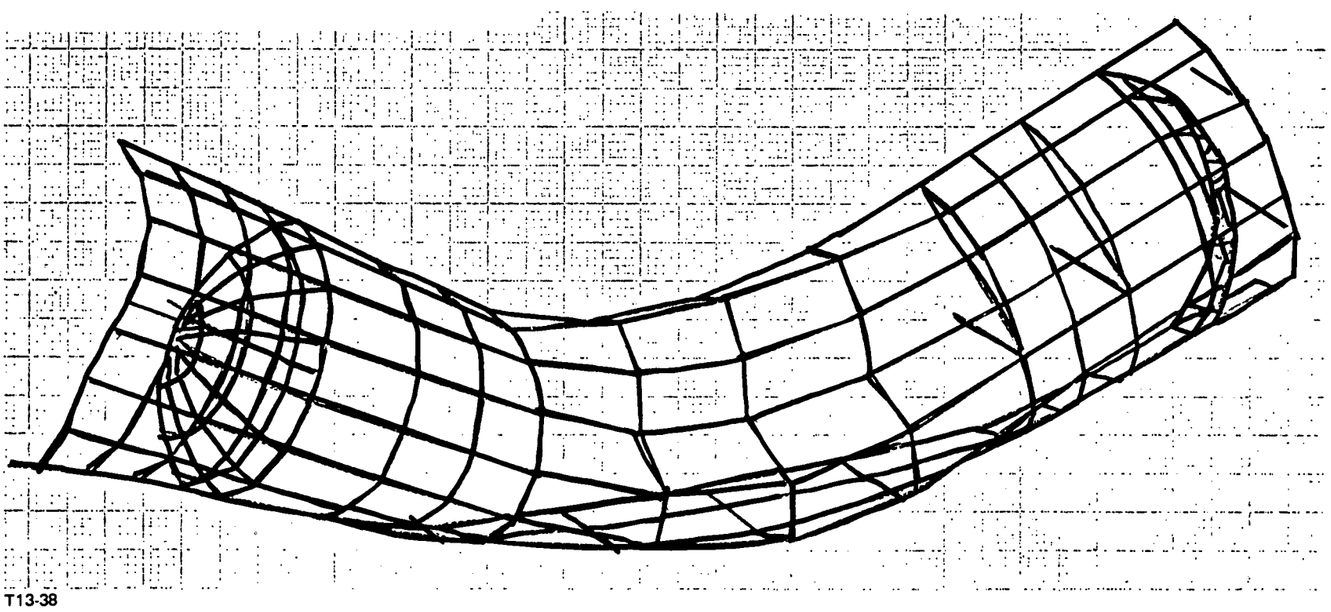

Fig. 3-27 1/8-Scale Model Liquid Hydrogen Tank, First Symmetric Mode — 139.25 Hz (Structure Only)

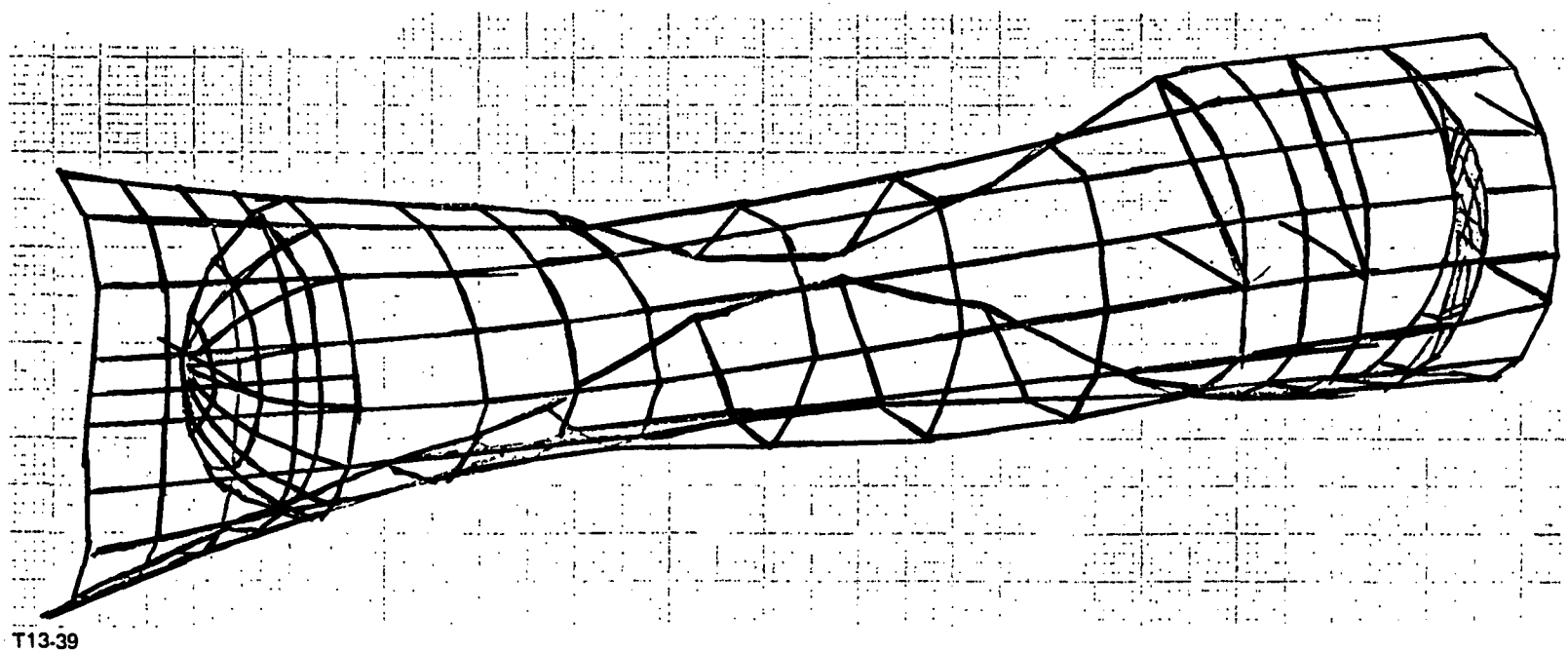

Fig. 3-28 1/8-Scale Model Liquid Hydrogen Tank, Second Symmetric Mode – 155.58 Hz (Structure Only)

3.4 COMPLETE MODEL OF EXTERNAL TANK

The data decks for both the hydrogen and oxygen tanks were joined together to form a single structure. The NASTRAN model is shown in Fig. 3-29. An attempt was made to run the hydroelastic analyses in Rigid Format 7 but NASTRAN time estimates indicated a cpu time in excess of 2 hours. A Rigid Format 3 run was made which effectively ignored the fluid and determined the modes for the empty structure. Five elastic modes were obtained which were primarily characterized as follows:

Frequency, Hz	Major Deformation
104.1	1st Bending
137.7	Breathing of LH_2 Tank
147.8	Local Shell Motion in LH_2 Tank
152.6	Local Shell Motion in LH_2 Tank
200.7	2nd Bending

The full model had also been submitted to Langley Research Center for computation on the CDC 6600 where it was determined that the problem was too large to be run.

In order to reduce the problem size, Guyan reduction was utilized and the problem was reduced to 412 DOF's and analyzed in Rigid Format 7. This version too ran out of time before extracting a root. The core requirements would have to be drastically reduced to avoid spillage and reduce time. Therefore, the READ module was substituted for the CEAD and a larger number of structural coordinates (1675 out of 2145 in the G set) were placed in the OMIT set leaving 198 DOF's in the A set. Only the zeroth fluid pressure harmonic was requested.

One eigenvalue was obtained at 45.2 Hz. A review of the mode indicated that in the cylindrical portions of the LO_2 and LH_2 tanks, radial motion occurred in higher order bending modes (i.e., 3 full waves about the circumference). Previous analyses of a small hemispherical tank, indicated that this radial pattern might be due to the coordinate reduction process and the problem was reformulated to retain more fluid loaded structural points. This was accomplished by including all interior fluid coordinates in OMIT set. In order to assure reasonable computer time the A set was kept at 252 DOF's which still required omitting many fluid loaded structural

grid points. The reformulated model was used to compute one low frequency mode, which now became 45.6 Hz. NASTRAN input data for this model is listed in Appendix C. Computer running times are listed in Table 3-4. The calculated modes for both models is similar, characterized primarily by longitudinal motion with the LO_2 tank and LH_2 tank moving in opposite directions. There is also some vertical bending as in the first mode of a free-free beam. The radial motion for both models, in the LH_2 tank light frame area is compared in Fig. 3-30. The motion on the reformulated model at one location where no structural elements were omitted, as shown on the bottom of the figure, is characterized as n = 1 circumferential motion as contrasted with the n = 3 motion for the original model shown in the upper part of the figure. Even with all interior fluid points in the OMIT set, the 224 remaining structural coordinates were not sufficient to avoid apparent anomalies in the tank sidewall motion. The mode shape for one location in the LO_2 tank in Fig. 3-31 presents two sets of adjacent grid points, 6 in. apart. At one station, motion in alternate points were in the OMIT set. The primary motion is similar along the Z-axis at both stations. The radial motion differs considerably, with the deflection at Station 71.78 in an N = 0 mode as anticipated, while that at Station 65.78 shows three full bending waves around the semi-circle. This variation in a mode where the pressure does not vary circumferentially (0th harmonic) is not convincing.

A more significant difference between the two models appears in the modal pressure coefficients. Table 3-5 presents a comparison at several locations in the LO_2 and LH_2 tanks. With only structural points omitted, the largest pressure occurs at the LO_2 tank bottom. When interior fluid points were omitted, the LO_2 tank bottom pressure was 7% less, LH_2 tank bottom pressure was 27% higher, and a pressure node surface occurs toward the top of the LO_2 tank. In addition to the LO_2 tank bottom pressure being lower, the generalized mass for the mode with interior fluid points in the OMIT set is twice as high (24.72 compared to 11.22). The tank bottom pressure response to an oscillating force at the SRB or Orbiter axial attachment points would be considerably lower (about 60%) for the mode calculated with omitted interior fluid points. This appears to be a significant difference between the models. Including fluid loaded structural coordinates in the OMIT set does not appear to give satisfactory model.

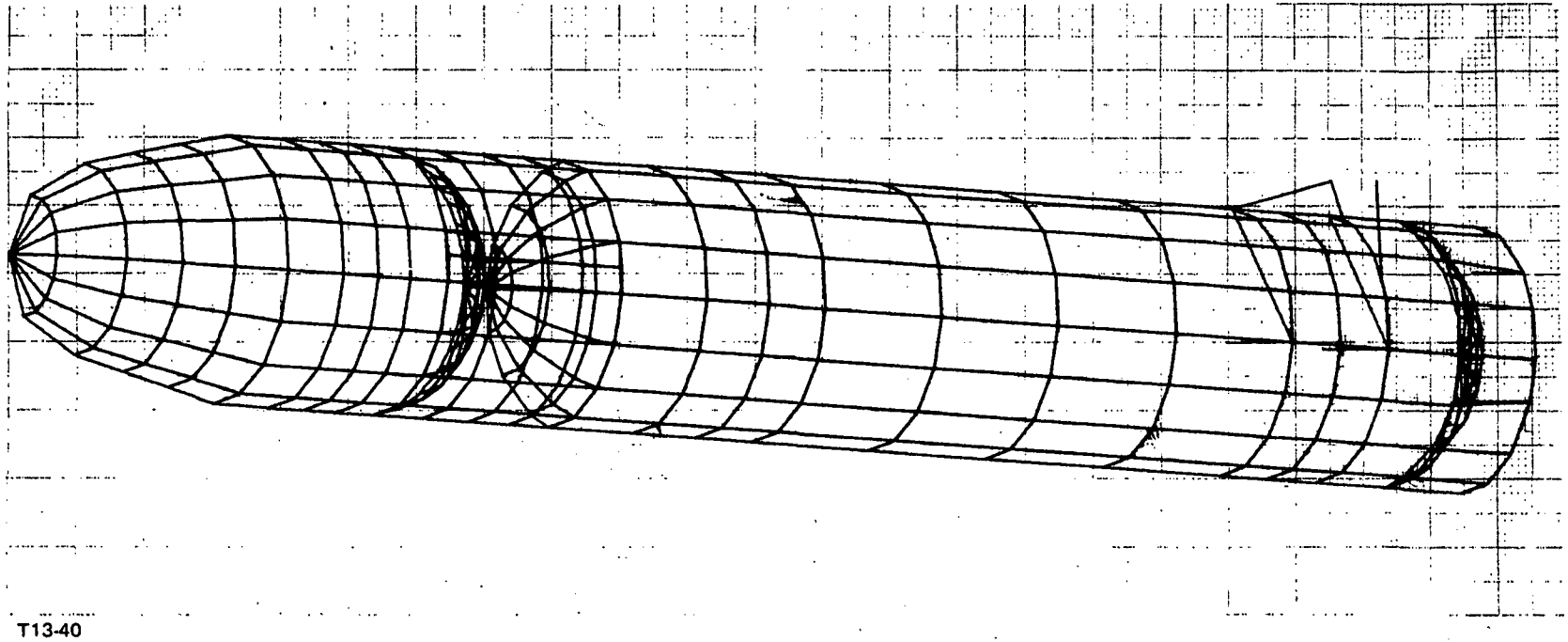

T13-40

Fig. 3-29 1/8-Scale Model External Tank NASTRAN Model

Table 3-4 Comparison of Computer Times for NASTRAN External Tank Hydroelastic Analysis

		Rigid Format 7 CEAD. OMIT Structure	READ(3) for CEAD. OMIT Structure Only	READ(3) for CEAD. OMIT Interior Fluid and Structure
Size of Analysis Sets	g	2145	2145	2145
	m	11	11	11
	n	2134	2134	2134
	s	262	262	262
	f	1872	1872	1872
	o	1460	1674	1620
	a (=d)	412	198	252
Time to SMP 1 Module – CPU (sec)		232	197	212
Elapsed (sec)		1135	1153	1566
% Full for Stiffness Matrix	K_{ff}(%)	2.4	2.4	2.4
Guyan Reduction	GO (%)	79	56.1	85.9
	K_{aa} (%)	63	32.6	79.6
Time to Reduce Stiffness	(In SMP 1)			
	CPU (sec)	982	307	458
	Elapsed (sec)	2577	1248	1006
% Full for Mass Matrices				
	M_{ff} (%)	0.1	0.1	0.1
	M_{aa} (%)	63	32.9	79.6
Time to Reduce Mass Matrix	(In SMP 2)			
	CPU (sec)	982	188	458
	Elapsed (sec)	2577	698	1006
Time from SMP 2 to GKAD				
	CPU (sec)	202	4	4
	Elapsed (sec)	647	1253	31
% Full for Dynamic Matrices				
	K_{dd} (%)	73.2	40.5	89.5
	M_{dd} (%)	63.7	40.9	89.5
Time in GKAD				
	CPU (sec)	1126	310	627
	Elapsed (sec)	4609	1253	1418
Time to do Eigenvalue Analysis				
Complex(1) (CEAD)	CPU (sec)	2354		
	Elapsed (sec)	23720		
Real (READ)	CPU (sec)		650	285
	Elapsed (sec)		2327	1706

T13-6(T)(1)

Table 3-4 Comparison of Computer Times for NASTRAN External Tank Hydroelastic Analysis (Cont)

(2)	Rigid Format 7 OMIT Structure	READ (3) for CEAD. OMIT Structure Only	READ (3) for CEAD. OMIT Interior Fluid and Structure
Total Time for Problem(5)			
CPU Time (min)	40	28.1	33.2
Channel Time (min)	279	11.8	33.4
Core Occupancy (Kbyte-hr)	2390	298.5	499.3

(1) Ran out of time; No eigenvalues found; Large spillage.

(2) All computer runs used 450 Kbytes of core.

(3) See Subsection 3.1 for demonstration problem showing substitution of READ module for CEAD, and eigenvalues and eigenvectors unchanged when omitting interior fluid points.

(4) Elapsed time indicates both input-output operations and delays due to other users occupying computer.

(5) All runs started from the same checkpoint tape 020951.

T13-6(T)(2)

Summary of Total NASTRAN Computing Time for External Tank

Item	Description	Debugging CPU Min	Debugging Sys Min	Debugging No. of Runs	Good Runs CPU Min	Good Runs Sys Min	Good Runs No. of Runs
I	**LOX TANK SYM. HYDRO-ELASTIC ANALYSIS** Using DET. method good runs gave 1 or 2 modes for 800 DOF (no omits)	96	250	12	150	904	10
	TOTAL TIME →				246	1154	22
II	**LH_2 TANK (LH_2 mass distributed to shell)** R.F.3						
	1. Symmetric Case (Phase 1) – INV gave 15 modes for 216 DOF	140	654	7	20	101	1
	2. Anti-symmetric Case (Phase 1) – INV gave 15 modes for 194 DOF	20	93	1	29	110	2
		160	747	8	49	211	3
	TOTAL TIME →				209	958	11
III	**COMBINED LOX AND LH_2 – SYM CASE**						
	1. No fluid – INV gave 10 modes for 130 DOF				36	141	3
	2. Fluid in LOX Only – DET gave 1 slosh mode	106	1555	7	30	250	1
	3. Fluid in Both – 1 mode after changing to INV for 412 DOF	99	1514	3	52	279	1
	(Not feasible to couple whole shuttle by this method)	205	3069	10	118	670	5
	TOTAL TIME →				323	3739	15

TT-192

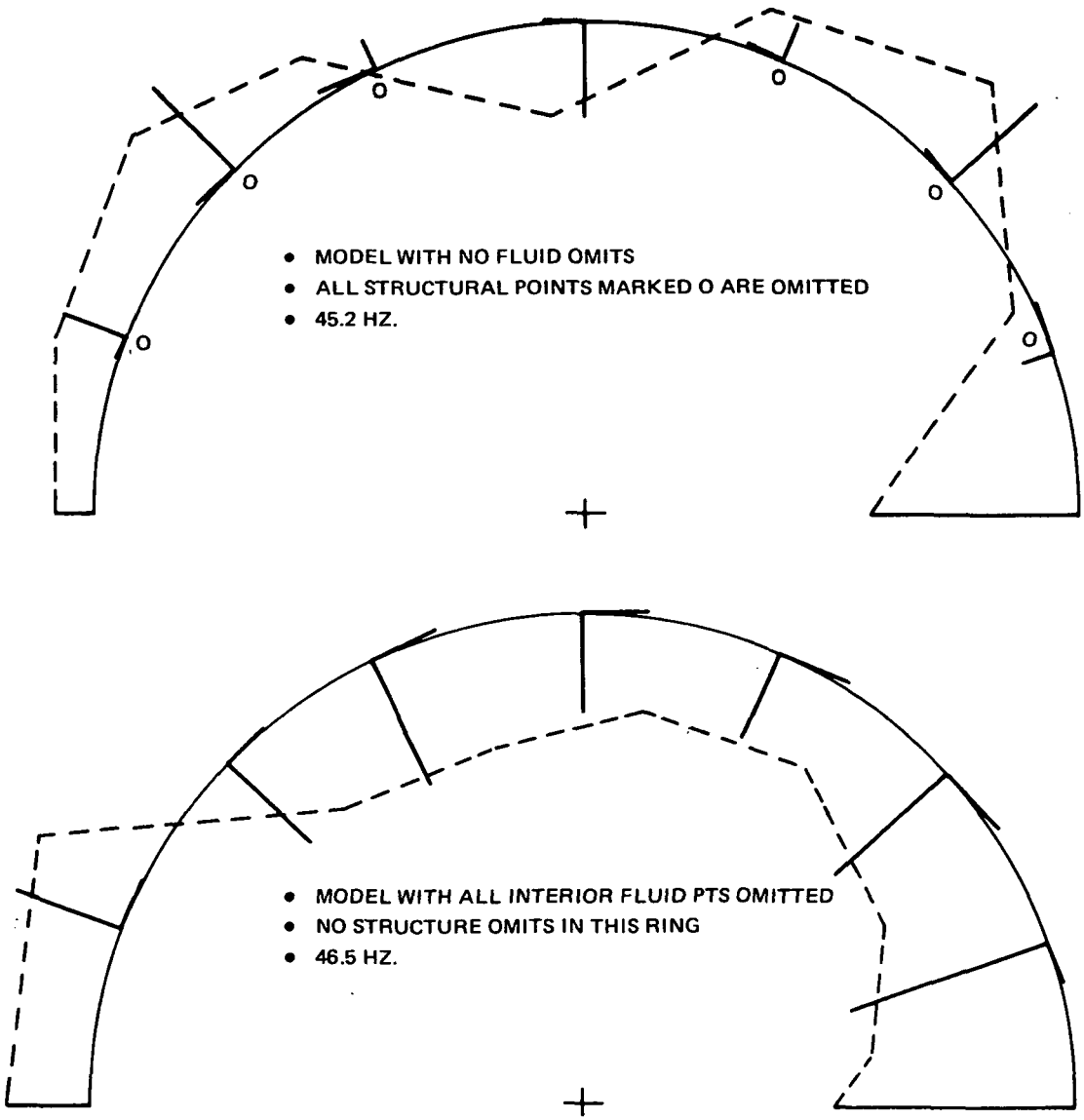

T13-41

Fig. 3-30 1/8-Scale Model External Tank – Comparison of Deflections of Light LH_2 Tank Ring at Station X 188.75

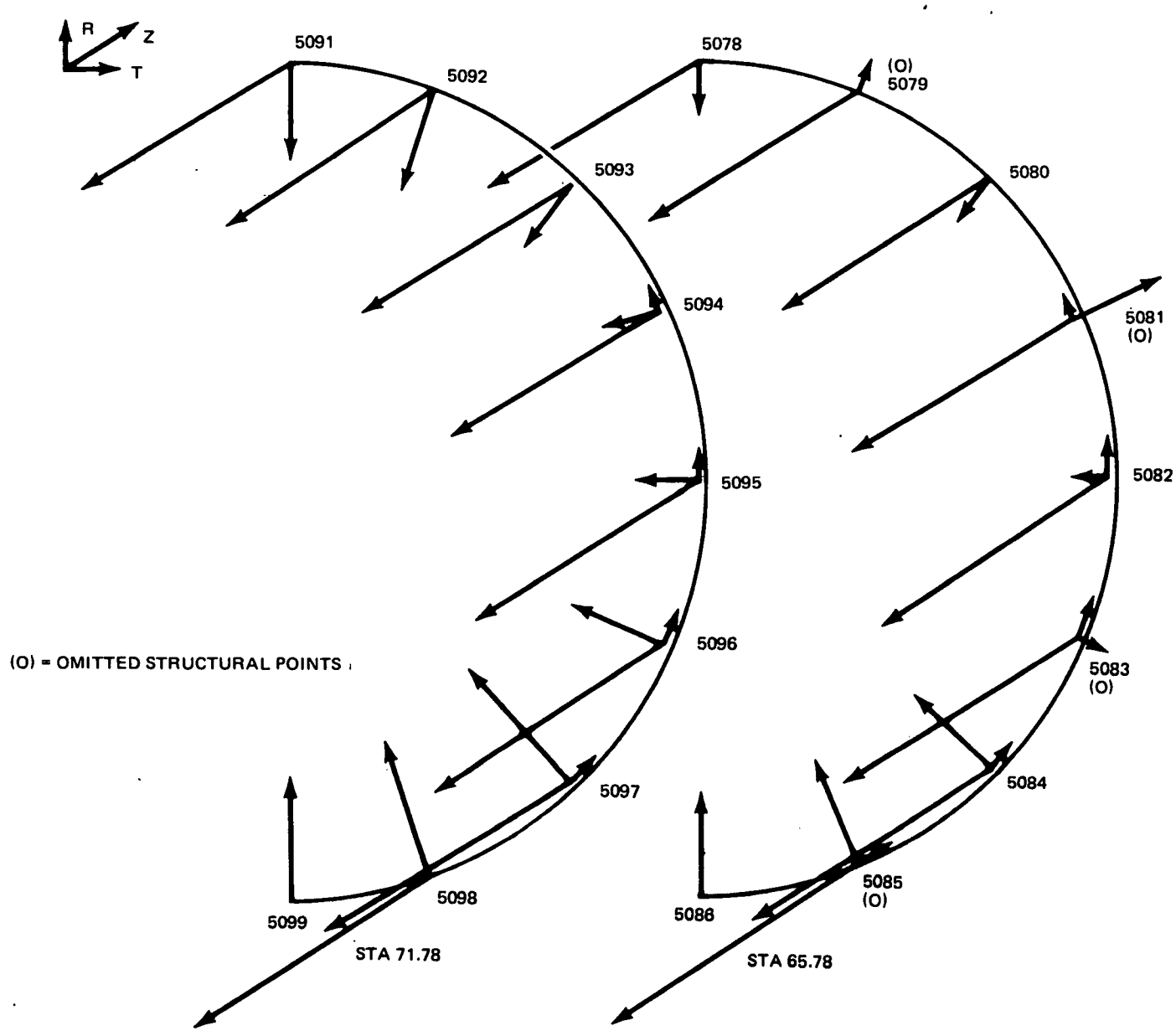

T13-42

Fig. 3-31 Comparison of Deflections on LO_2 Tank in 45.6 Hz Mode.

Table 3-5 Comparison of Tank Modal Pressures

Location	Tank	Distance		Modal Pressure	
		Axial From Bottom (inches)	Radial From Center Line (inches)	Interior Fluid Omits (45.6 Hz)	No Fluid Omits (45.2 Hz)
8439	LH_2	0	6.4	1.00	0.73
8419		3.5	6.4	0.99	0.72
8420		3.5	12.6	0.99	0.72
8399		8.5	6.4	0.97	0.72
8400		8.5	12.6	0.97	0.71
8401		8.5	17.9	0.97	0.71
8379		10.3	6.4	0.96	0.71
8380		11.3	12.6	0.96	0.71
8381		11.3	19.8	0.96	0.71
5178	LO_2	0	1.8	–.93	–1.00
5179		0.6	5.3	–.93	– .99
5165		1.3	5.0	–.88	– .97
5166		1.3	9.3	–.88	– .96
5152		3.4	5.0	–.85	– .95
5153		3.4	9.0	–.84	– .94
5154		3.4	12.3	–.83	– .93
5139		6.7	5.0	–.77	– .90
5140		6.7	10.0	–.76	– .89
5141		6.7	13.6	–.74	– .88
5142		6.7	16.3	–.73	– .87
5022		66.0	5.0	0.29	– .15
5023		66.0	7.8	0.32	– .15
5024		66.0	10.8	0.37	– .15
5025		66.0	14.2	0.47	– .16

T13-7(T)

Section 4
NASTRAN MODIFICATIONS

4 - NASTRAN MODIFICATIONS

4.1 DEVELOPMENT OF THE MODIFIED NASTRAN HYDROELASTIC ANALYSIS

A re-formulation of the NASTRAN hydroelastic analysis technique was developed on the basis of assumed fluid incompressibility for application in the study of liquid filled tank dynamics. The incompressible fluid formulation results in a set of algebraic equations relating the fluid bounding surface pressures to outward normal surface accelerations. Internal fluid pressures are dependent on surface pressures and (in the special case of negligible free surface gravitational potential) free surface displacements are dependent on structural interface displacements. The final representation of the fluid is in terms of a mass matrix which is symmetric, positive-definite, and directly related to the fluid kinetic energy. Expressed in terms of fluid/structure interface motion, this matrix is added to the structural mass matrix in a typical hydroelastic analysis problem. The form of the dynamic equations is the same as for an empty structure with the dynamic state completely determined by structural motion. Data such as surface pressure, internal pressure and free surface displacement are recoverable through algebraic relationships. Details of the basic theoretical development are presented in Appendix B1.

The re-formulated hydroelastic analysis utilizes the fluid finite elements in NASTRAN which describe relationships between circumferential harmonic pressure distributions and discrete displacements for polygons of revolution. These relationships have the potential of describing the fluid dynamics in an over-or-under determined sense; a consistent and more concise description is realized by constraining rings of grid points to displace in the harmonic shapes specified by the pressure DOF's. Since the displacements are vector quantities (3 displacements, 3 rotations per grid point) each component must be expressed in terms of harmonics as described in Appendix B2. The procedure described in Appendix B2 serves as an efficient general reduction scheme for structures of axisymmetric geometry (harmonic reduction). Implementation of harmonic reduction in NASTRAN is accomplished by

use of MPC's which relate physical grid displacements to harmonic grid displacements (the Fourier coefficients) defined by extra GRID or GRIDB cards. Due to the voluminous number of MPC statements required to define the harmonic reduction, an automatic transformation data generation program (HARM) has been written; a FORTRAN listing of HARM is presented in Appendix C. Harmonic reduction was initially demonstrated on a 60 degree spherical cap model for which natural frequencies resulting from Guyan reduction and harmonic reduction were compared to STARS-2 results (assumed exact). The results summarized in Appendix B2.3 indicate that harmonic reduction is inherently more accurate and efficient than Guyan reduction for this geometry.

Modification of the NASTRAN hydroelastic formulation was accomplished by utilization of ALTER-DMAP statements in Rigid Formats 7 and 3 for calculation of fluid matrix data and hydroelastic modes, respectively. Listings of the modified Rigid Formats are presented in Appendix C with bulk data for a basic checkout problem consisting of a circular cylinder with fluid. The results of elementary assembled hydroelastic analysis problems consisting of a fluid-filled hemispherical elastic container and a fluid-filled circular cylindrical shell are summarized in Appendix B3.

The results of this initial study clearly indicate the accuracy and efficiency inherent in the modified hydroelastic analysis for the two problems considered. Excellent agreement between finite element and exact analytical solutions was achieved.

4.2 ANALYSIS OF THE 1/8-SCALE EXTERNAL TANK

Upon verification of the re-formulated NASTRAN hydroelastic analysis, a study of 1/8-scale model ET dynamics was initiated. The structural and fluid models utilized were nearly identical to those discussed in the previous sections; the current mathematical model utilizes symmetric harmonics n = 0, 1, 2, 3 for the fluid. Normal and tangential motion of the tank surface is conveniently described in terms of local spherical and cylindrical reference frames. Harmonic reduction with harmonics n = 0, 1, 2, 3 retained, is utilized on the structural model with ultimate reduction to an analysis set of 128 outward normal harmonic DOF's.

Computational efficiency in the ET study is very good with the total run time per liquid level never exceeding 20 cpu min computation times plus 5 cpu min plot tape preparation (for approximately 130 plots) on Grumman's IBM 370/168 computer. In a typical run, 128 eigenvalues were extracted by the Givens method and the lowest 25 free-free mode shapes with modal pressure distributions computed. In the attempt to study ET dynamics with the old NASTRAN hydroelastic analysis, computation time was in excess of 70 cpu min with multiple submissions and only one eigenvalue and mode shape extracted by the unsymmetric inverse power method. Some further cost savings are anticipated due to checkpoint-restart capability; an inconsistency in Grumman's NASTRAN job control language (JCL) data, causing errors in checkpoint runs has recently been detected and corrected. By utilization of checkpointing in a first case liquid level NASTRAN run, structural and fluid data may be saved on tapes eliminating much of the computation time associated with preparation of matrix data common to all liquid levels. It is expected that the total running time per liquid level will be reduced to about 10 cpu min for cases subsequent to the initial run.

To date, three liquid fill conditions have been studied consisting of:

- Liftoff - $h_{LOX} = 75$ in., $h_{LH_2} = 141$ in.
- Post max Q - $h_{LOX} = 50$ in., $h_{LH_2} = 130$ in.
- Empty - $h_{LOX} = h_{LH_2} = 0$.

Modal data for each of these fill conditions is summarized in Tables 4-1 through 4-3 with dome pressure gain presented as a measure of POGO sensitivity (A derivation of the pressure gain parameter is presented in Appendix B4). CALCOMP plots of the current analysis mode shapes are presented in Fig. 4-1 through 4-72. Unrealistic behavior of the individual tank dome apexes is present in the liftoff configuration (Fig. 4-1 through 4-23) and in the post max Q configuration (Fig. 4-24 through 4-28). This localized behavior is eliminated by an "apex fix" in the post max Q configuration (Fig. 4-29 through 4-50) and in the empty configuration (Fig. 4-51 through 4-72) with negligible effect on natural frequencies. The apex fix consists of a set of MPC's forcing the apex and the set of grid points connected to it by triangular elements to move as a rigid body in the zeroth harmonic. *

- - - - -

* This should not be confused with the preliminary apex fix presented in Appendix B2.4.

In order to verify the current NASTRAN results, the dynamic pressure distributions in the first bending (Fig. 4-73) and axial modes (Fig. 4-74) were studied and found to be consistent with structural deformation and modal generalized mass. Additional confidence in the current analysis results was achieved upon comparison of the current empty tank modes presented in Fig. 4-51 through 4-53 with the few modes calculated in a previous analysis based on no reductions (Fig. 4-75 through 4-77). The frequency comparisons for this case are as follows:

Mode	"Exact" No Reductions	Harmonic Reduction
1st Bending	104.4	105.6
LH_2 Cylinder N = 3	151.6	153.0

T13-1(T)

The above comparisons indicate the accuracy associated with harmonic reduction applied to geometrically axisymmetric but structurally non-axisymmetric tanks. Analysis/test comparisons are currently in progress and will be fully documented in the Task 21 final report.

Table 4-1 1/8-Scale External Tank (ET) Hydroelastic Mode Summary (at Lift-off)

Mode No.	Freq. (Hz)	Modal Mass (lb-sec²/in)	Description of Mode	LOX Dome Pressure Gain x10³	LH_2 Dome Pressure Gain x10³
4 *	29.7	4.751	ET 1st Axial n=0	0.84	0.22
5	34.5	0.857	LOX n=2 (No Dome)	0.02	0.005
6 *	35.7	0.760	ET 1st Bending n=1	0.26	0.11
7	36.6	0.428	LOX n=3 (No Dome)	0.05	0.03
8 *	54.9	2.667	ET 2nd Axial n=0	0.43	0.59
9 *	57.8	0.131	LH_2 Cylinder n=2,3	0.10	0.12
10 *	61.4	0.067	LH_2 Cylinder n=3,2	0.11	0.22
11	62.1	0.395	LOX n=3 (No Dome)	0.07	0.03
12 *	63.8	0.520	ET 2nd Bending n=1	0.45	0.04
13	68.4	0.581	LOX n=2 (No Dome)	0.01	0.02
14 *	96.0	0.618	LOX n=1	0.66	0.005
15 *	96.1	0.433	LOX n=0	1.95	0.04
16 *	109.4	0.465	LOX, LH_2 n=0	1.00	0.18
17	114.5	0.741	LOX, LH_2 n=2,3	0.06	0.009
18	117.8	0.277	LOX n=3 (No Dome)	0.04	0.003
19 *	119.7	0.142	LH_2 Cylinder, LOX n=2,0	0.55	0.010
20 *	119.8	0.254	LOX n=0	1.78	0.11
21 *	124.2	0.221	LOX n=1	1.63	0.02
22	128.6	0.062	LH_2 Cylinder n=3	0.01	0.007
23 *	135.0	0.475	LOX n=0	0.97	0.16
24 *	135.9	0.431	ET, LOX Dome n=1,0	1.25	0.03
25	138.2	0.589	LOX n=2	0.04	0.01

* = POGO Sensitive Mode

Note: Modes 1, 2, 3 are Rigid Body Pitch Plane Modes

T13-8(T)

Table 4-2 1/8-Scale External Tank (ET) Hydroelastic Mode Summary (Post Max Q)

Mode No.	Freq. (Hz)	Modal Mass (lb-sec^2/in.)	Description of Mode	LOX Dome Pressure Gain x10^3	LH_2 Dome Pressure Gain x10^3
4	42.0	0.549	LOX n=2 (No Dome)	0.085	0.055
5	45.5	0.294	LOX n=3 (No Dome)	0.044	0.040
6 *	49.2	0.427	ET 1st Bending n=1	0.500	0.478
7 *	51.8	1.809	ET 1st Axial n=0	0.799	0.684
8	58.6	0.140	LH_2 Cylinder n=2, 3	0.041	0.034
9 *	61.7	0.074	LH_2 Cylinder n=3, 2	0.121	0.099
10 *	79.2	1.158	ET 2nd Axial n=0	0.529	0.256
11 *	79.7	1.135	ET 2nd Bending n=1	0.718	0.102
12	105.7	0.359	LOX n=2 (No Dome)	0.019	0.006
13	107.8	0.177	LOX n=3 (No Dome)	0.033	0.004
14 *	113.7	0.244	LOX n=0	2.72	0.033
15 *	120.7	0.160	LOX n=1, ET n=1	2.66	0.021
16 *	120.9	0.346	LOX n=0	1.28	0.215
17	125.5	0.126	LH_2 Cylinder n=3, 2	0.038	0.003
18	130.6	0.106	LH_2 Cylinder n=3, 2	0.085	0.014
19	144.6	0.396	LOX n=2	0.097	0.010
20 *	146.2	0.125	LOX n=1	2.59	0.057
21 *	148.6	0.338	LOX n=0	1.25	0.095
22	149.1	0.211	LOX n=3 (No Dome)	0.03	0.004
23 *	150.6	0.283	ET Bending, LOX Dome n=1	0.828	0.114
24 *	162.9	0.089	LOX n=2	0.911	0.008
25 *	167.8	0.079	LOX Dome, ET n=0	4.27	1.76

*=POGO Sensitive Mode

T13-9(T)

Table 4-3 Empty 1/8-Scale External Tank (ET) Mode Summary

Mode No.	Freq. (Hz)	Modal Mass (lb-sec^2/in.)	Description of Mode
4	105.6	0.0425	ET 1st Bending n=1
5	153.0	0.0094	LH_2 Cylinder n=3
6	161.7	0.0172	LH_2 Cylinder n=2, 3
7	226.0	0.0497	ET 2nd Bending n=1
8	257.8	0.0770	ET 1st Axial n=0
9	274.7	0.0271	LH_2 Cylinder n=2, 3
10	328.3	0.0122	LH_2 Cylinder, LOX n=3, 2
11	332.0	0.0149	LOX, LH_2 n=3, 2
12	332.8	0.0234	LOX, LH_2 n=3, 2
13	343.7	0.0118	ET n=3
14	357.8	0.0696	ET Bending n=1, 3
15	431.0	0.0210	LH_2 Cylinder n=2
16	459.1	0.0615	LH_2 Cylinder n=3, ET n=1
17	472.9	0.0114	LH_2 Cylinder n=3
18	482.2	0.0185	ET n=2
19	498.6	0.0076	LOX n=3
20	513.2	0.0697	ET n=1, 2, 3
21	533.1	0.0243	ET n=2, 1
22	567.2	0.0487	ET n=1, 2, 3
23	604.6	0.0391	ET n=2, 1, 3
24	625.4	0.0116	LOX n=3
25	628.0	0.0144	ET n=3, 2

T13-10(T)

HARMONIC REDUCTION
UNDEFORMED SHAPE

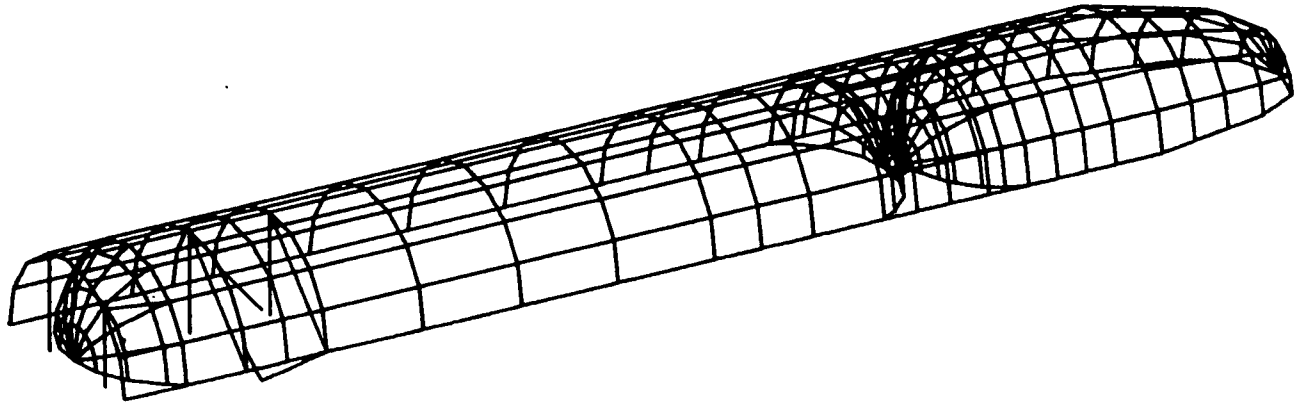

T13-51

Fig. 4-1 External Tank With Fluid, Liftoff Configuration

HARMONIC REDUCTION
MODAL DEFORMATION – SUBCASE 1 MODE 4 EIGENVALUE = 34936 (RADIANS/SEC)²

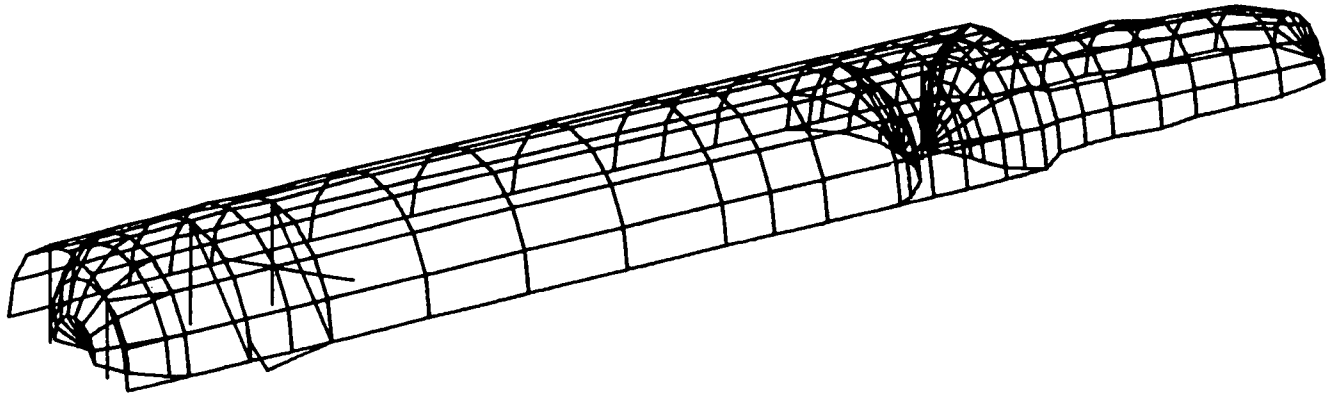

T13-52

Fig. 4-2 External Tank With Fluid, Liftoff Configuration

HARMONIC REDUCTION
MODAL DEFORMATION – SUBCASE 1 MODE 5 EIGENVALUE = 46981 (RADIANS/SEC)^2

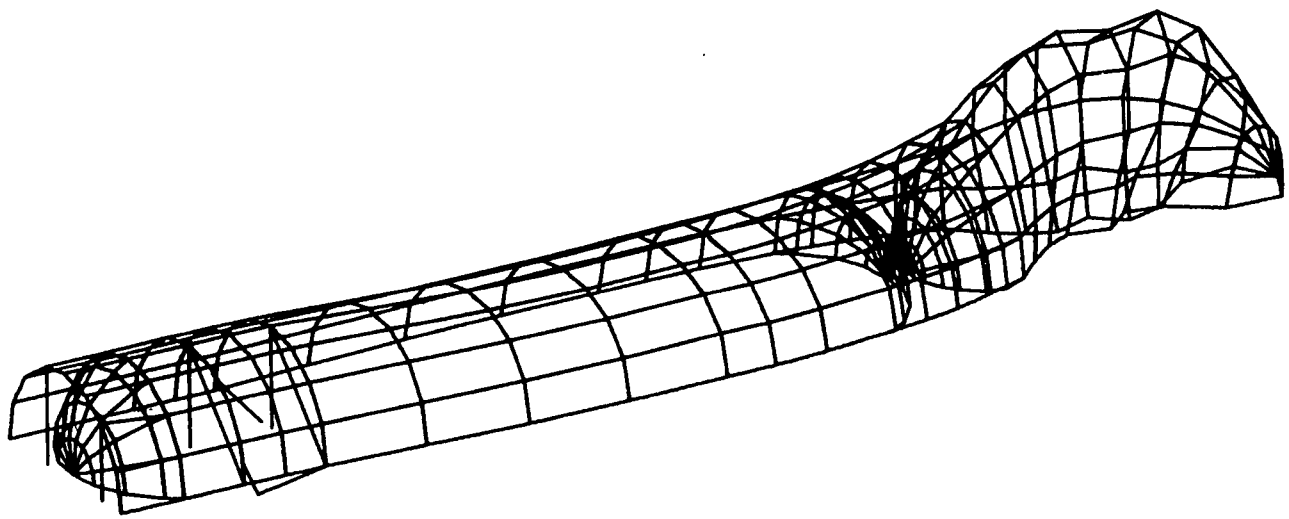

T13-53

Fig. 4-3 External Tank With Fluid, Liftoff Configuration

HARMONIC DEFORMATION
MODAL DEFORMATION – SUBCASE 1 MODE 6 EIGENVALUE = 50367 (RADIANS/SEC)^2

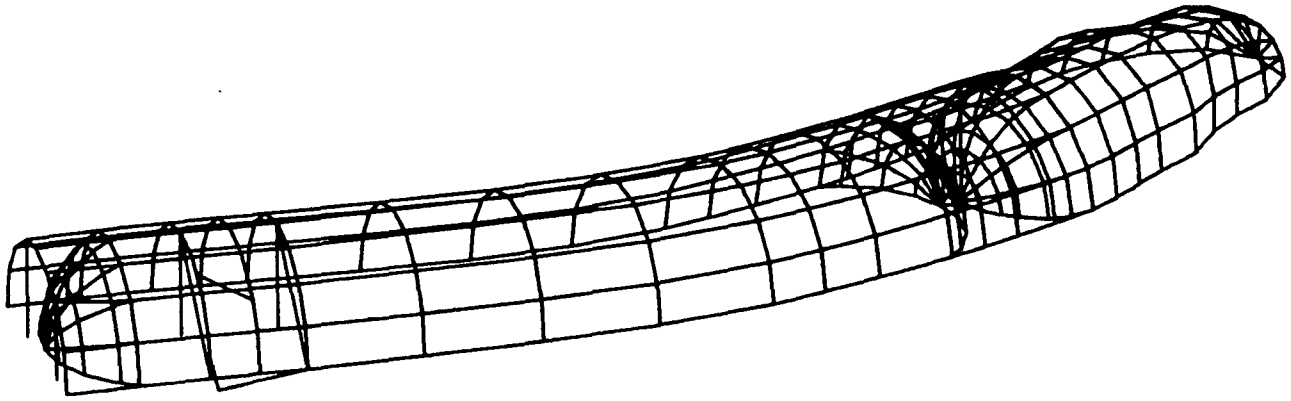

T13-54

Fig. 4-4 External Tank With Fluid, Liftoff Configuration

HARMONIC REDUCTION
MODAL DEFORMATION – SUBCASE 1 MODE 7 EIGENVALUE = 53045 (RADIANS/SEC)^2

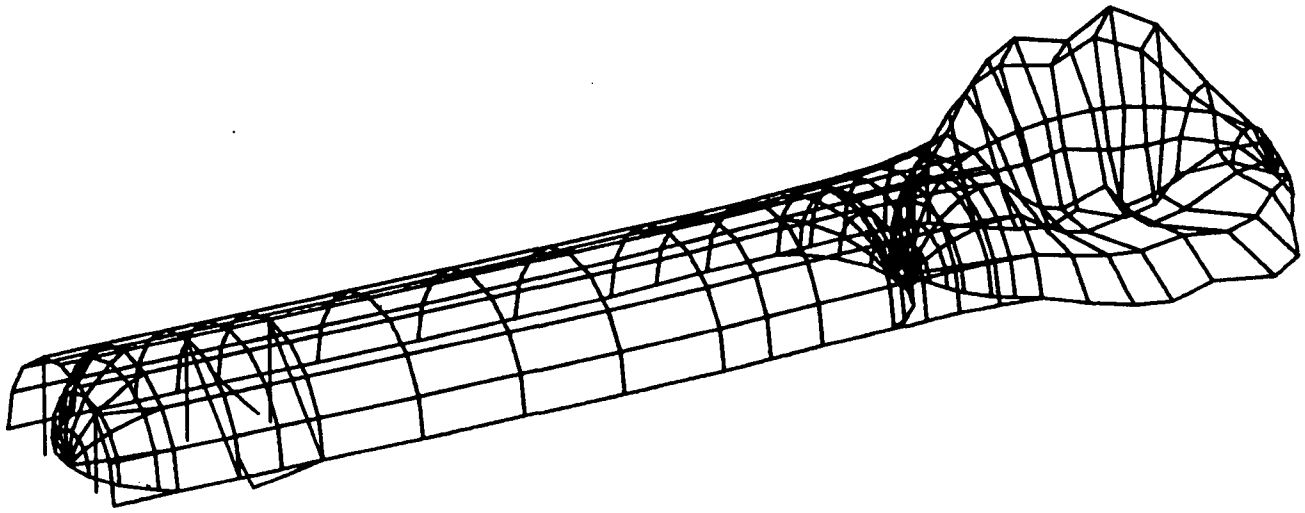

T13-55

Fig. 4-5 External Tank With Fluid, Liftoff Configuration

HARMONIC REDUCTION
MODAL DEFORMATION – SUBCASE 1 MODE 8 EIGENVALUE = 118959 (RADIANS/SEC)²

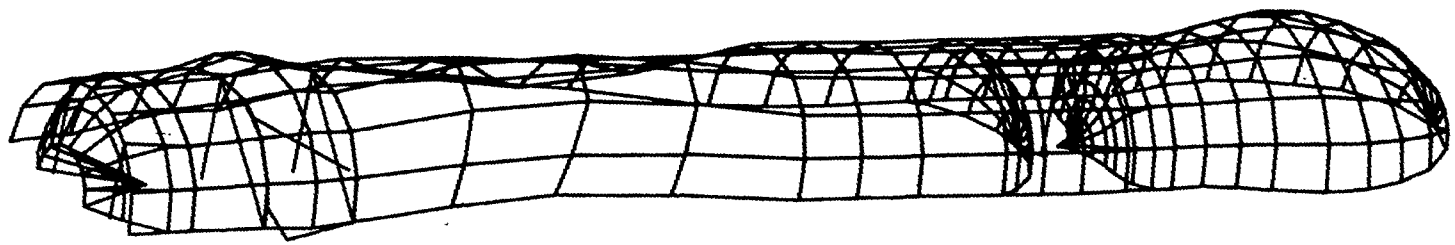

T13-56

Fig. 4-6 External Tank With Fluid, Liftoff Configuration

HARMONIC REDUCTION
MODAL DEFORMATION – SUBCASE 1 MODE 9 EIGENVALUE = 132080 (RADIANS/SEC)²

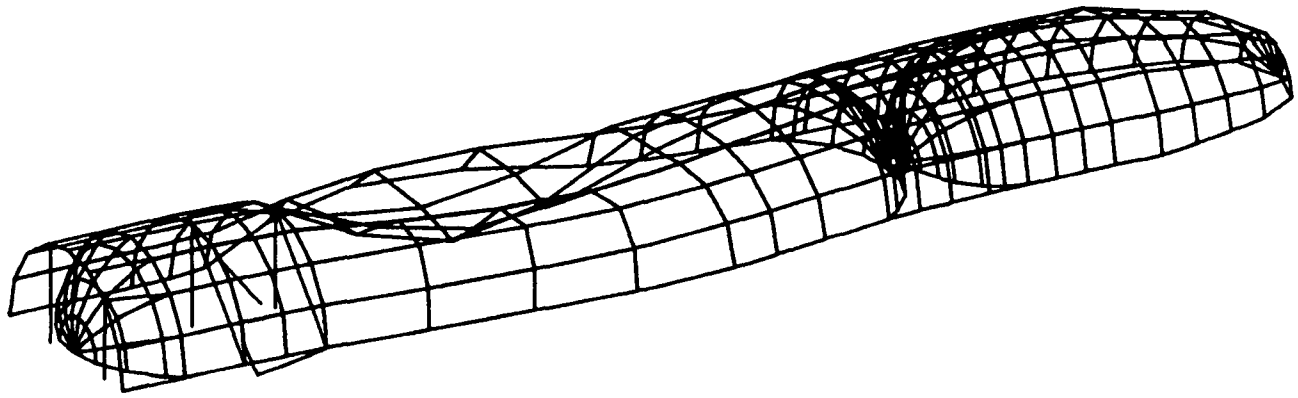

T13-57

Fig. 4-7 External Tank With Fluid, Liftoff Configuration

HARMONIC REDUCTION
MODAL DEFORMATION -- SUBCASE 1 MODE 10 EIGENVALUE = 148882 (RADIANS/SEC)^2

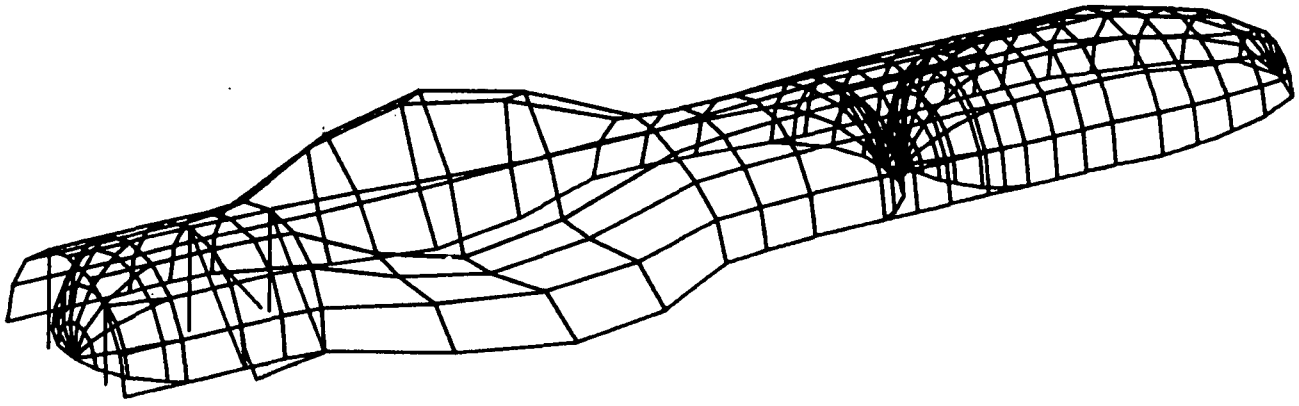

.T13-58

Fig. 4-8 External Tank With Fluid, Liftoff Configuration

HARMONIC REDUCTION
MODAL DEFORMATION – SUBCASE 1 MODE 11 EIGENVALUE = 162007 (RADIANS/SEC)^2

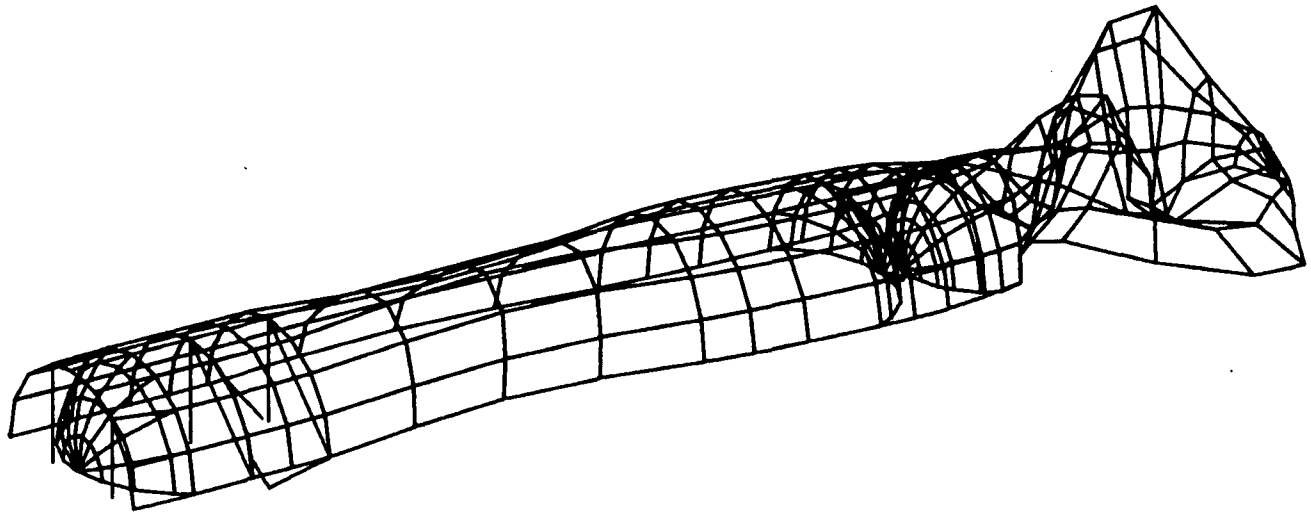

T13-59

Fig. 4-9 External Tank With Fluid, Liftoff Configuration

HARMONIC REDUCTION
MODAL DEFORMATION – SUBCASE 1 MODE 12 EIGENVALUE = 160621 (RADIANS/SEC)²

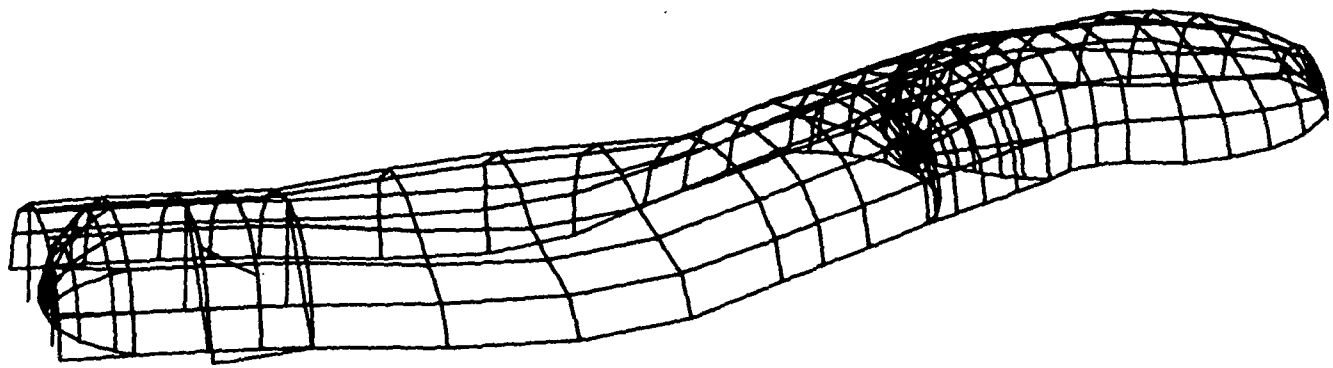

T13-60

Fig. 4-10 External Tank With Fluid, Liftoff Configuration

HARMONIC REDUCTION
MODAL DEFORMATION – SUBCASE 1 MODE 13 EIGENVALUE = 184897 (RADIANS/SEC)^2

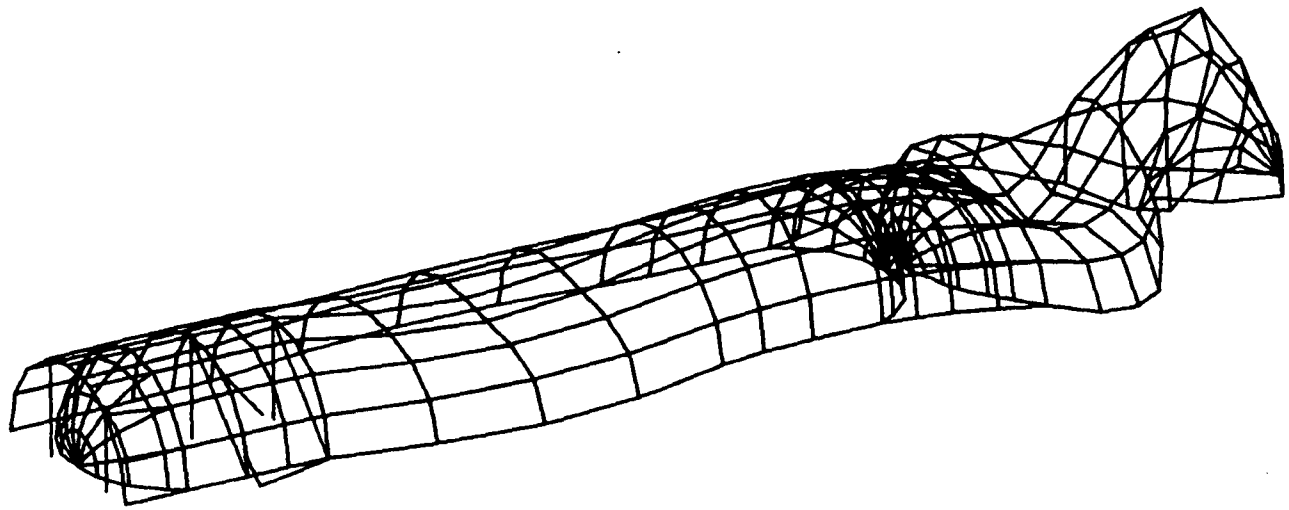

T13-61

Fig. 4-11 External Tank With Fluid, Liftoff Configuration

HARMONIC REDUCTION
MODAL DEFORMATION – SUBCASE 1 MODE 14 EIGENVALUE = 363684 (RADIANS/SEC)²

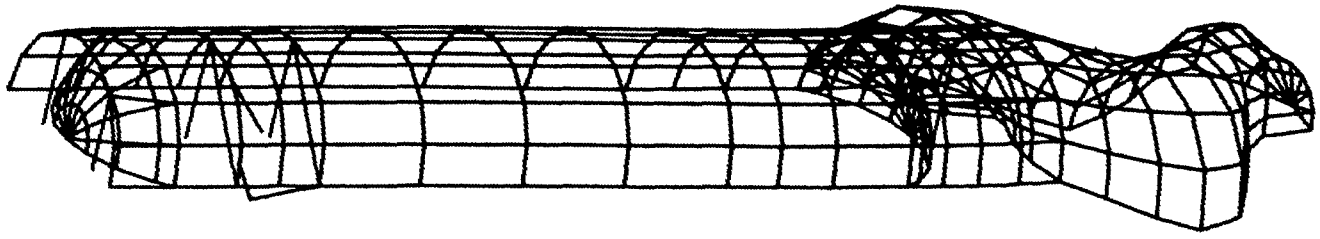

T13-62

Fig. 4-12 External Tank With Fluid, Liftoff Configuration

HARMONIC REDUCTION
MODAL DEFORMATION – SUBCASE 1 MODE 15 EIGENVALUE = 364909 (RADIANS/SEC)²

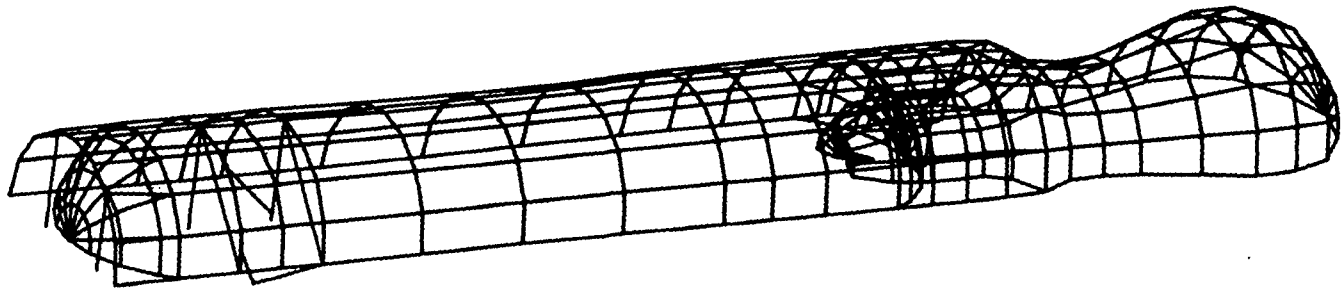

T13-63

Fig. 4-13 External Tank With Fluid, Liftoff Configuration

HARMONIC REDUCTION
MODAL DEFORMATION – SUBCASE 1 MODE 16 EIGENVALUE = 472148 (RADIANS/SEC)^2

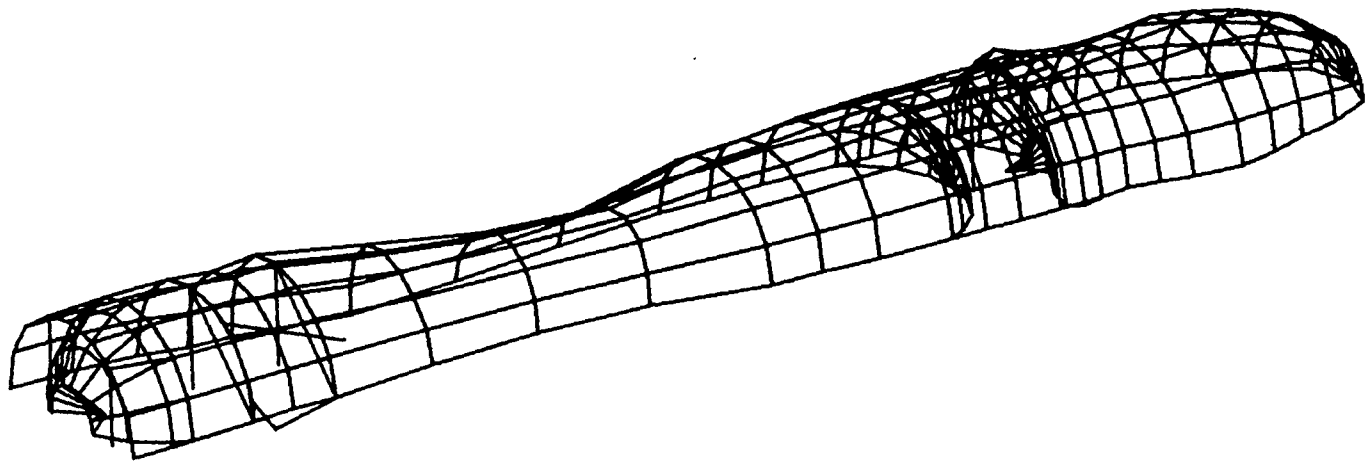

Fig. 4-14 External Tank With Fluid, Liftoff Configuration

T13-64

HARMONIC REDUCTION
MODAL DEFORMATION – SUBCASE 1 MODE 17 EIGENVALUE = 517366 (RADIANS/SEC)^2

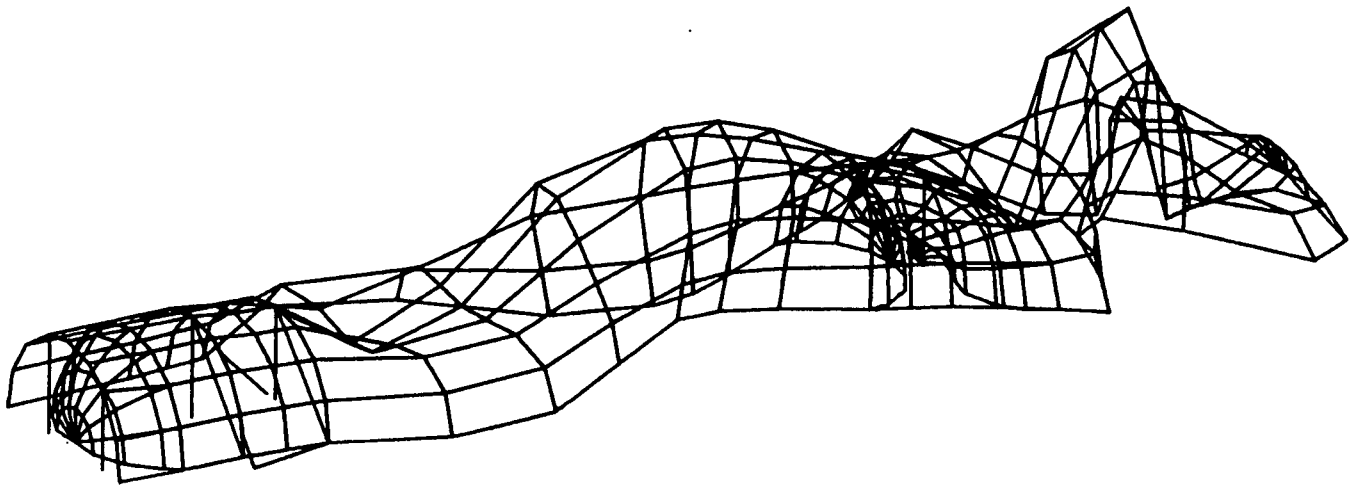

T13-65

Fig. 4-15 External Tank With Fluid, Liftoff Configuration

HARMONIC REDUCITON
MODAL DEFORMATION – SUBCASE 1 MODE 18 EIGENVALUE = 548146 (RADIANS/SEC)^2

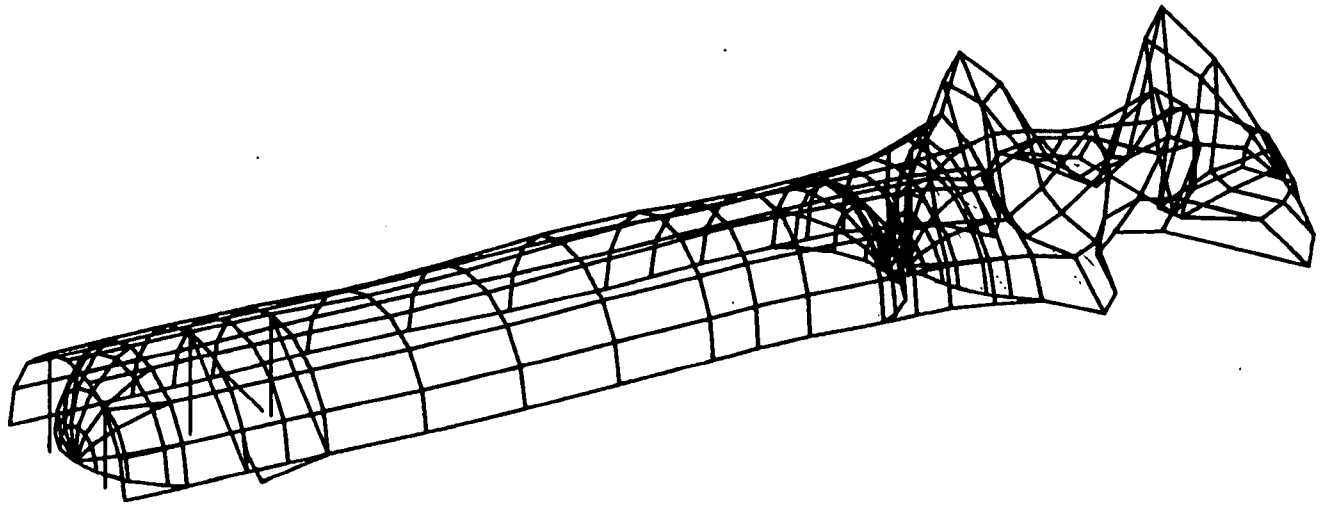

T13-66

Fig. 4-16 External Tank With Fluid, Liftoff Configuration

HARMONIC REDUCTION
MODAL DEFORMATION – SUBCASE 1 MODE 19 EIGENVALUE = 565369 (RADIANS/SEC)^2

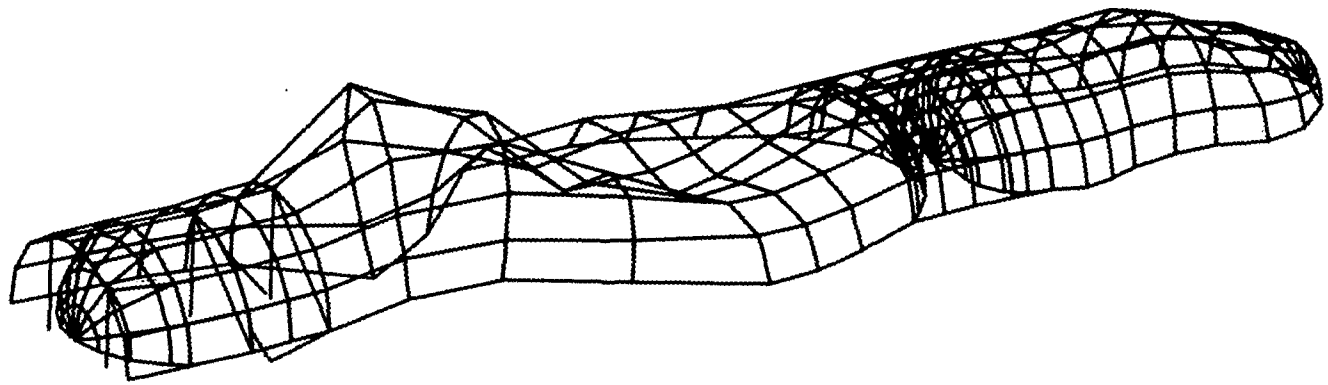

T13-67

Fig. 4-17 External Tank With Fluid, Liftoff Configuration

HARMONIC REDUCTION
MODAL DEFORMATION – SUBCASE 1 MODE 20 EIGENVALUE = 566502 (RADIANS/SEC)^2

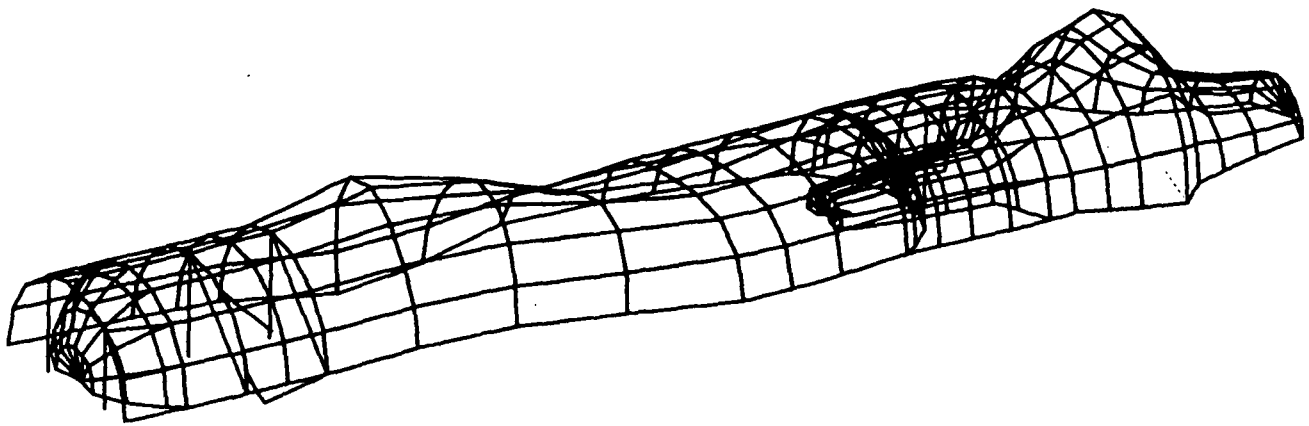

T13-68

Fig. 4-18 External Tank With Fluid, Liftoff Configuration

HARMONIC REDUCTION
MODAL DEFORMATION – SUBCASE 1 MODE 21 EIGENVALUE = 609237 (RADIANS/SEC)^2

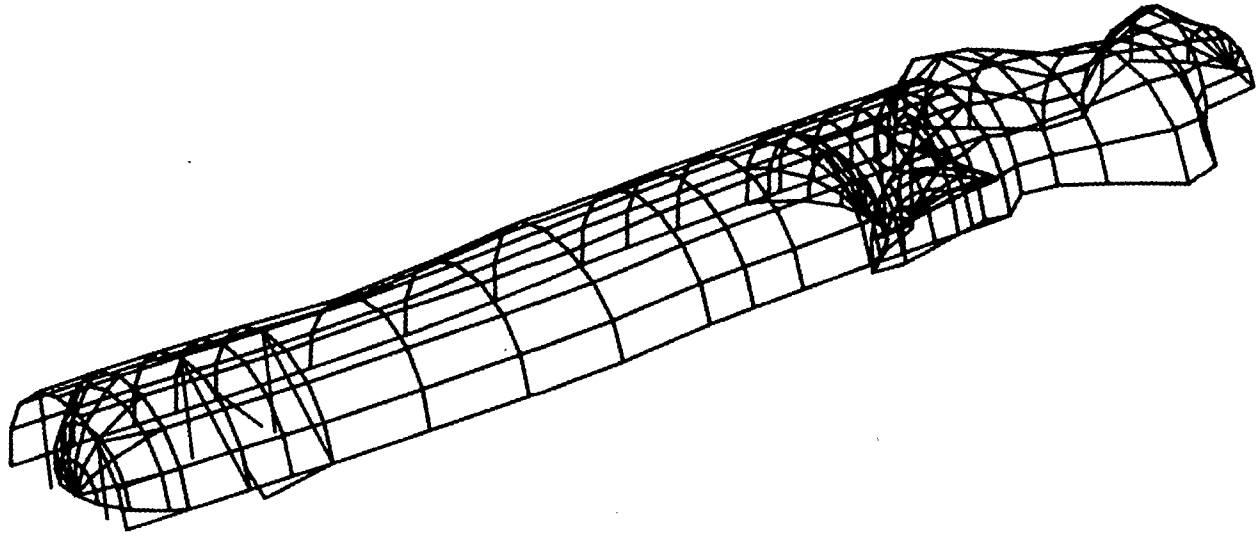

Fig. 4-19 External Tank With Fluid, Liftoff Configuration

T13-69

HARMONIC REDUCTION
MODAL DEFORMATION – SUBCASE 1 MODE 22 EIGENVALUE = 662844 (RADIANS/SEC)²

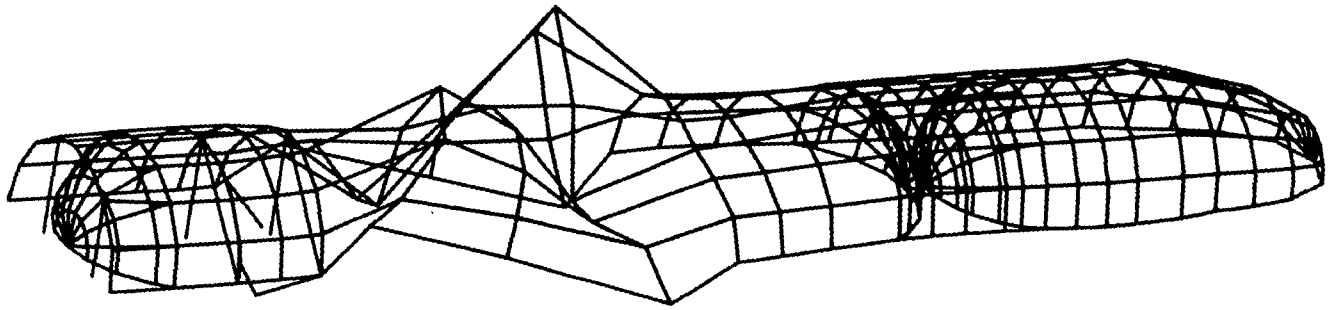

T13-70

Fig. 4-20 External Tank With Fluid, Liftoff Configuration

HARMONIC REDUCTION
MODAL DEFORMATION – SUBCASE 1 MODE 23 EIGENVALUE = 719923 (RADIANS/SEC)^2

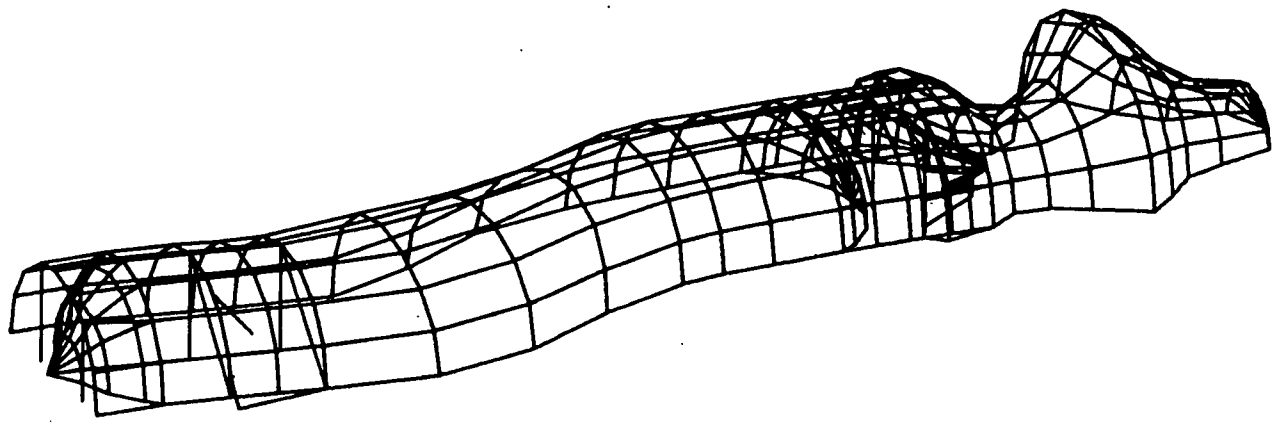

T13-71

Fig. 4-21 External Tank With Fluid, Liftoff Configuration

HARMONIC REDUCTION
MODAL DEFORMATION – SUBCASE 1 MODE 24 EIGENVALUE = 728992 (RADIANS/SEC)²

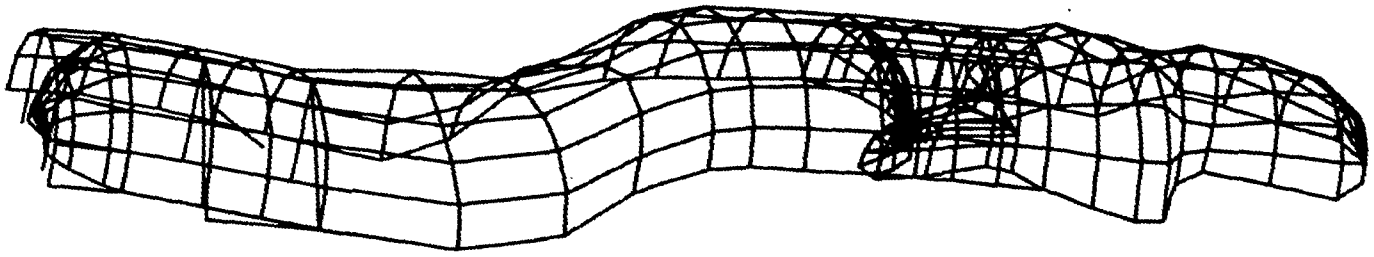

T13-72

Fig. 4-22 External Tank With Fluid, Liftoff Configuration

HARMONIC REDUCTION
MODAL DEFORMATION – SUBCASE 1 MODE 25 EIGENVALUE = 754276 (RADIANS/SEC)^2

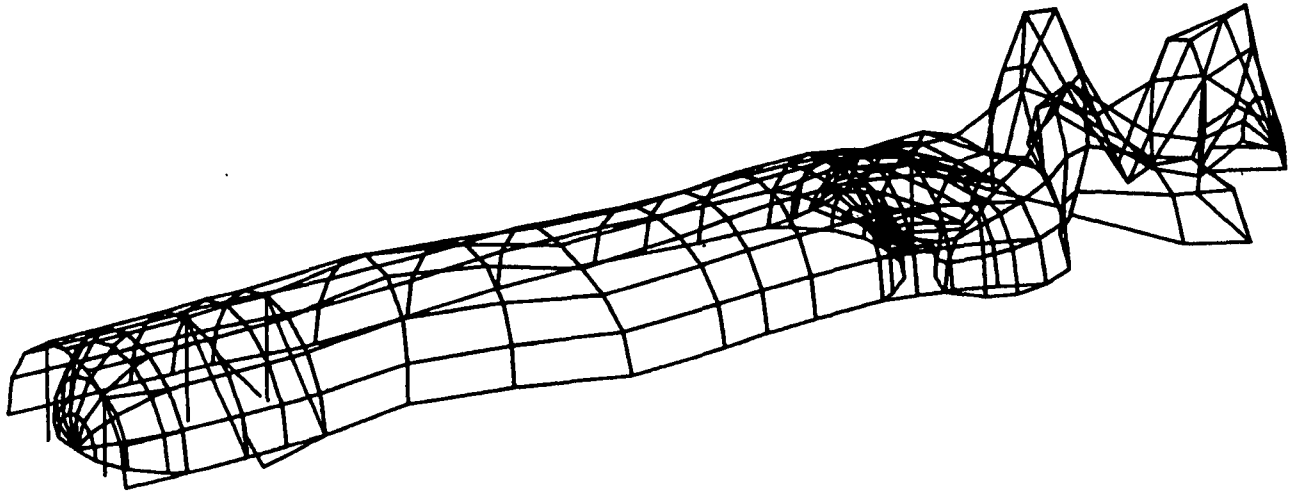

T13-73

Fig. 4-23 External Tank With Fluid, Liftoff Configuration

HARMONIC REDUCTION
MODAL DEFORMATION – SUBCASE 1 MODE 4 EIGENVALUE = 69707 (RADIANS/SEC)²

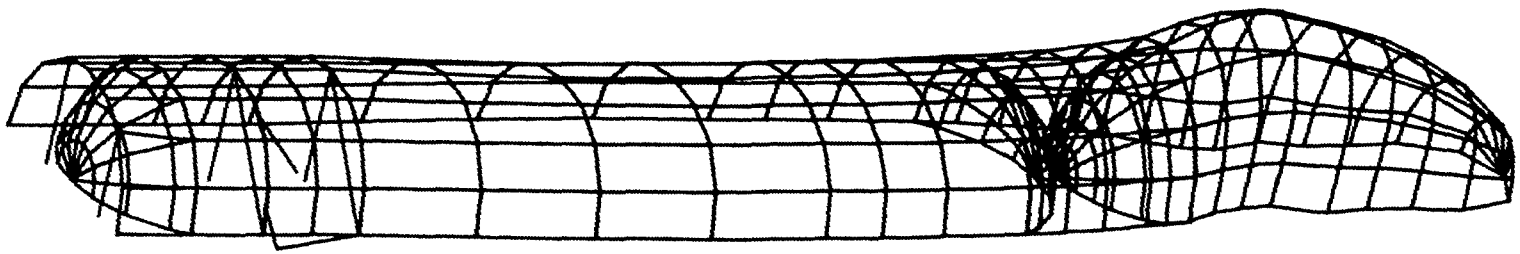

T13-74

Fig. 4-24 External Tank With Fluid, Post Max. Q Configuration

HARMONIC REDUCTION
MODAL DEFORMATION – SUBCASE 1 MODE 5 EIGENVALUE = 78016 (RADIANS/SEC)²

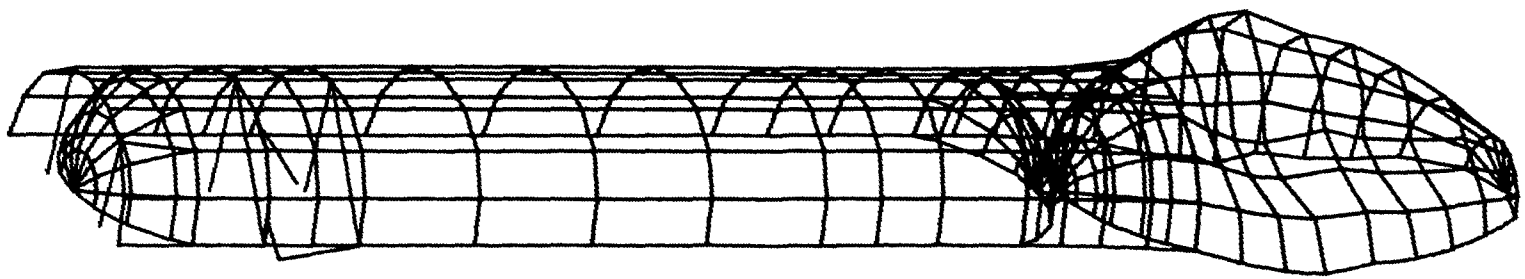

T13-75

Fig. 4-25 External Tank With Fluid, Post Max. Q Configuration

HARMONIC REDUCTION
MODAL DEFORMATION – SUBCASE 1 MODE 6 EIGENVALUE = 96602 (RADIANS/SEC)²

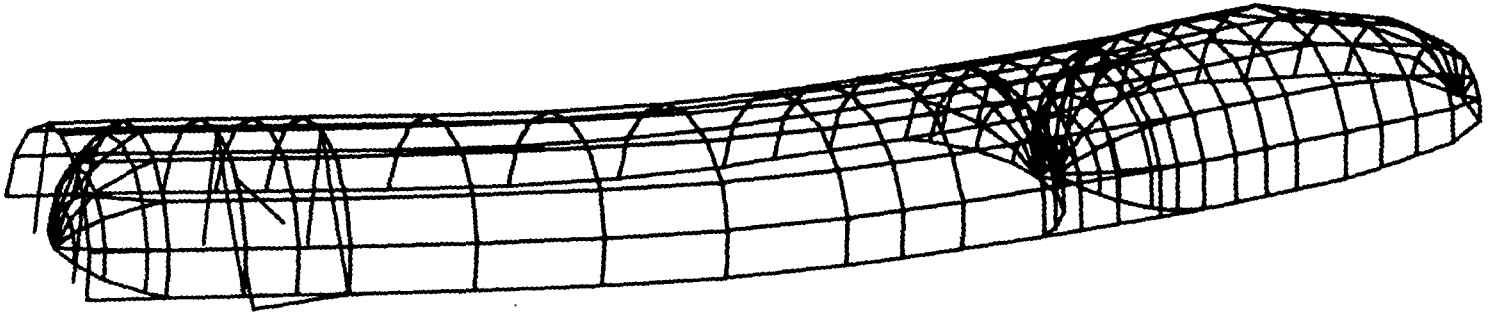

T13-76

Fig. 4-26 External Tank With Fluid, Post Max. Q Configuration

HARMONIC REDUCTION
MODAL DEFORMATION – SUBCASE 1 MODE 7 EIGENVALUE = 104736 (RADIANS/SEC)²

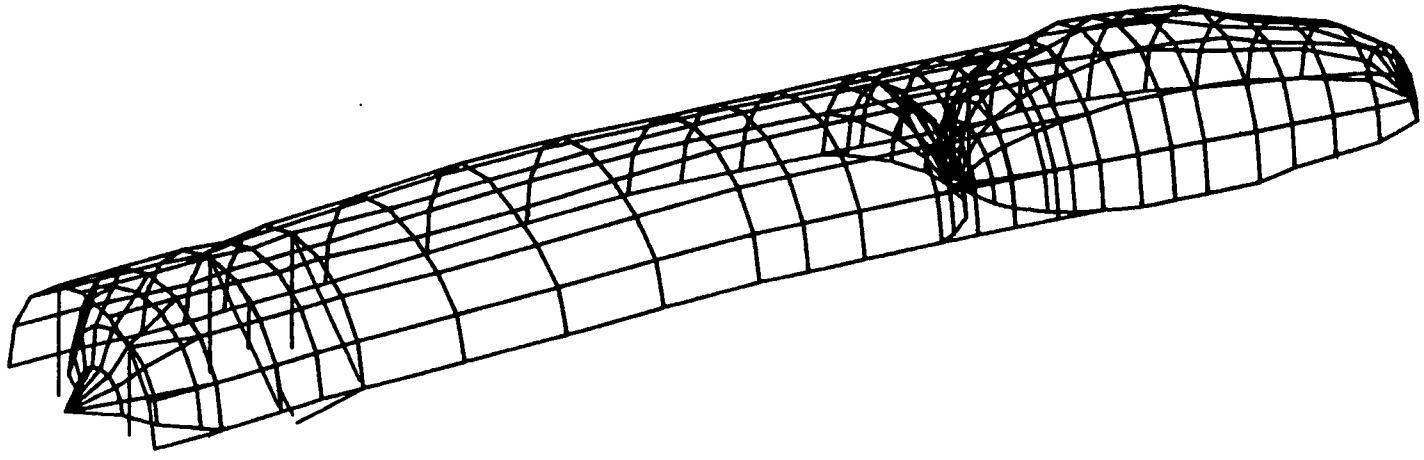

T13-77

Fig. 4-27 External Tank With Fluid, Post Max. Q Configuration

HARMONIC REDUCTION
MODAL DEFORMATION – SUBCASE 1 MODE 15 EIGENVALUE = 676228 (RADIANS/SEC)²

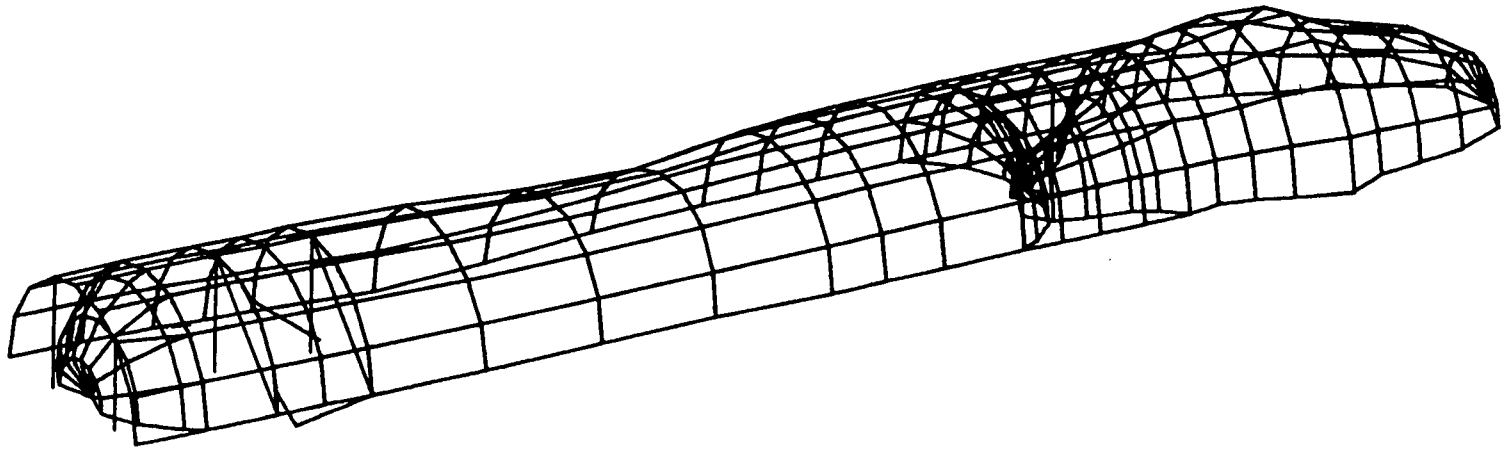

T13-78

Fig. 4-28 External Tank With Fluid, Post Max. Q Configuration

HARMONIC REDUCTION
MODAL DEFORMATION – SUBCASE 1 MODE 14 EIGENVALUE 510477 (RADIANS/SEC)^2

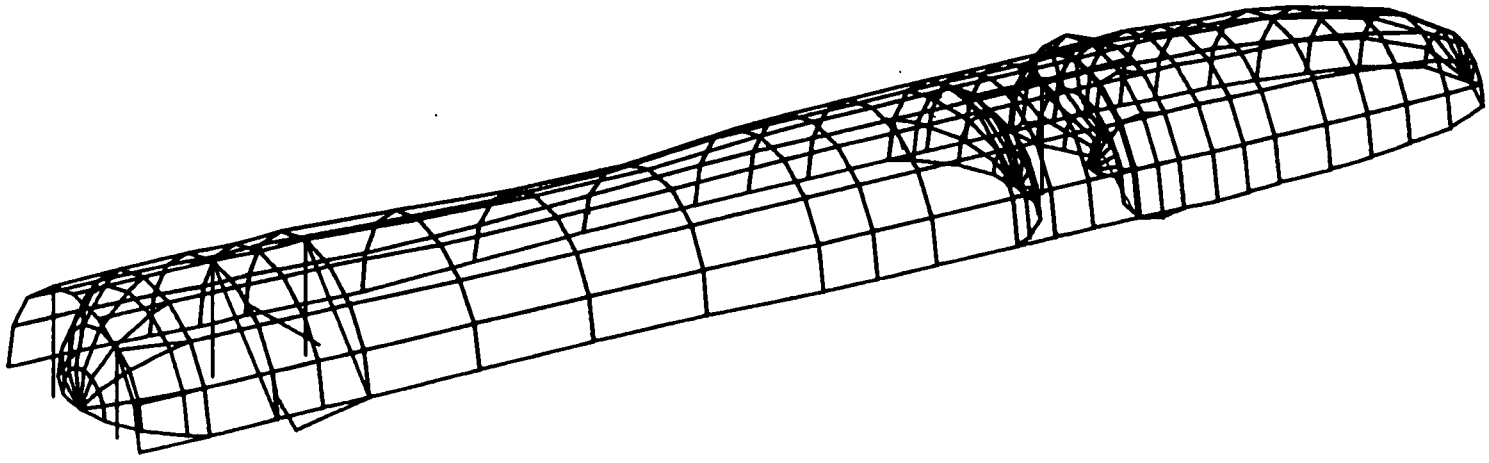

T13-89

Fig. 4-39 External Tank With Fluid, Post Max. Q Configuration

HARMONIC REDUCTION
MODAL DEFORMATION – SUBCASE 1 MODE 5 EIGENVALUE = 78017 (RADIANS/SEC)^2

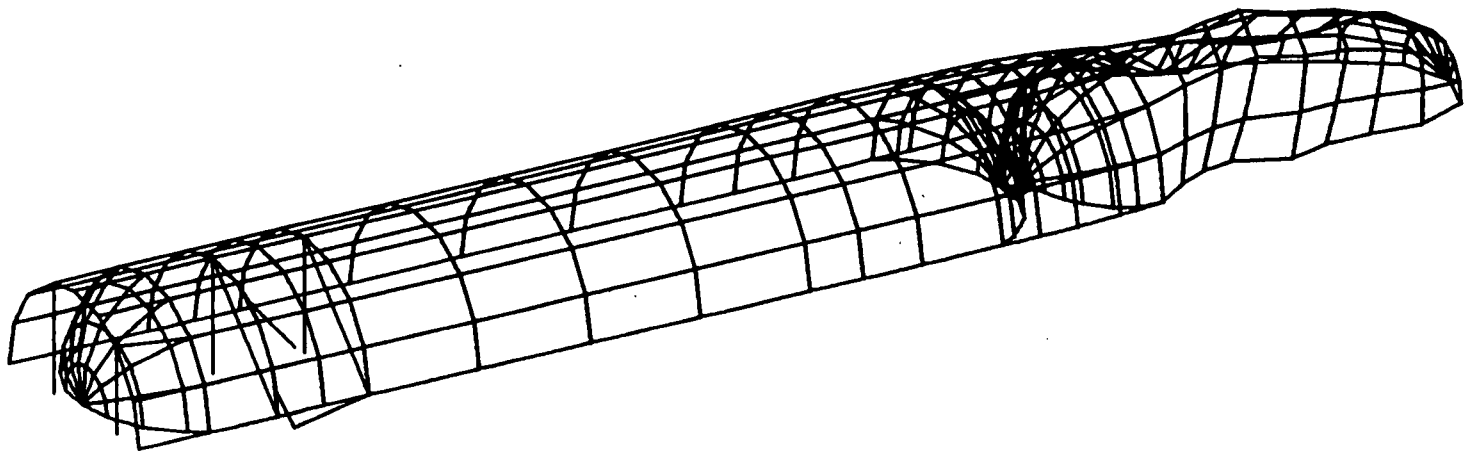

T13-80

Fig. 4-30 External Tank With Fluid, Post Max. Q Configuration

HARMONIC REDUCTION
MODAL DEFORMATION – SUBCASE 1 MODE 6 EIGENVALUE = 95561 (RADIANS/SEC)^2

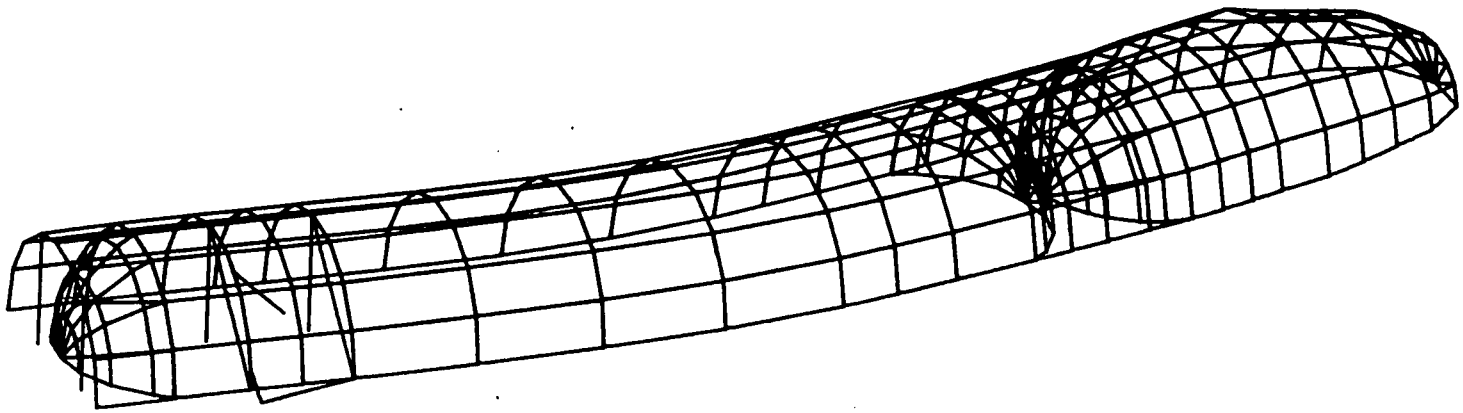

T13-81

Fig. 4-31 External Tank With Fluid, Post Max. Q Configuration

HARMONIC REDUCTION
MODAL DEFORMATION – SUBCASE 1 MODE 7 EIGENVALUE = 105919 (RADIANS/SEC)^2

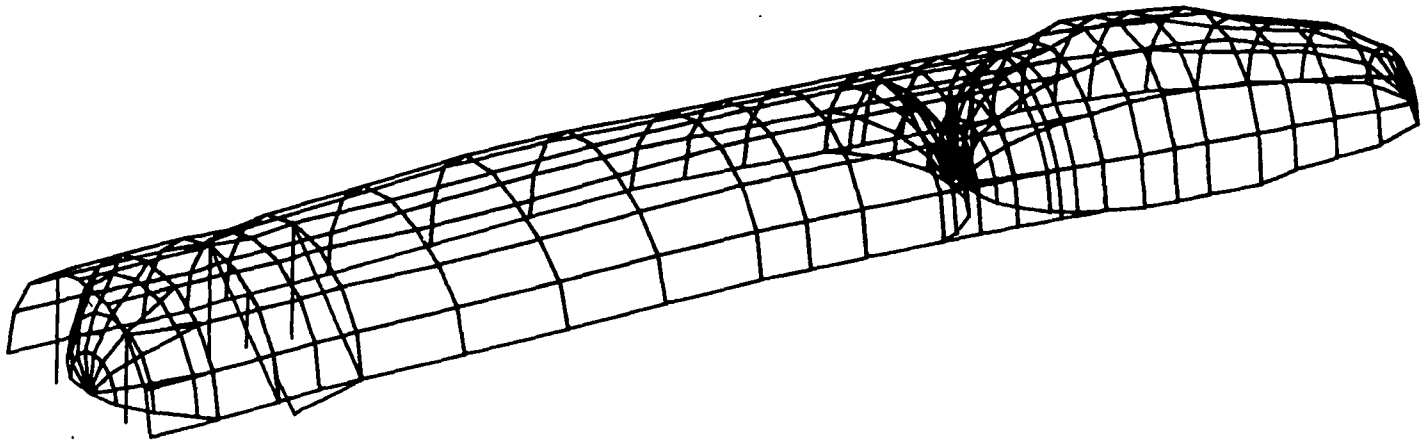

T13-82

Fig. 4-32 External Tank With Fluid, Post Max. Q Configuration

HARMONIC REDUCTION
MODAL DEFORMATION – SUBCASE 1 MODE 8 EIGENVALUE = 135425 (RADIANS/SEC)^2

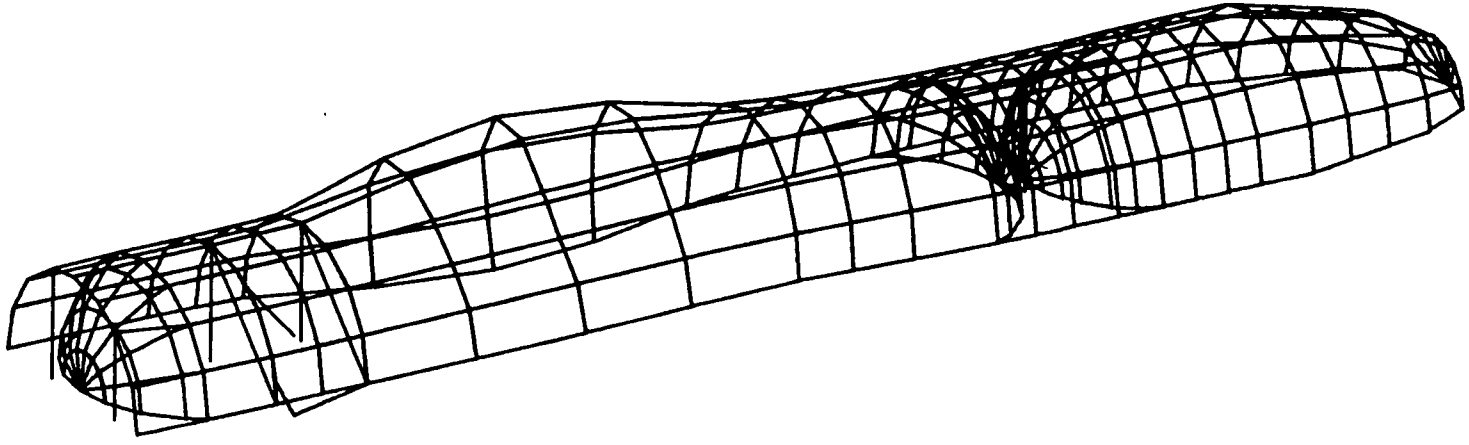

T13-83

Fig. 4-33 External Tank With Fluid, Post Max. Q Configuration

HARMONIC REDUCTION
MODEL DEFORMATION – SUBCASE 1 MODE 9 EIGENVALUE = 150184 (RADIANS/SEC)^2

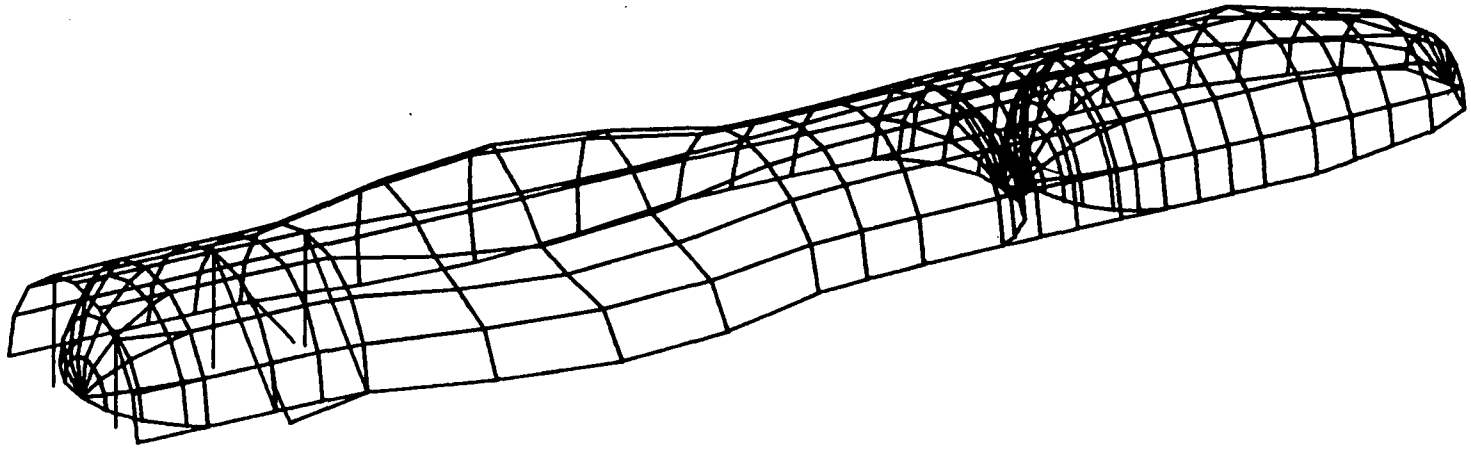

T13-84

Fig. 4-34 External Tank With Fluid, Post Max. Q Configuration

HARMONIC REDUCTION
MODAL DEFORMATION – SUBCASE 1 MODE 10 EIGENVALUE = 247567 (RADIANS/SEC)^2

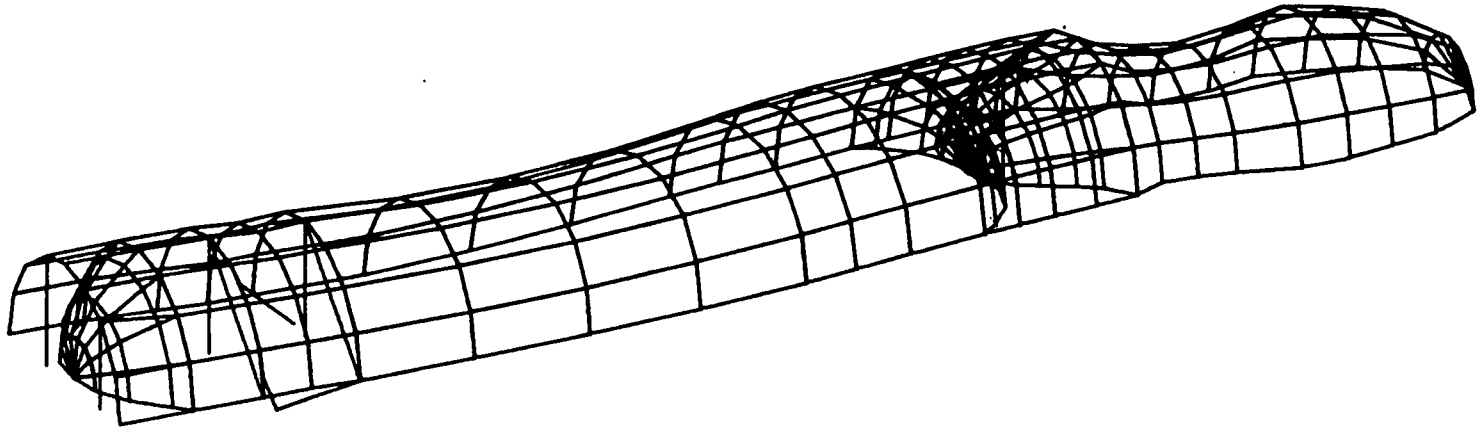

T13-85

Fig. 4-35 External Tank With Fluid, Post Max. Q Configuration

HARMONIC REDUCTION
MODAL DEFORMATION – SUBCASE 1 MODE 11 EIGENVALUE = 250847 (RADIANS/SEC)^2

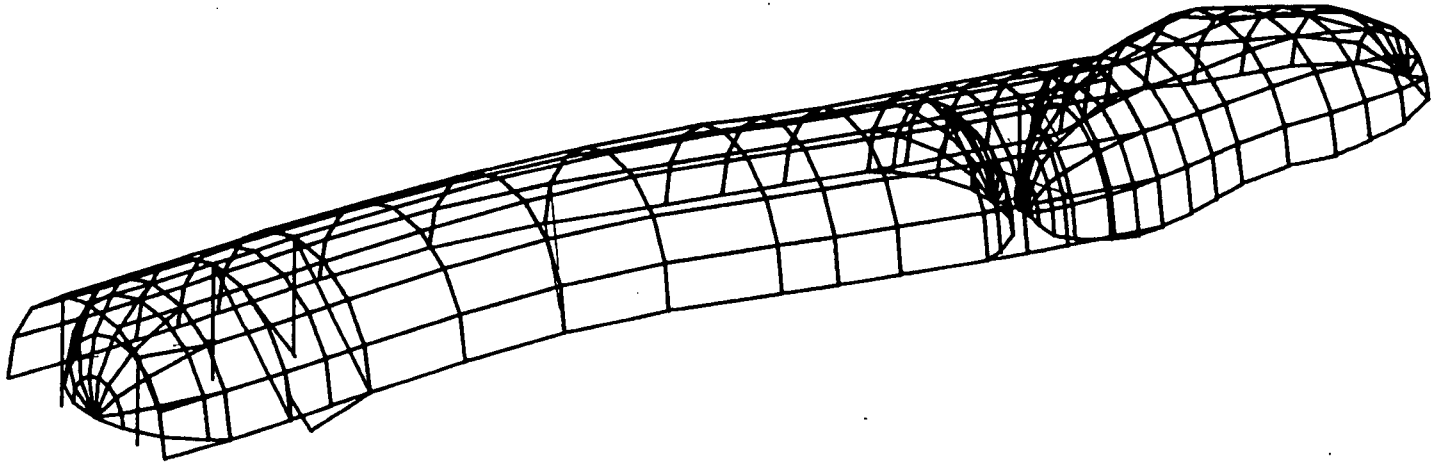

T13-86

Fig. 4-36 External Tank With Fluid, Post Max. Q Configuration

HARMONIC REDUCTION
MODAL DEFORMATION – SUBCASE 1 MODE 12 EIGENVALUE = 441298 (RADIANS/SEC)²

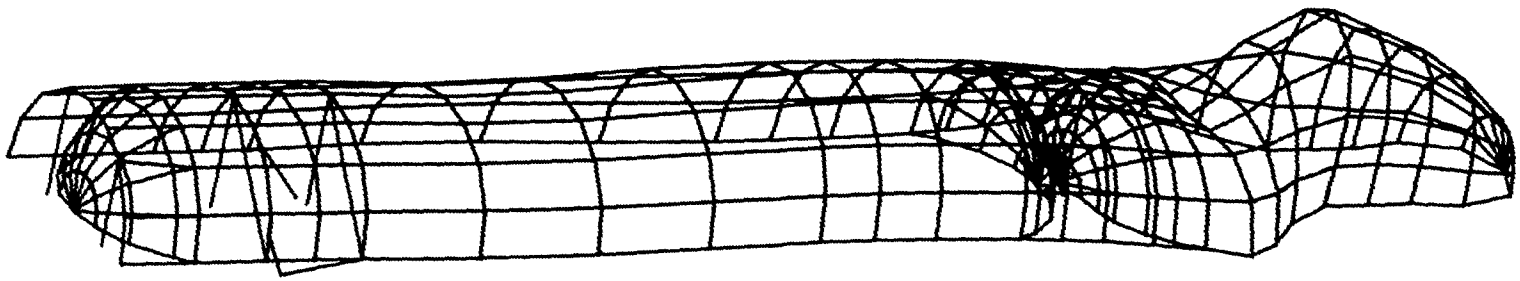

T13-87

Fig. 4-37 External Tank With Fluid, Post Max. Q. Configuration

HARMONIC REDUCTION
MODAL DEFORMATION – SUBCASE 1 MODE 13 Eigenvalue = 458951 (RADIANS/SEC)^2

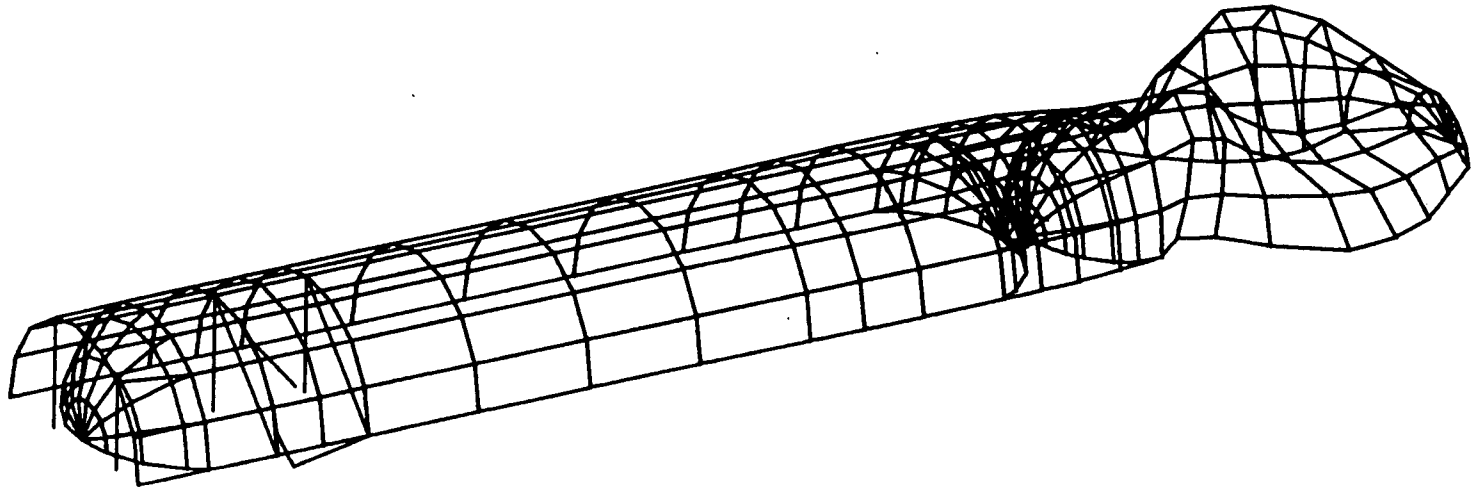

T13-88

Fig. 4-38 External Tank With Fluid, Post Max. Q Configuration

HARMONIC REDUCTION
MODAL DEFORMATION – SUBCASE 1 MODE 14 EIGENVALUE 510477 (RADIANS/SEC)^2

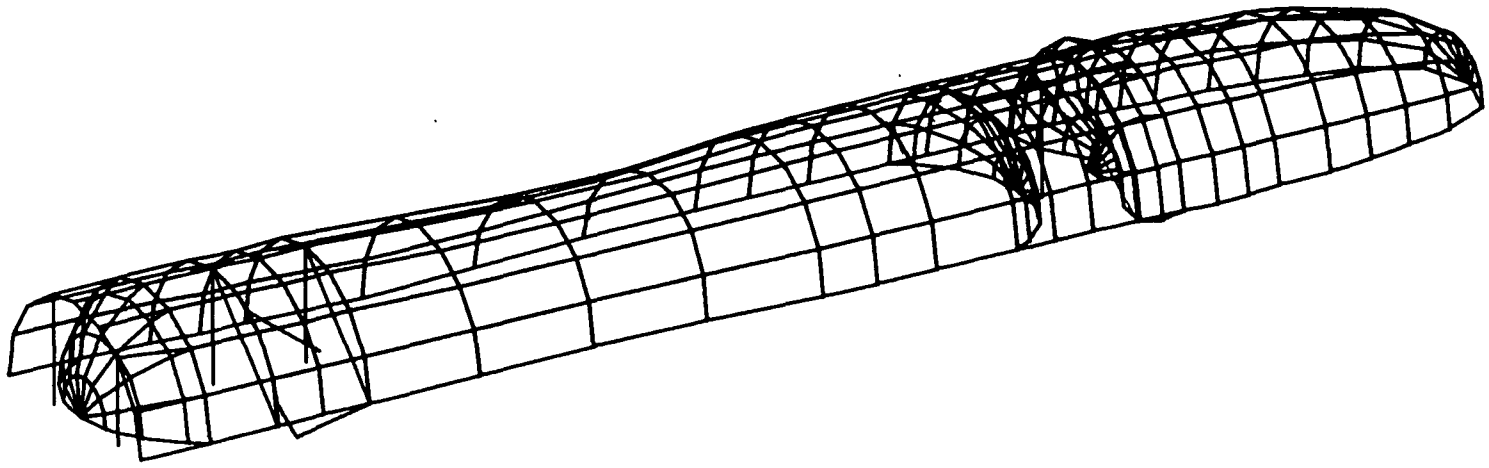

T13-89

Fig. 4-39 External Tank With Fluid, Post Max. Q Configuration

HARMONIC REDUCTION
MODAL DEFORMATION – SUBCASE 1 MODE 15 EIGENVALUE = 575589 (RADIANS/SEC)^2

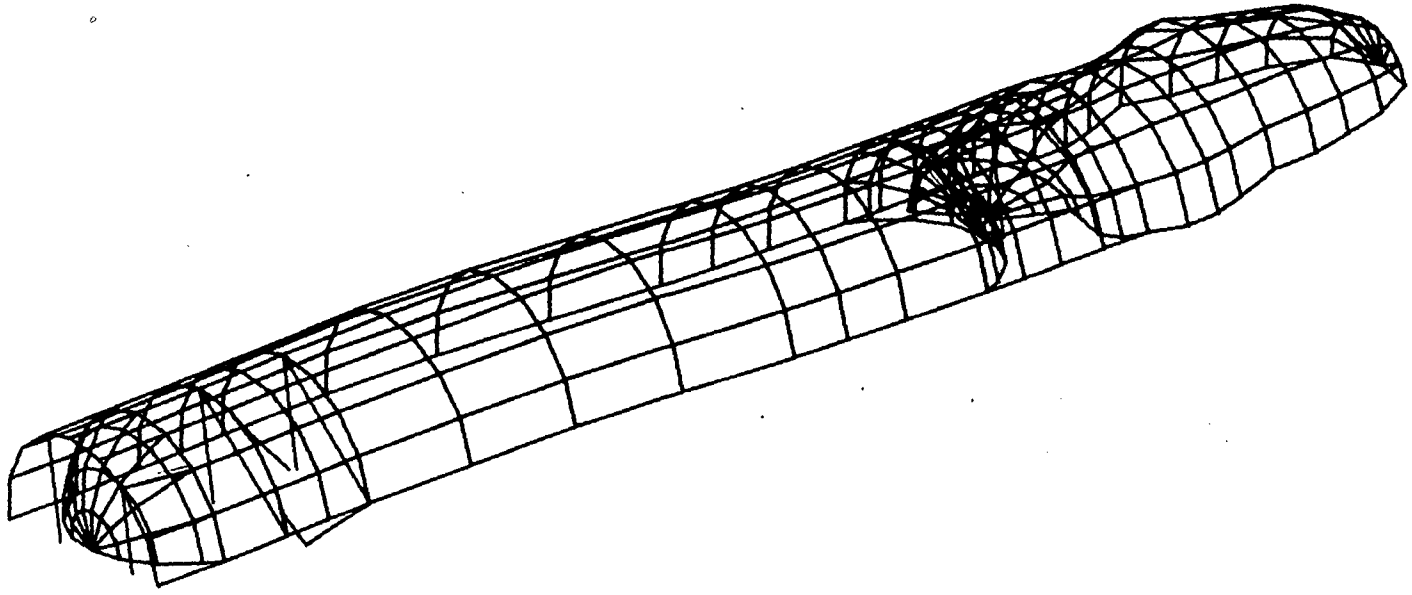

Fig. 4-40 External Tank With Fluid, Post Max. Q Configuration

T13-90

HARMONIC REDUCTION
MODAL DEFORMATION – SUBCASE 1 MODE 16 EIGENVALUE = 576571 (RADIANS/SEC)^2

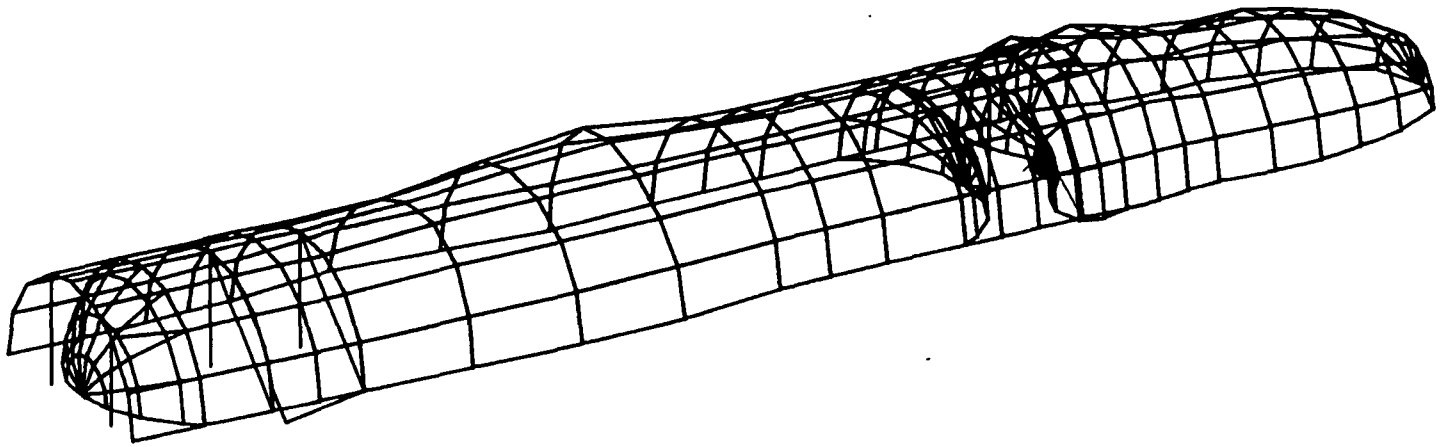

T13-91

Fig. 4-41 External Tank With Fluid, Post Max. Q Configuration

HARMONIC REDUCTION
MODAL DEFORMATION – SUBCASE 1 MODE 17 EIGENVALUE = 621326 (RADIANS/SEC)^2

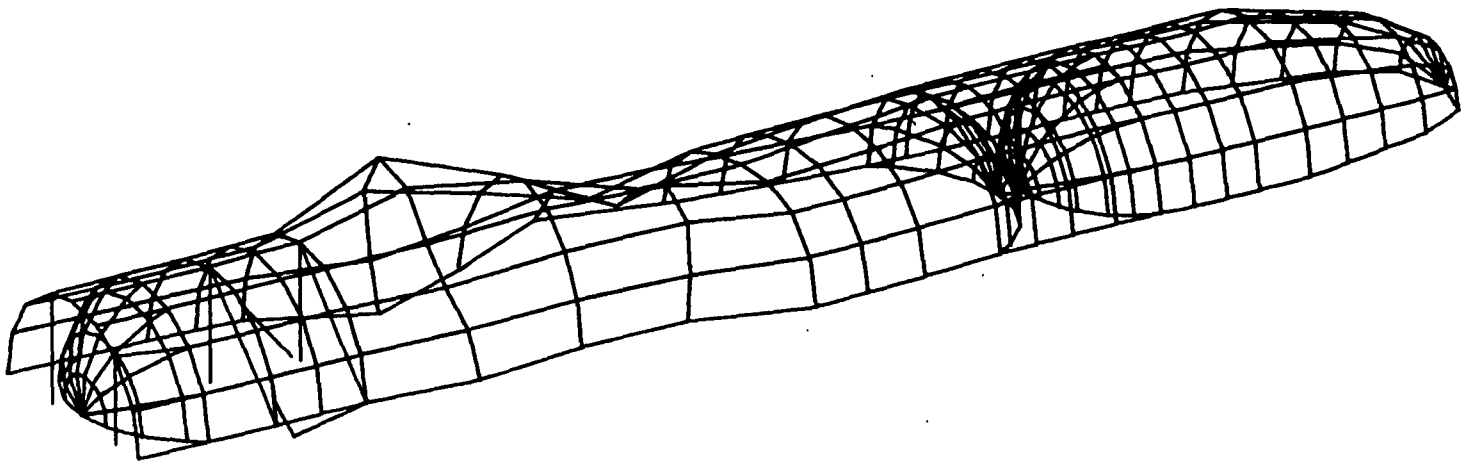

T13-92

Fig. 4-42 External Tank With Fluid, Post Max. Q Configuration

HARMONIC REDUCTION
MODAL DEFORMATION – SUBCASE 1 MODE 18 EIGENVALUE = 672842 (RADIANS/SEC)^2

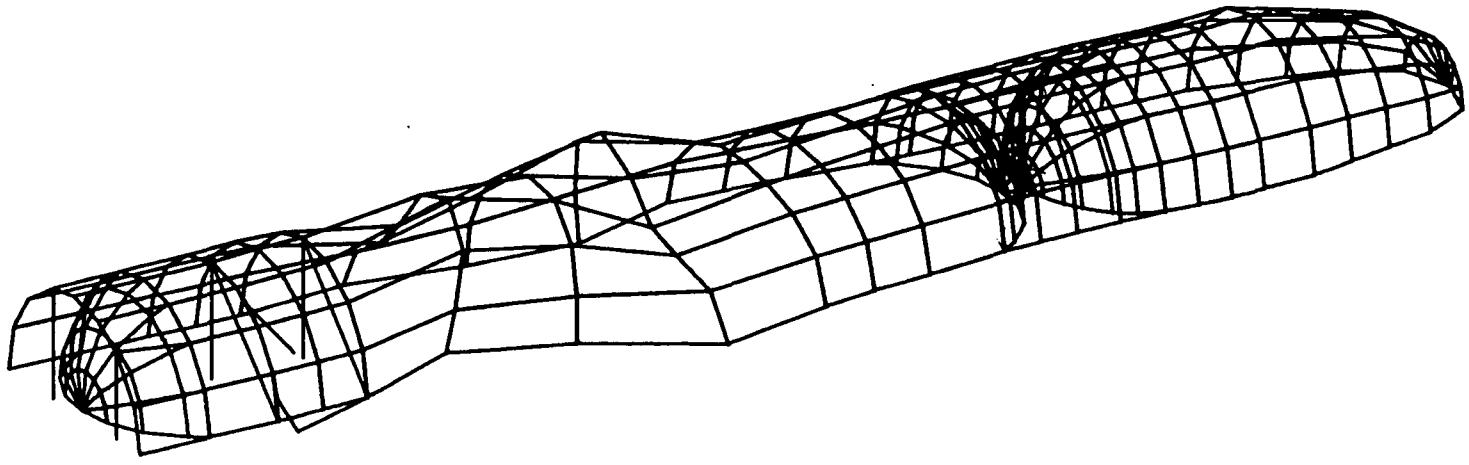

T13-93

Fig. 4-43 External Tank With Fluid, Post Max. Q Configuration

MOA
HARMONIC REDUCTION
MODAL DEFORMATION – SUBCASE 1 MODE 19 EIGENVALUE = 825279 (RADIANS/SEC)^2

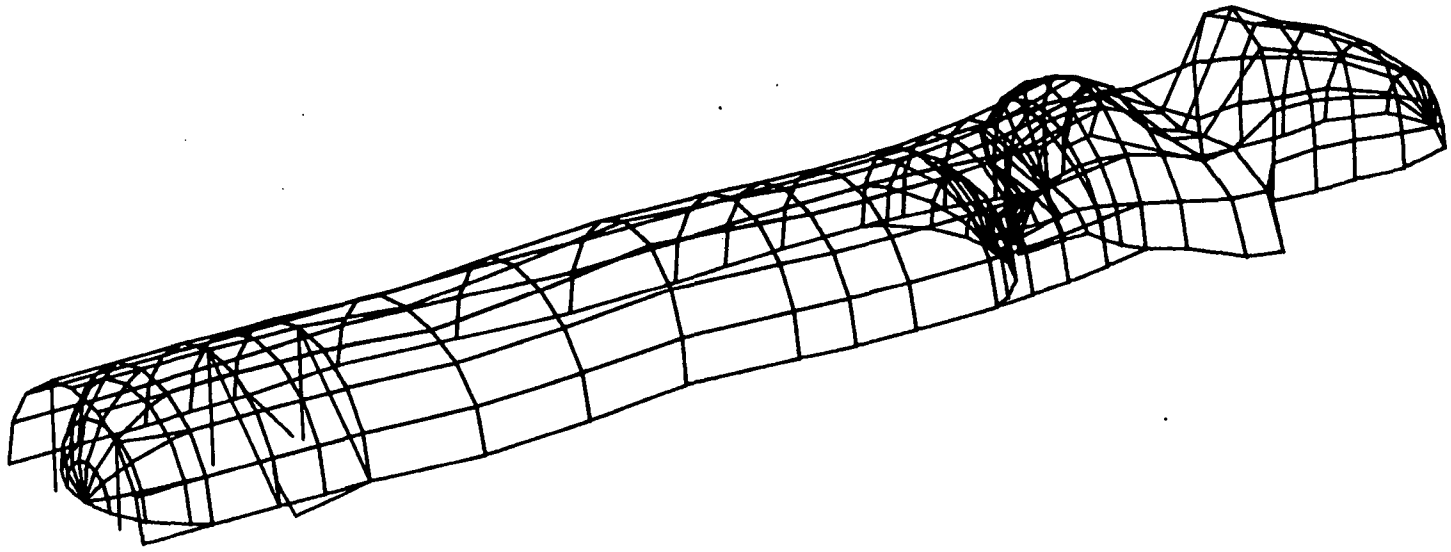

T13-94

Fig. 4-44 External Tank With Fluid, Post Max. Q Configuration

HARMONIC REDUCTION
MODAL DEFORMATION – SUBCASE 1 MODE 20 EIGENVALUE = 843961 (RADIANS/SEC)^2

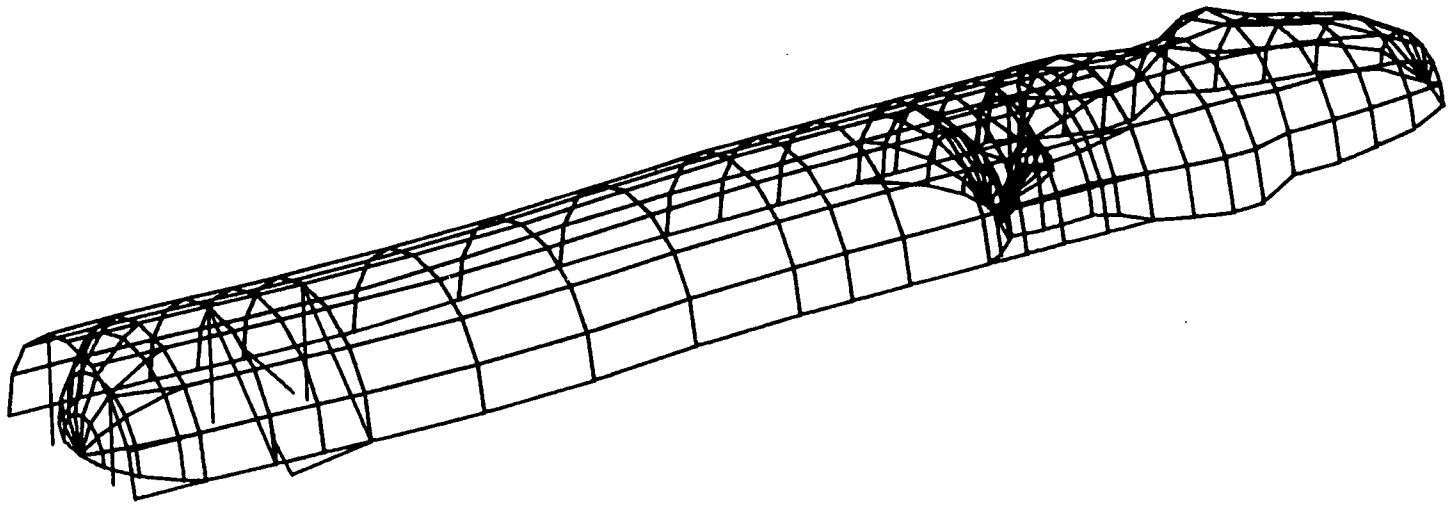

T13-95

Fig. 4-45 External Tank With Fluid, Post Max. Q Configuration

HARMONIC REDUCTION
MODAL DEFORMATION – SUBCASE 1 MODE 21 EIGENVALUE = 871814 (RADIANS/SEC)^2

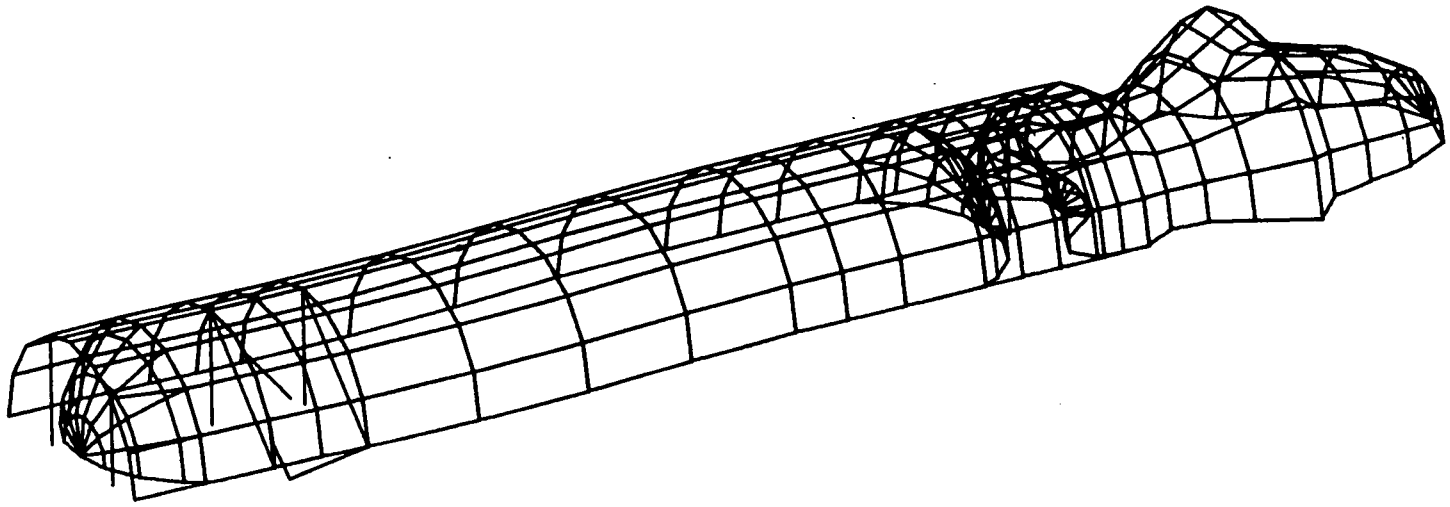

T13-96

Fig. 4-46 External Tank With Fluid, Post Max. Q Configuration

HARMONIC REDUCTION
MODAL DEFORMATION – SUBCASE 1 MODE 22 EIGENVALUE = 877137 (RADIANS/SEC)^2

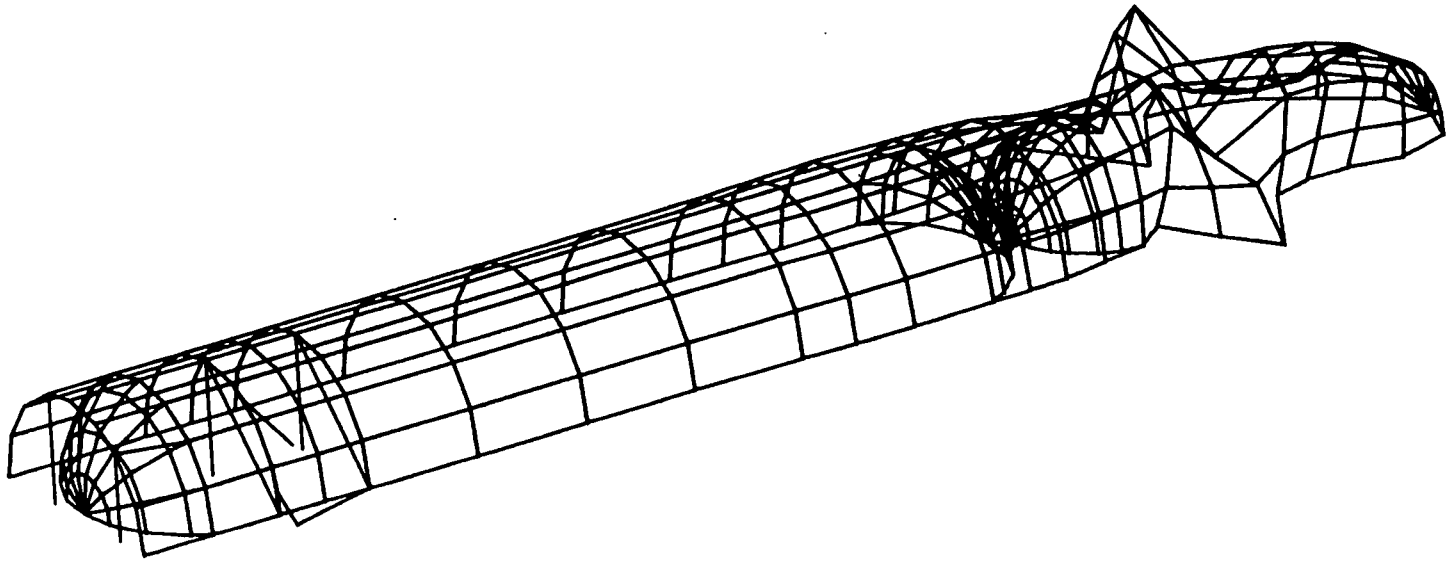

T13-97

Fig. 4-47 External Tank With Fluid, Post Max. Q Configuration

HARMONIC REDUCTION
MODAL DEFORMATION – SUBCASE 1 MODE 23 EIGENVALUE = 895894 (RADIANS/SEC)²

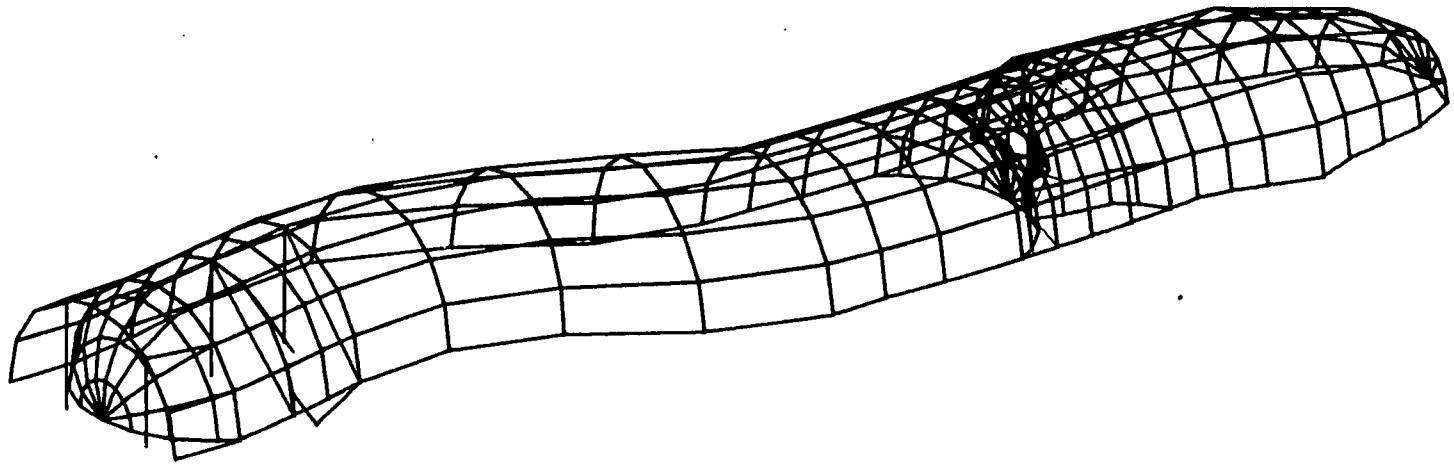

T13-98

Fig. 4-48 External Tank With Fluid, Post Max. Q Configuration

HARMONIC REDUCTION
MODAL DEFORMATION – SUBCASE 1 MODE 24 EIGENVALUE = 1047303 (RADIANS/SEC)^2

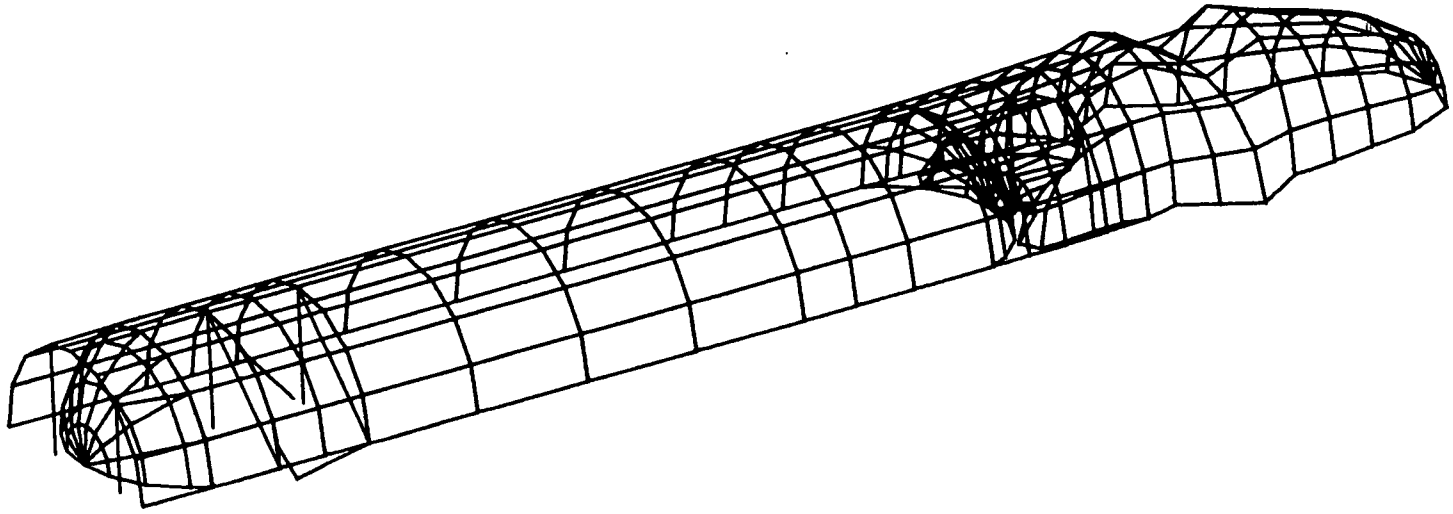

T13-99

Fig. 4-49 External Tank With Fluid, Post Max. Q Configuration

HARMONIC REDUCTION
MODAL DEFORMATION – SUBCASE 1 MODE 25 EIGENVALUE = 1112063 (RADIANS/SEC)²

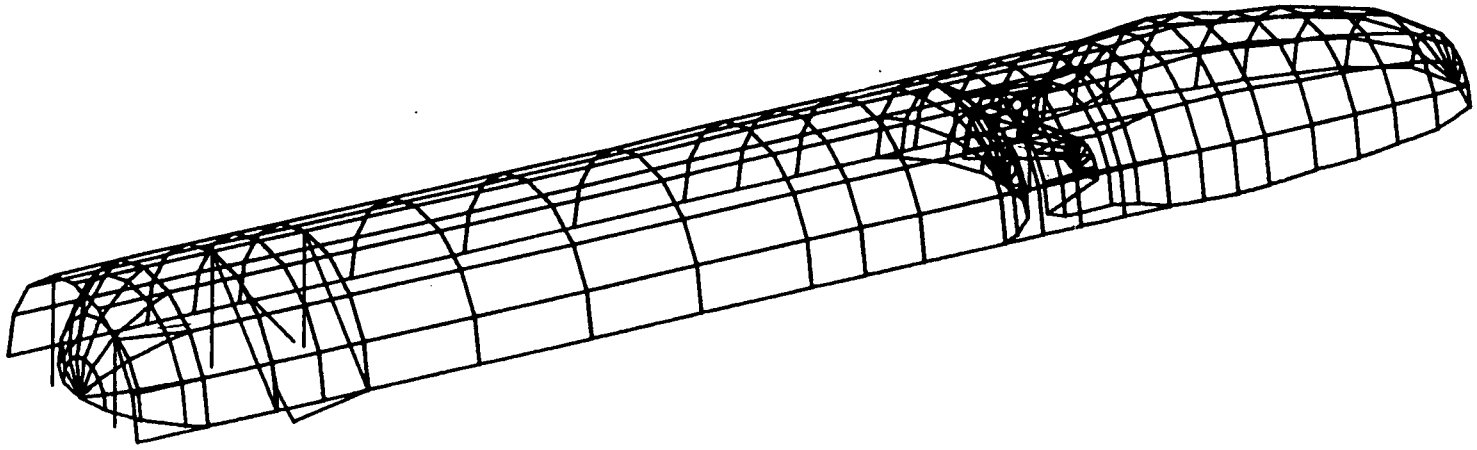

T13-100

Fig. 4-50 External Tank With Fluid, Post Max. Q Configuration

HARMONIC REDUCTION
MODAL DEFORMATION – SUBCASE 1 MODE 4 EIGENVALUE = 440452 (RADIANS/SEC)^2

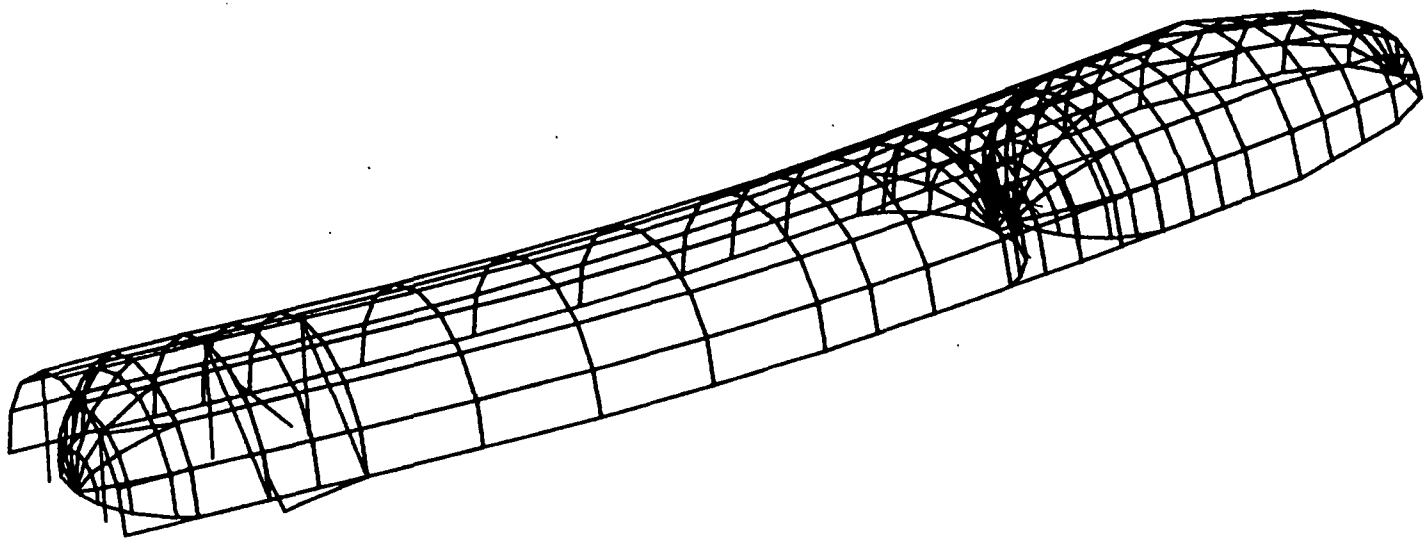

T13-101

Fig. 4-51 External Tank Without Fluid

HARMONIC REDUCTION
MODAL DEFORMATION – SUBCASE 1 MODE 5 EIGENVALUE = 923919 (RADIANS/SEC)²

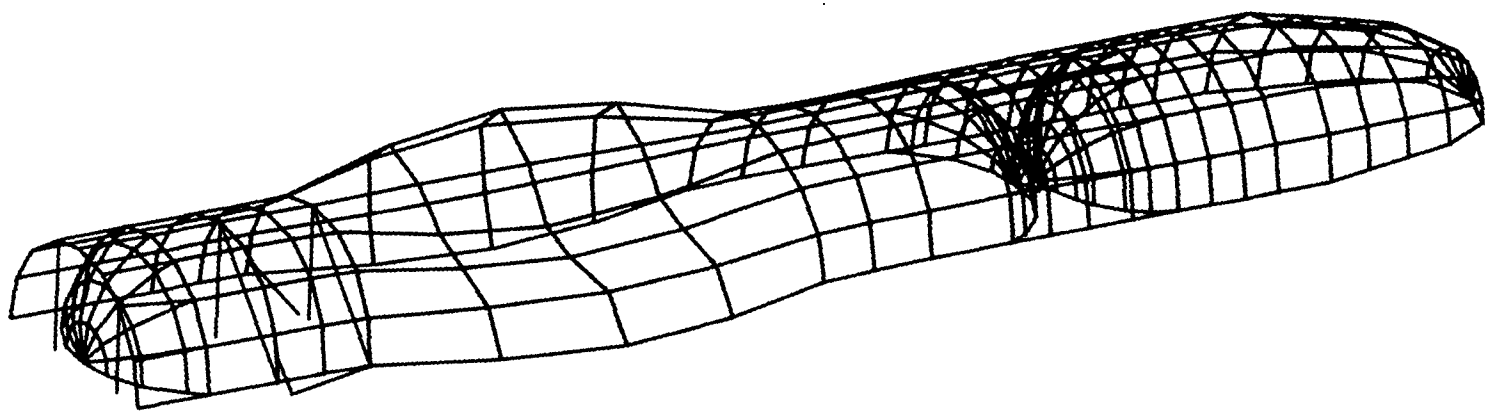

T13-102

Fig. 4-52 External Tank Without Fluid

T13-103 HARMONIC REDUCTION
MODAL DEFORMATION – SUBCASE 1 MODE 6 EIGENVALUE = 1031670 (RADIANS/SEC)^2

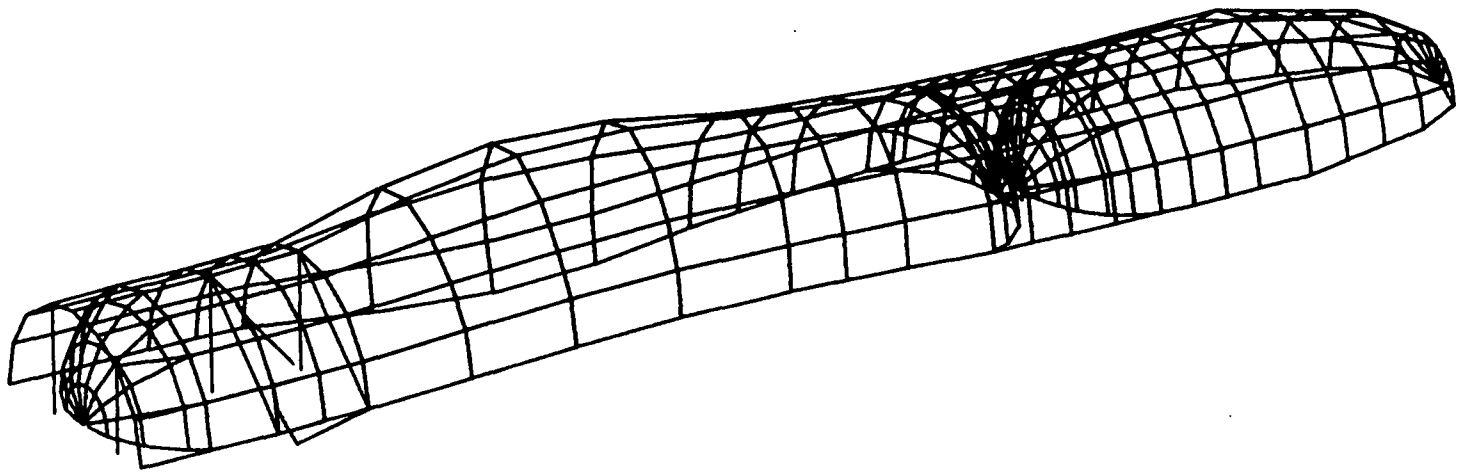

T13-5

Fig. 4-53 External Tank Without Fluid

HARMONIC REDUCTION
MODAL DEFORMATION – SUBCASE 1 MODE 7 EIGENVALUE = 2016352 (RADIANS/SEC)²

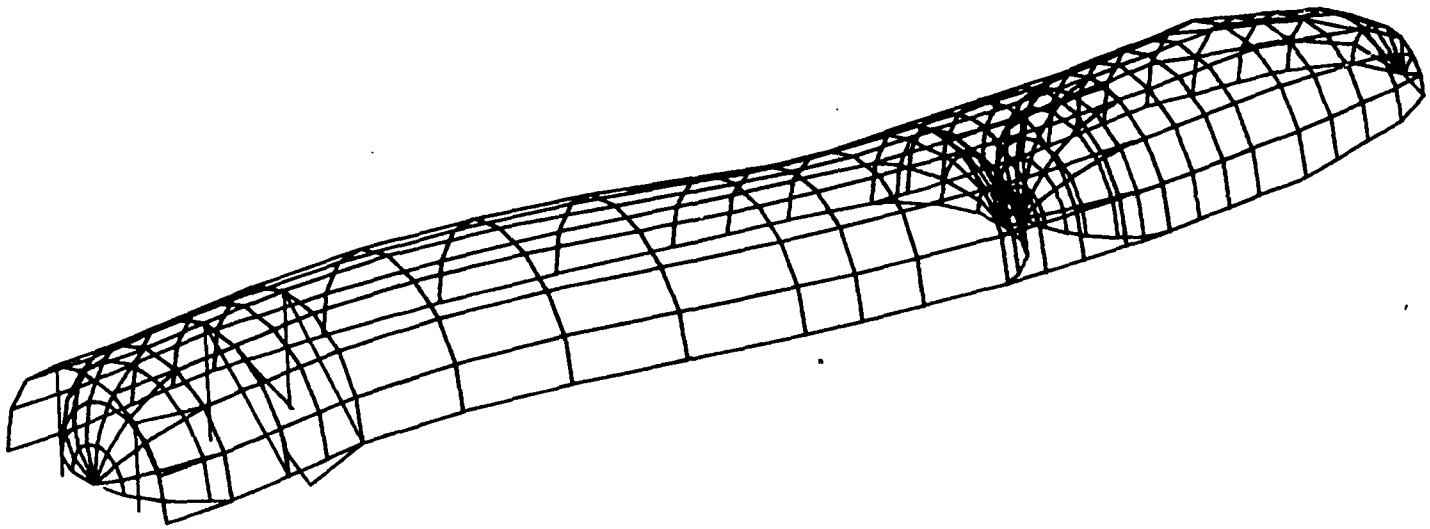

T13-104

Fig. 4-54 External Tank Without Fluid

HARMONIC REDUCTION
MODAL DEFORMATION – SUBCASE 1 MODE 8 EIGENVALUE = 2624686 (RADIANS/SEC)^2

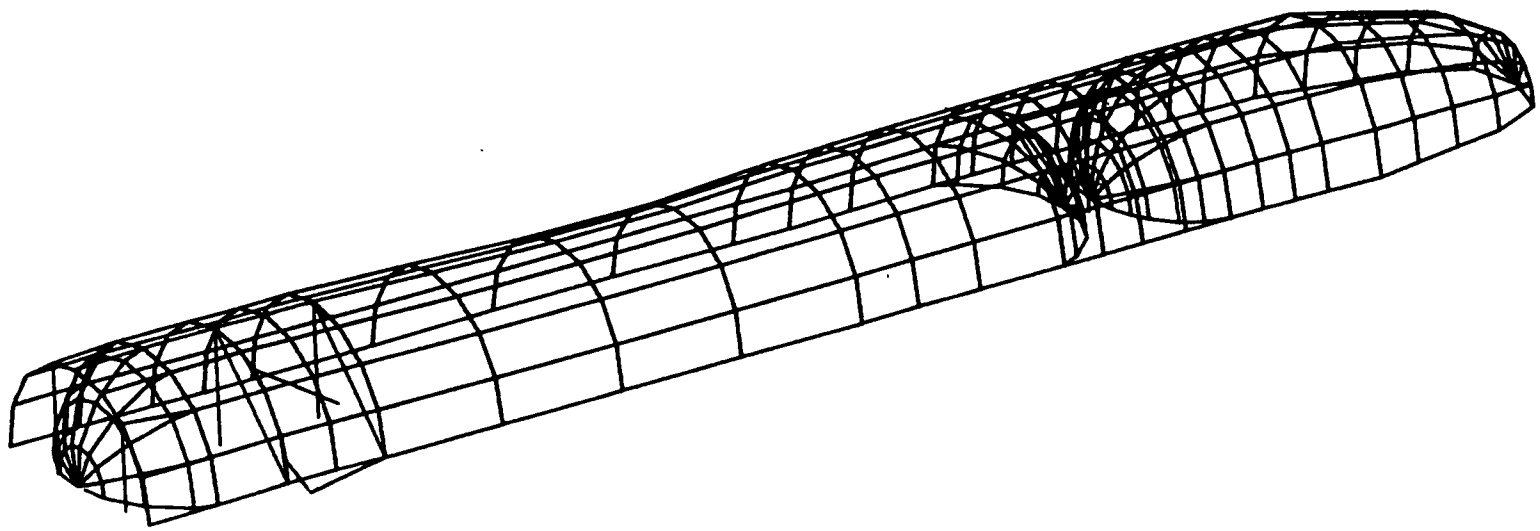

T13-105

Fig. 4-55 External Tank Without Fluid

HARMONIC REDUCTION
MODAL DEFORMATION – SUBCASE 1 MODE 9 EIGENVALUE = 2976288 (RADIANS/SEC)^2

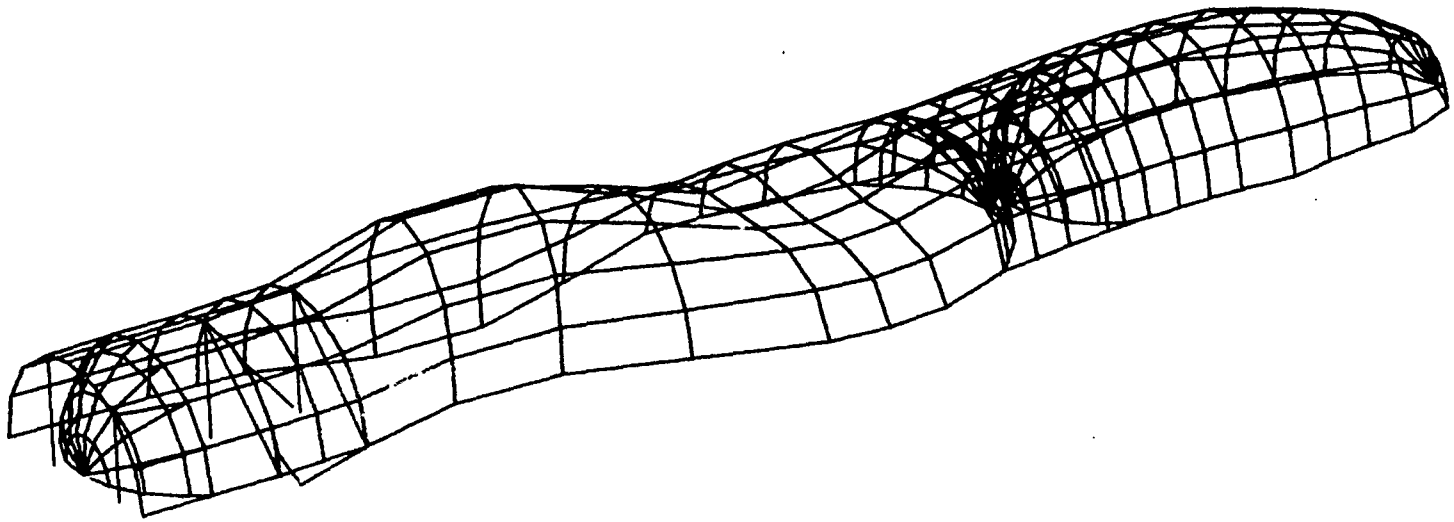

[illegible] External Tank Without Fan.

HARMONIC REDUCTION
MODAL DEFORMATION – SUBCASE 1 MODE 10 EIGENVALUE = 4254448 (RADIANS/SEC)²

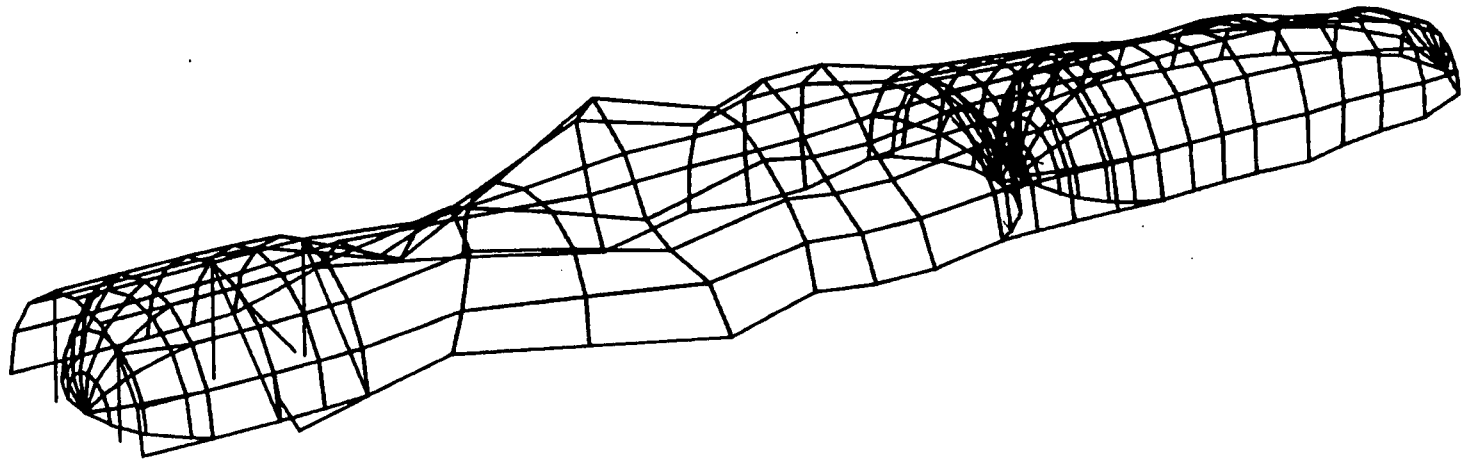

T13-107

Fig. 4-57 External Tank Without Fluid

HARMONIC REDUCTION
MODAL DEFORMATION – SUBCASE 1 MODE 11 EIGENVALUE = 4351788 (RADIANS/SEC)^2

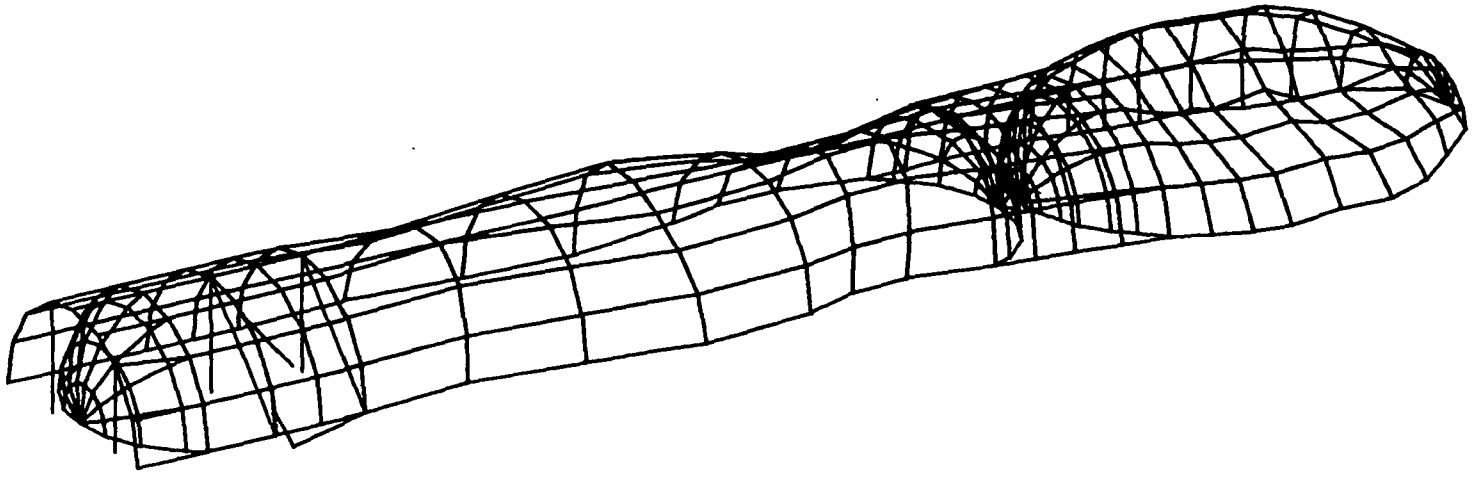

T13-108

Fig. 4-58 External Tank Without Fluid

HARMONIC REDUCTION
MODAL DEFORMATION – SUBCASE 1 MODE 12 EIGENVALUE = 4372603 (RADIANS/SEC)²

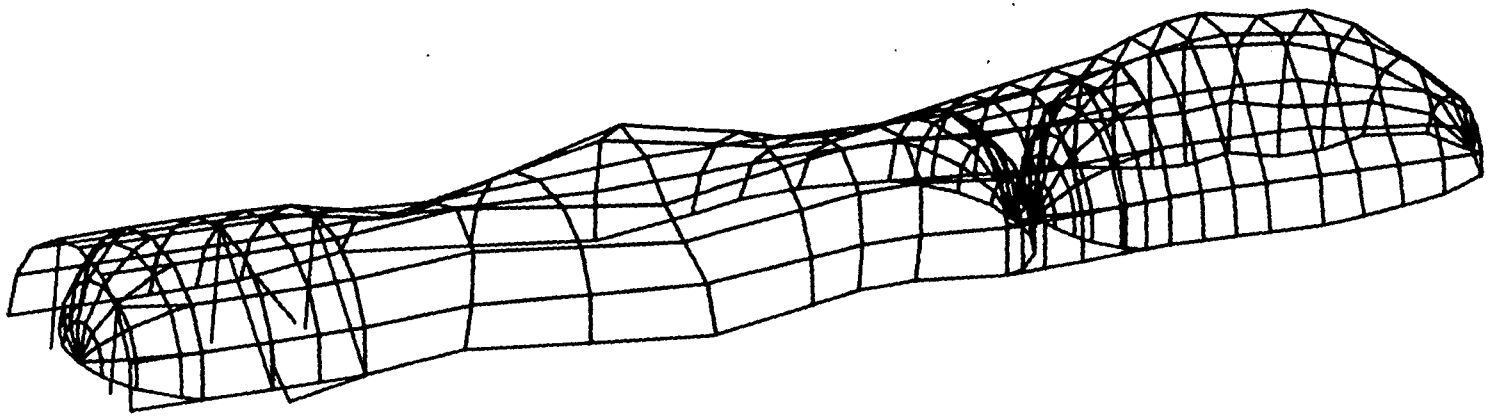

T13-109

Fig. 4-59 External Tank Without Fluid

HARMONIC REDUCTION
MODAL DEFORMATION – SUBCASE 1 MODE 13 EIGENVALUE = 4662576 (RADIANS/SEC)^2

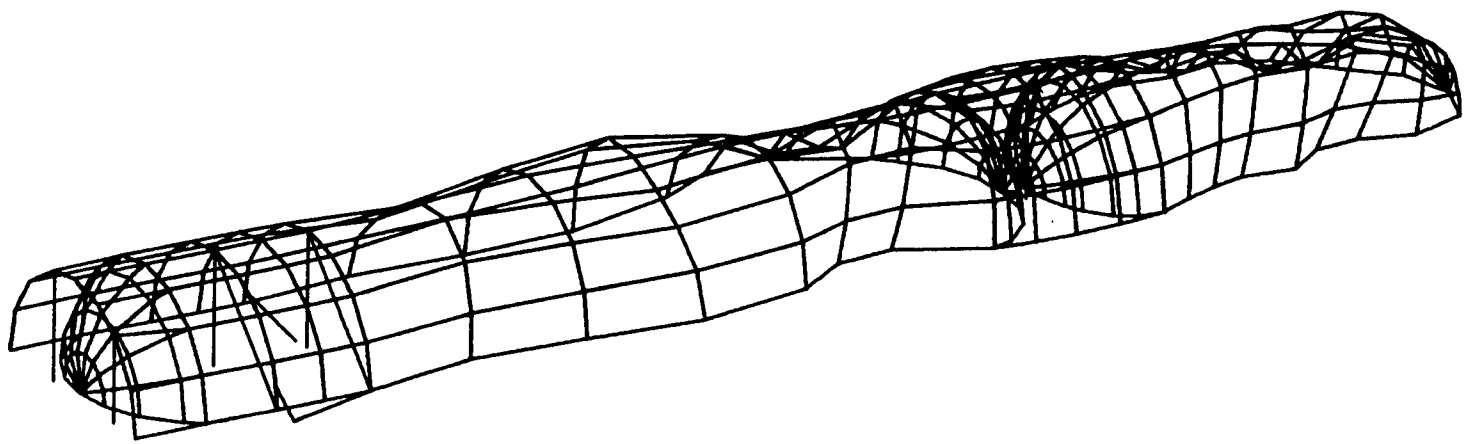

T13-110

Fig. 4-60 External Tank Without Fluid

HARMONIC REDUCTION
MODAL DEFORMATION – SUBCASE 1 MODE 14 EIGENVALUE = 5052284 (RADIANS/SEC)^2

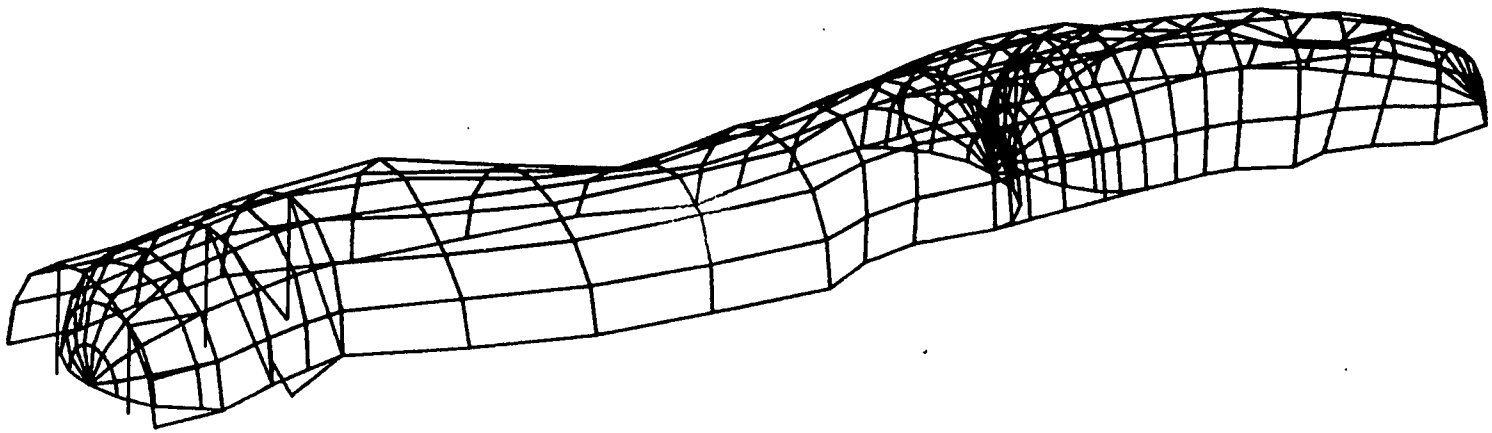

T13-111

Fig. 4-61 External Tank Without Fluid

HARMONIC REDUCTION
MODAL DEFORMATION – SUBCASE 1 MODE 15 EIGENVALUE = 7333198 (RADIANS/SEC)²

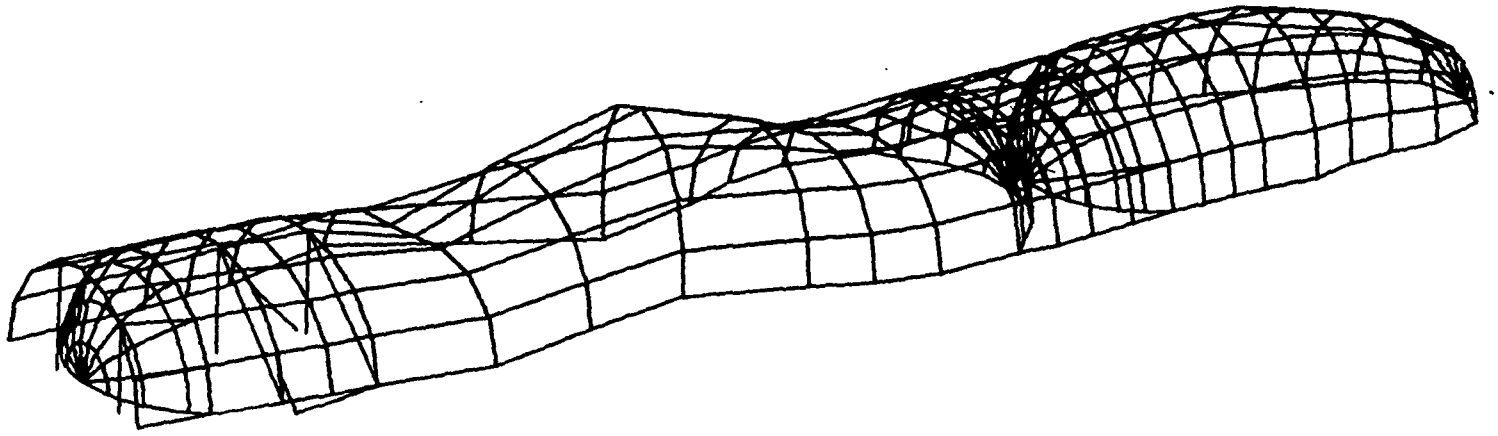

T13-112

Fig. 4-62 External Tank Without Fluid

HARMONIC REDUCTION

MODAL DEFORMATION – SUBCASE 1 MODE 16 EIGENVALUE = 8320355 (RADIANS/SEC)^2

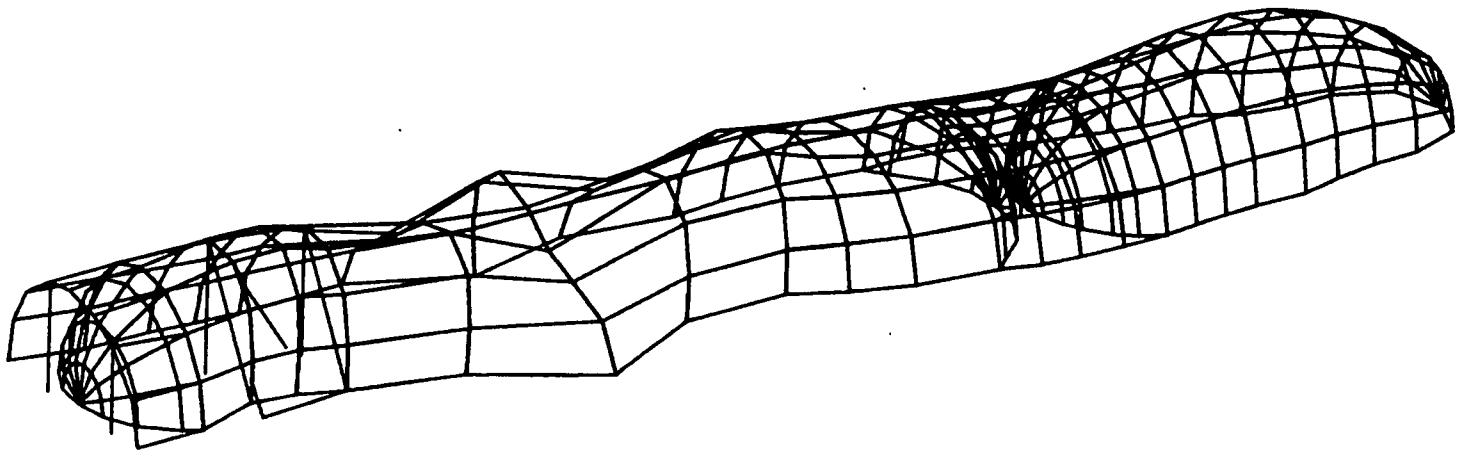

T13-113

Fig. 4-63 External Tank Without Fluid

HARMONIC REDUCTION
MODAL DEFORMATION – SUBCASE 1 MODE 17 EIGENVALUE = 8826886 (RADIANS/SEC)^2

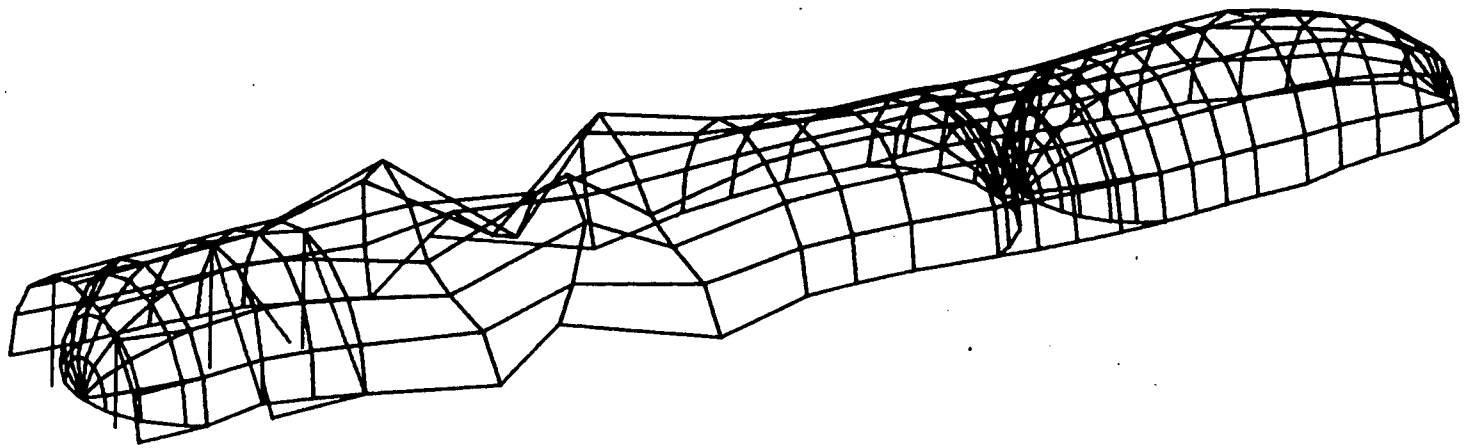

T13-114

Fig. 4-64 External Tank Without Fluid

HARMONIC REDUCTION
MODAL DEFORMATION – SUBCASE 1 MODE 18 EIGENVALUE = 9180132 (RADIANS/SEC)^2

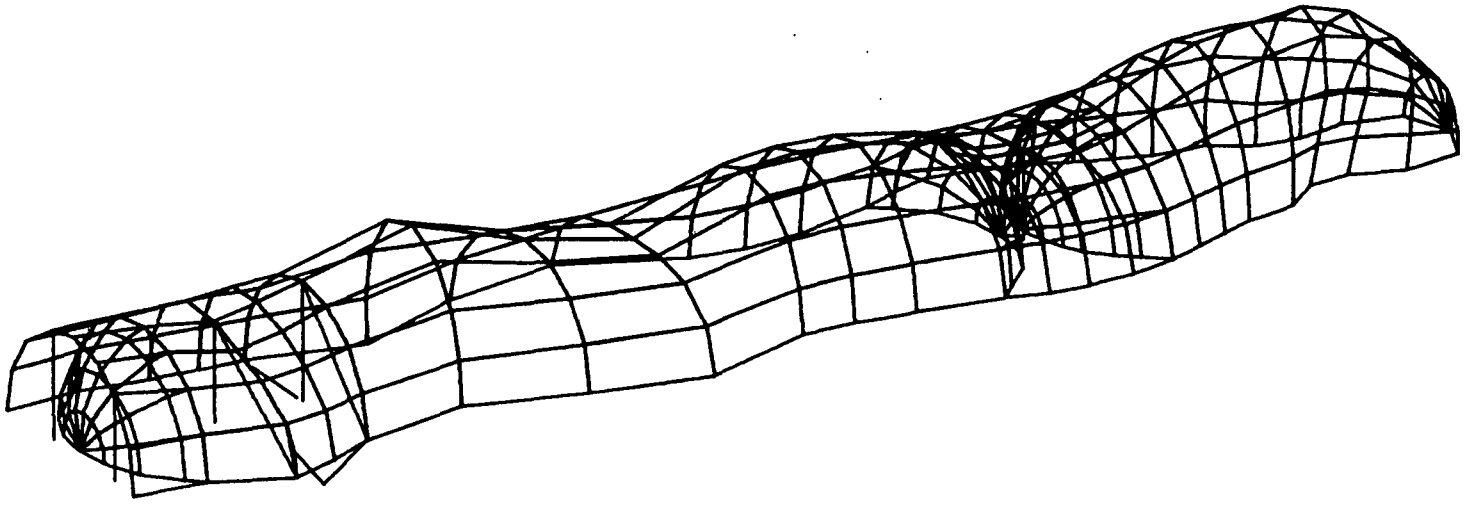

T13-115

Fig. 4-65 External Tank Without Fluid

HARMONIC REDUCTION
MODAL DEFORMATION – SUBCASE 1 MODE 19 EIGENVALUE = 9812092 (RADIANS/SEC)²

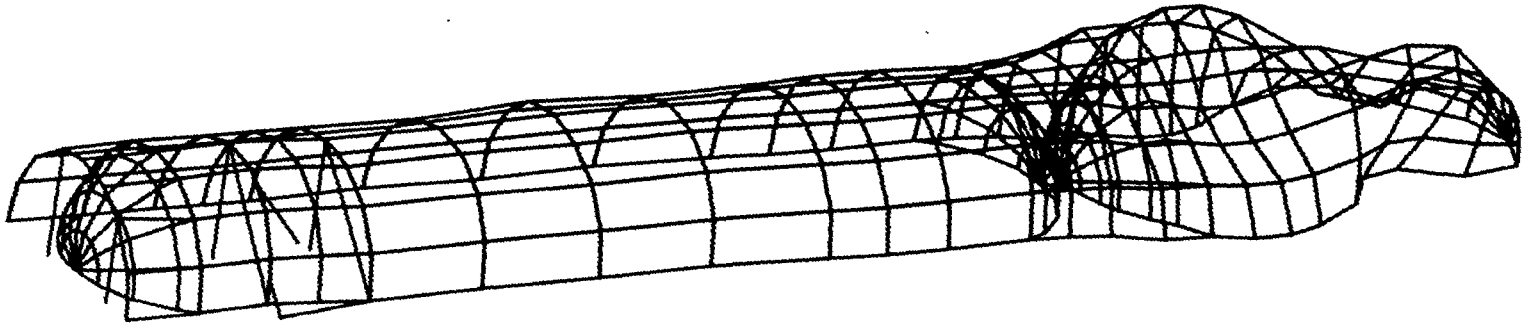

T13-116

Fig. 4-66 External Tank Without Fluid

HARMONIC REDUCTION
MODAL DEFORMATION – SUBCASE 1 MODE 20 EIGENVALUE = 10397898 (RADIANS/SEC)^2

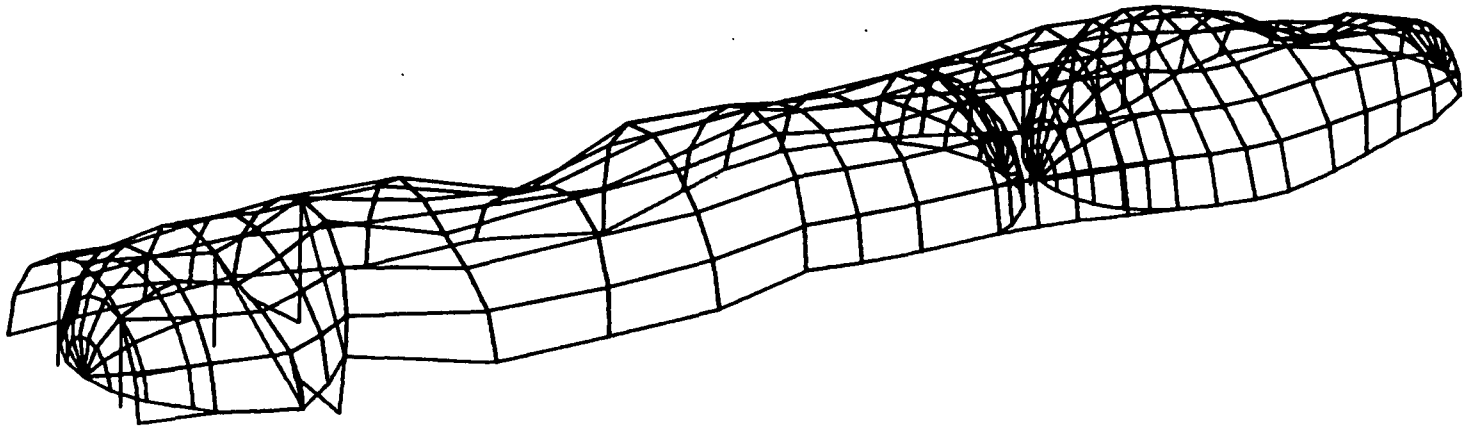

T13-117

Fig. 4-67 External Tank Without Fluid

HARMONIC REDUCTION
MODAL DEFORMATION – SUBCASE 1 MODE 21 EIGENVALUE = 11217576 (RADIANS/SEC)²

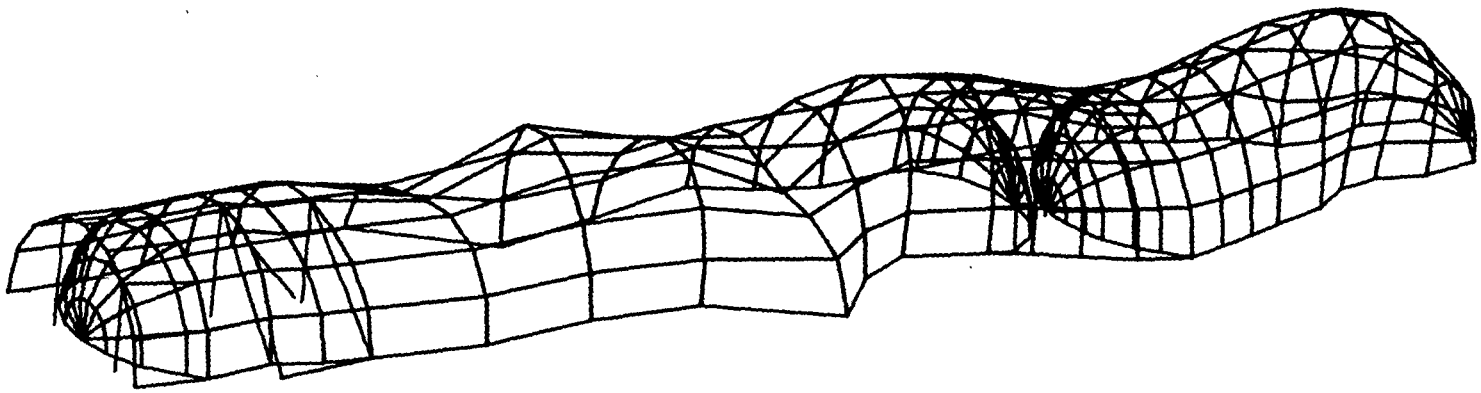

T13-118

Fig. 4-68 External Tank Without Fluid

HARMONIC REDUCTION
MODAL DEFORMATION – SUBCASE 1 MODE 22 EIGENVALUE = 12700159 (RADIANS/SEC)^2

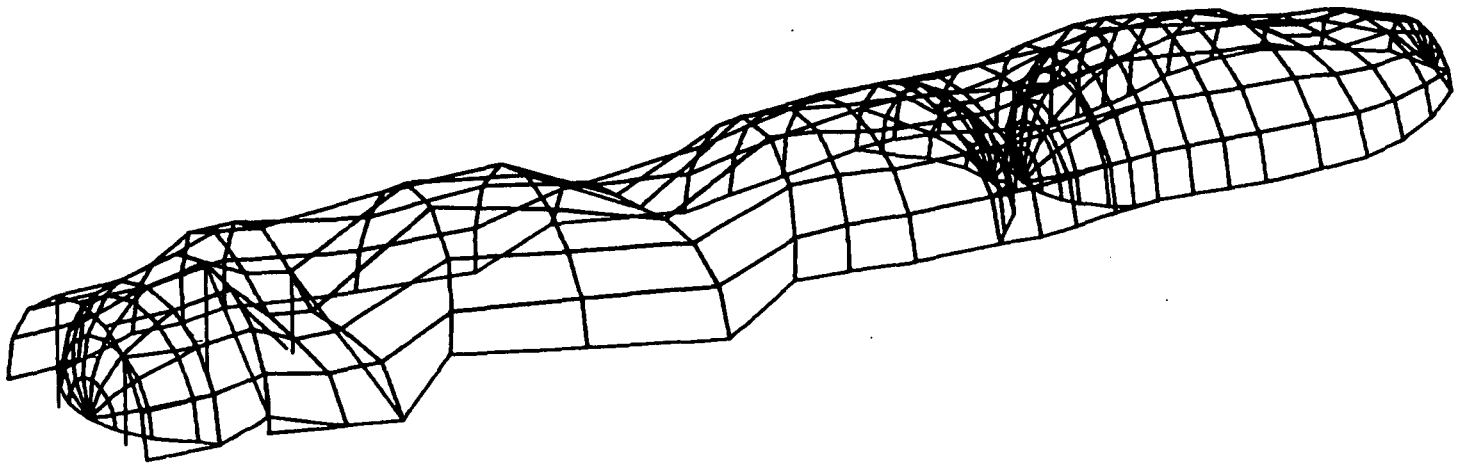

T13-119

Fig. 4-69 External Tank Without Fluid

HARMONIC REDUCTION
MODAL DEFORMATION – SUBCASE 1 MODE 23 EIGENVALUE = 14432951 (RADIANS/SEC)^2

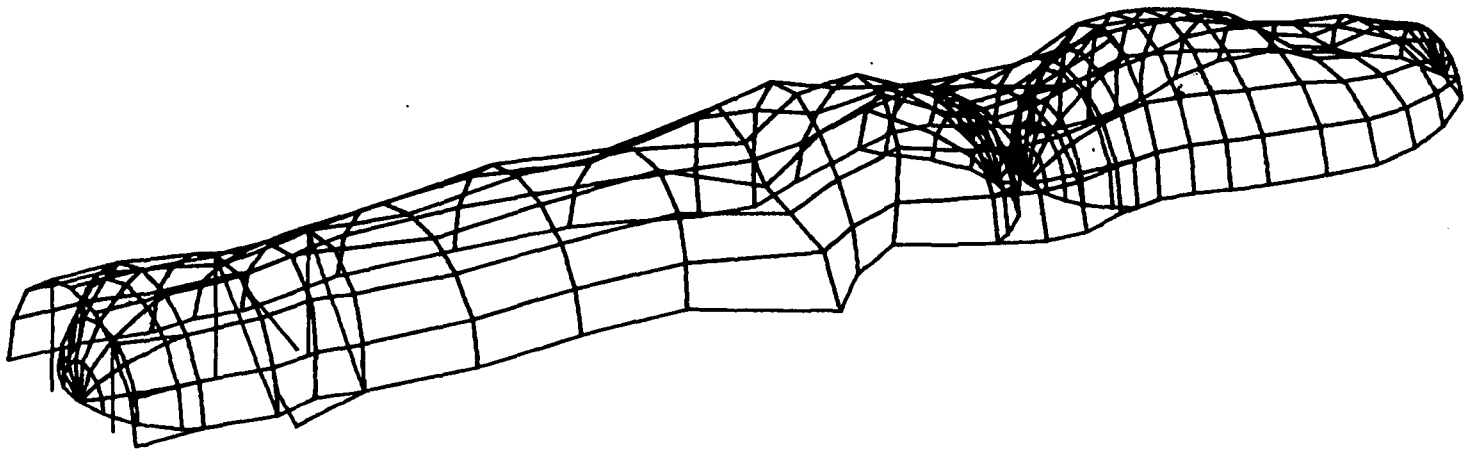

T13-120

Fig. 4-70 External Tank Without Fluid

HARMONIC REDUCTION
MODAL DEFORMATION – SUBCASE 1 MODE 24 EIGENVALUE = 15443116 (RADIANS/SEC)^2

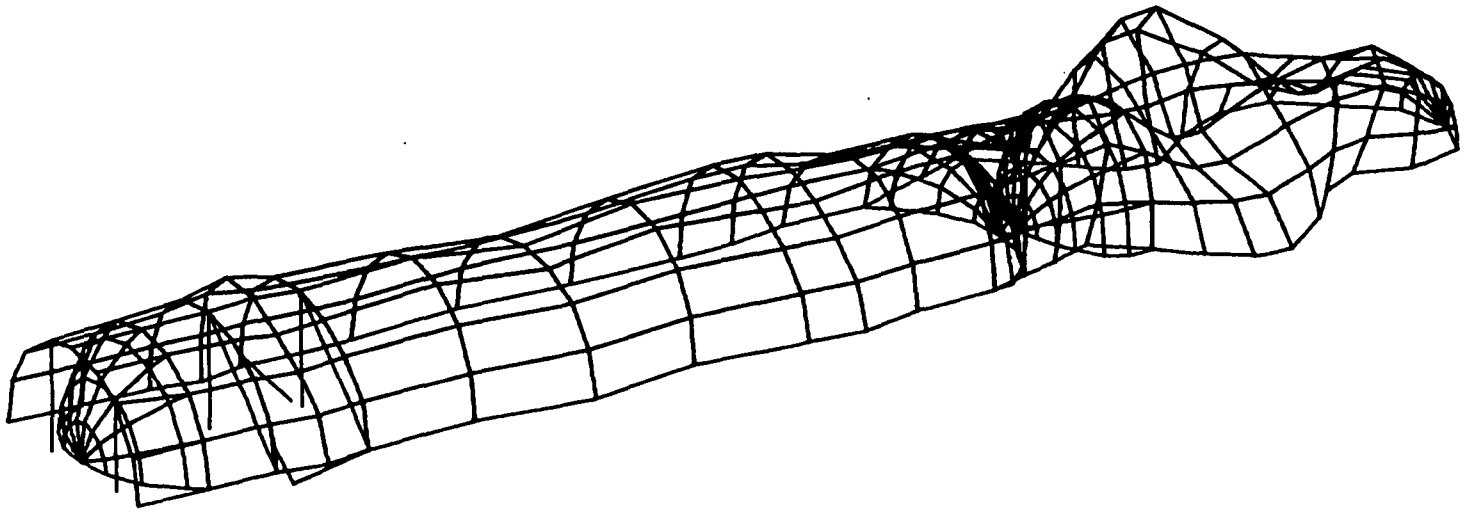

T13-121

Fig. 4-71 External Tank Without Fluid

HARMONIC REDUCTION
MODAL DEFORMATION – SUBCASE 1 MODE 25 EIGENVALUE = 15569283 (RADIANS/SEC)²

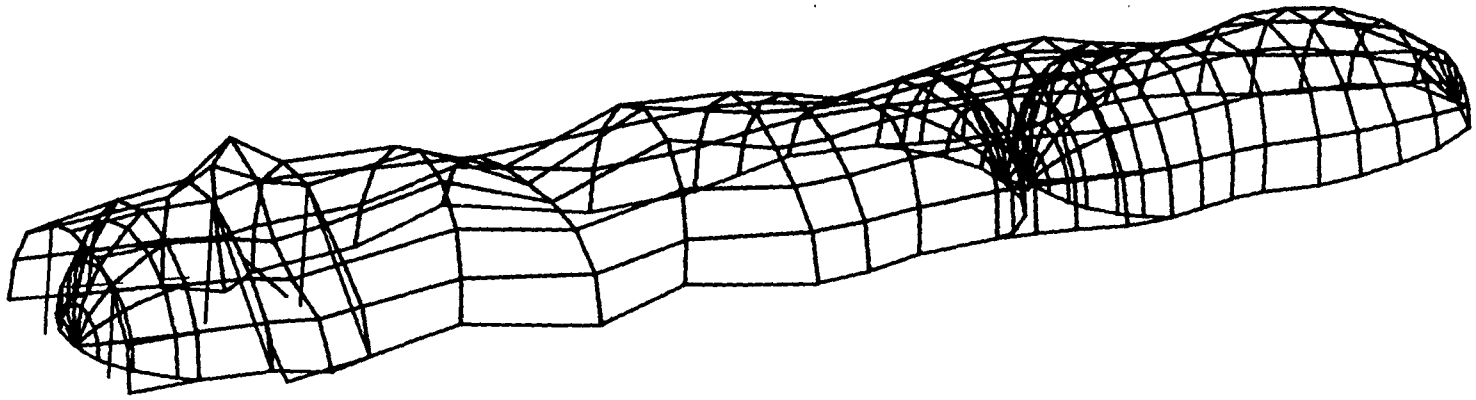

T13-122

Fig. 4-72 External Tank Without Fluid

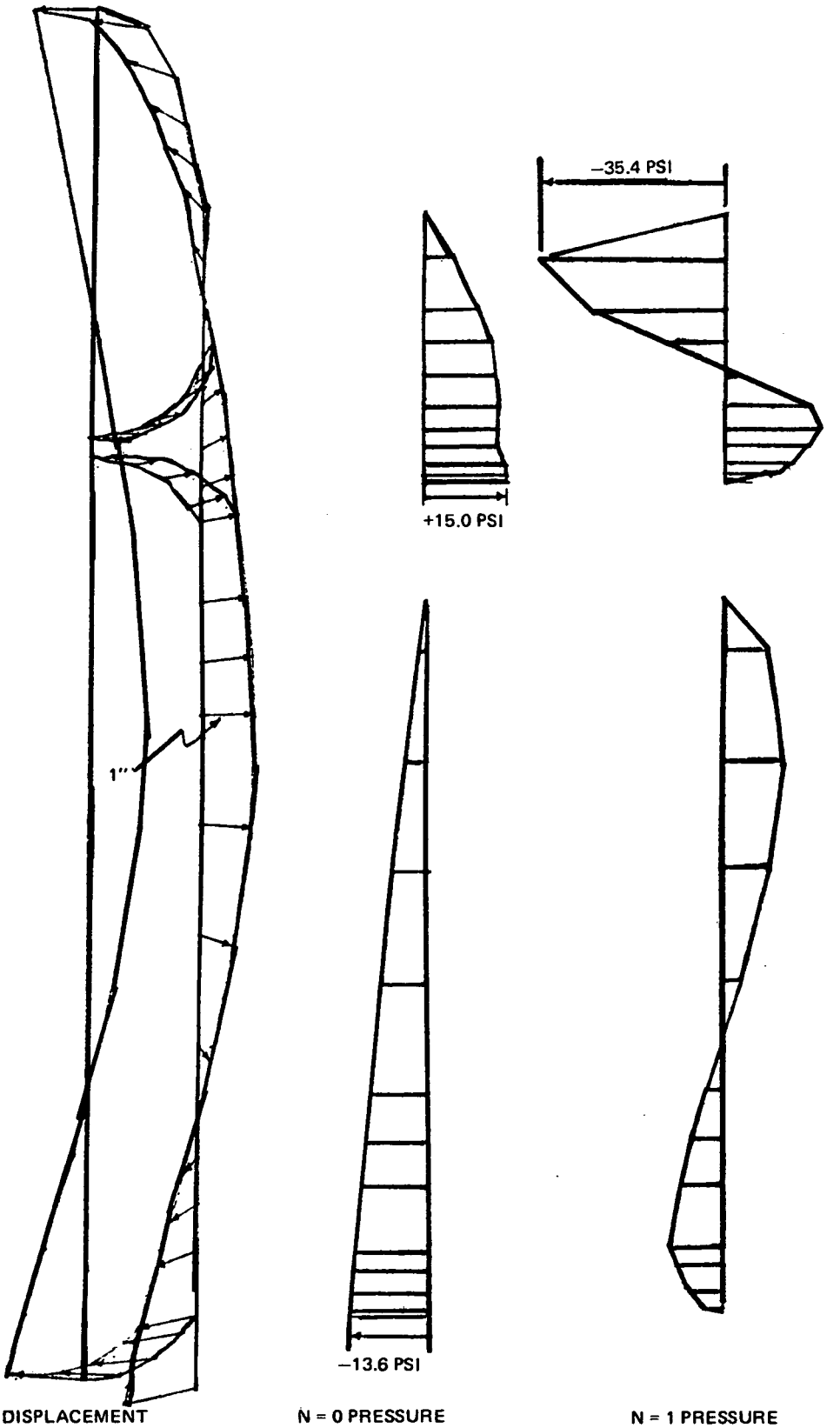

Fig. 4-73 Post Max Q External Tank 1st Bending Mode (Mode 6)

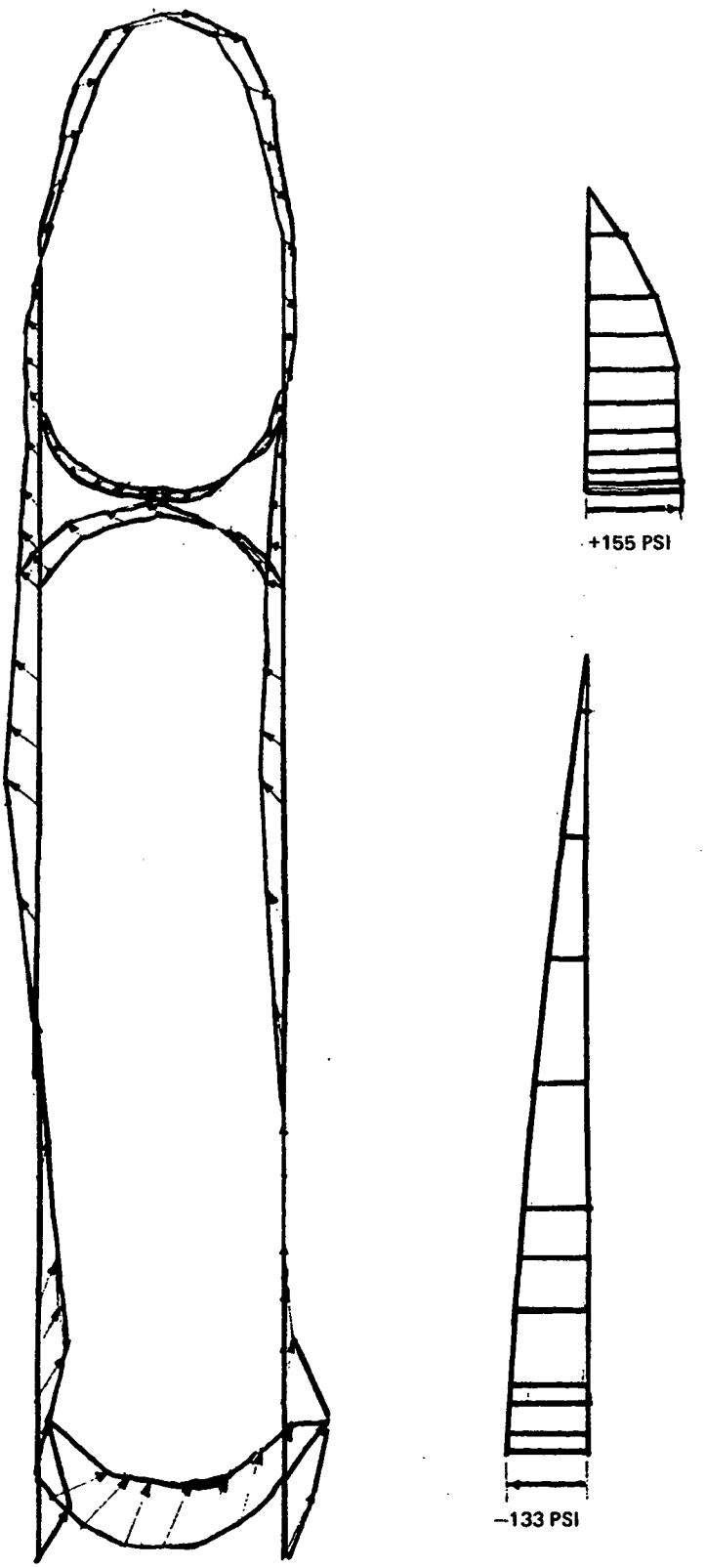

T13-124 DISPLACEMENT N = 0 PRESSURE

Fig. 4-74 Post Max Q External Tank 1st Axial Mode (Mode 7)

METHOD INV. NO OMITS
FREE FREE MODES
MODAL DEFOR, SUBCASE 1 MODE4 FREQ. 151,6242

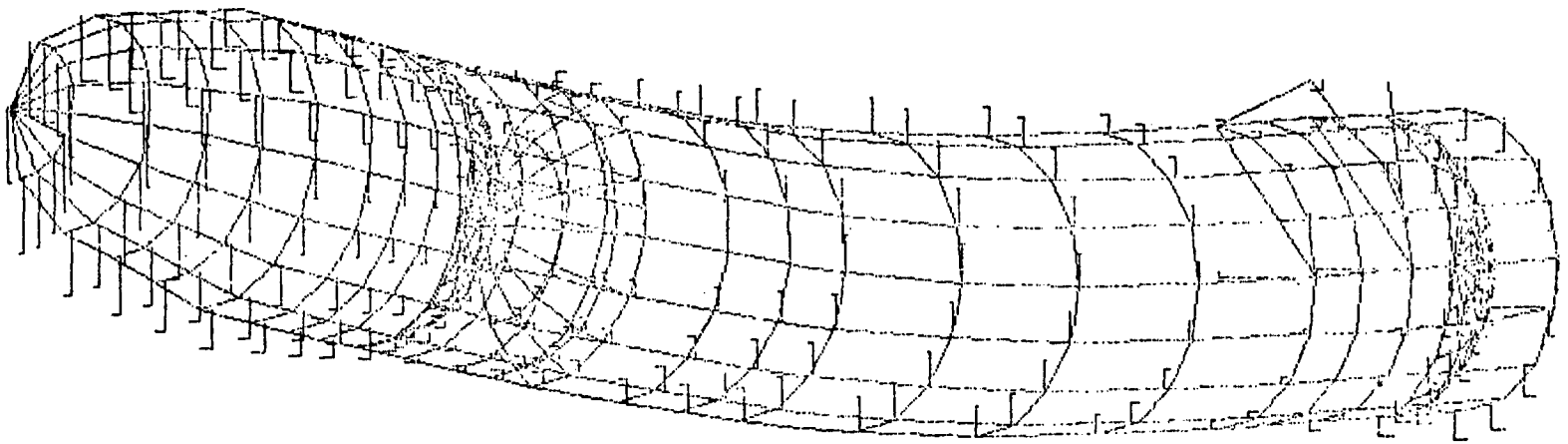

T13-125

Fig. 4-75 NASTRAN Model of External Tank Structure

METHOD INV. NO OMITS
FREE FREE MODES
MODAL DEFOR. SUBCASE 1 MODE4 FREQ. 151.6242

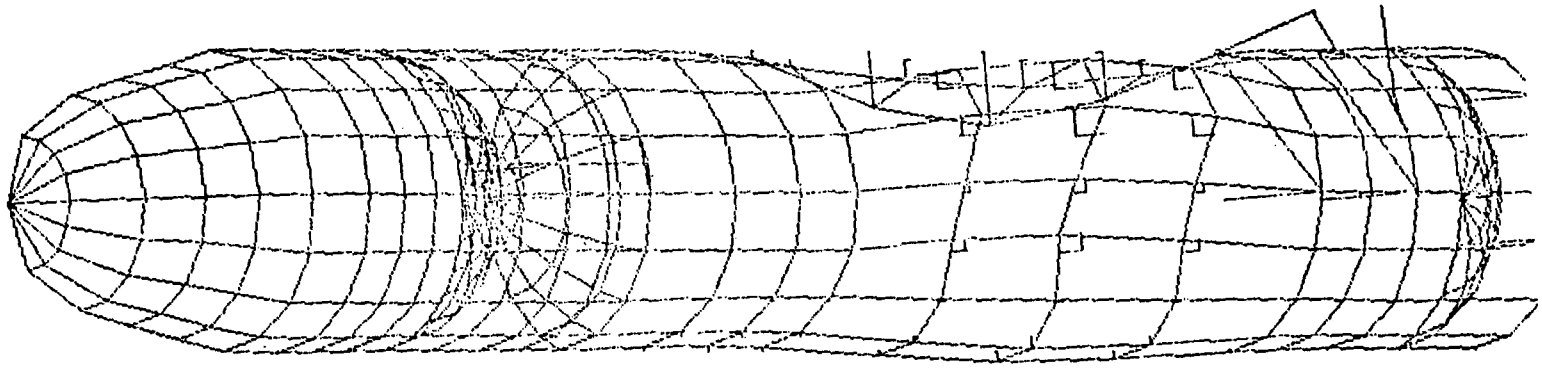

T13-126

Fig. 4-76 NASTRAN Model of External Tank Structure

METHOD INV. NO OMITS
FREE FREE MODES
MODAL DEFOR, SUBCASE 1 MODE 4 FREQ. 151.6242

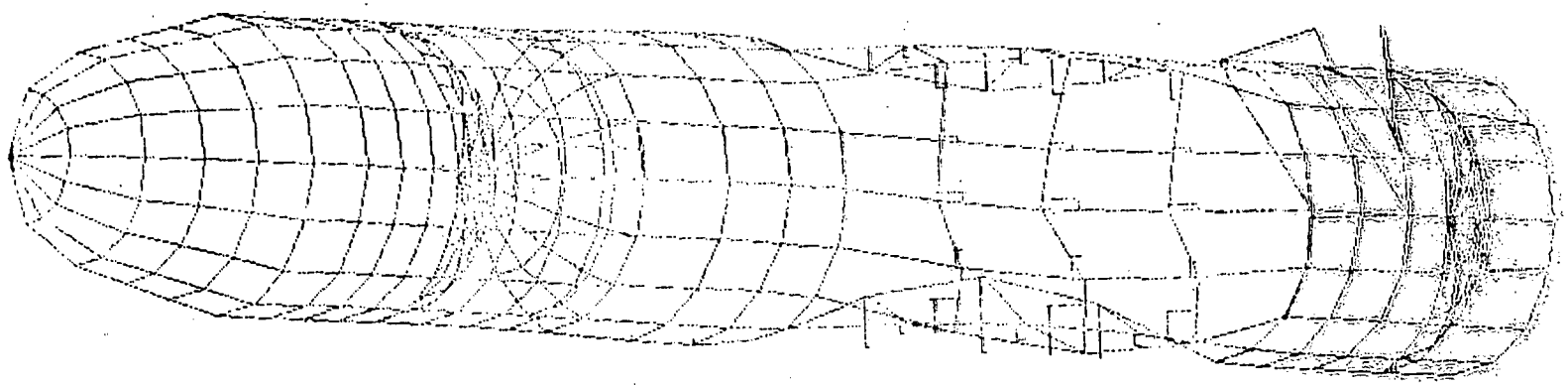

T13-127

Fig. 4-77 NASTRAN Model of External Tank Structure

Section 5
REFERENCES

5 - REFERENCES

5-1 "NASTRAN Analysis of the 1/8-Scale Space Shuttle Dynamic Model", Paper II in NASA TMX 2893, NASTRAN User's Experiences, September 1973.

5-2 Bernstein, M., et al., "Design of Space Shuttle Structural Dynamics Model", NASA CR-112205, Revision A, 1973.

GRUMMAN AEROSPACE CORPORATION
BETHPAGE, NEW YORK 11714

2210-74